University of Zimbabwe

Research Topic:

Designing of Large Scale Grid Connected PV Systems

By

FUNGISAI MUZOKOMBA

R015278L

Research Proposal submitted in partial fulfilment of the requirements for the degree of Master of Renewable Energy, University of Zimbabwe

Supervisor: Eng. T. Hove

July 2017

Abstract

Grid-connected PV systems are usually installed to increase power availability and at the same time enhancing the performance of the electricity network by reducing the power losses and improving the voltage profile of the network. However, this tend not to be always the case as these systems might impose several negative impacts on the network, especially if their level of penetration is high. These negative impacts include power and voltage fluctuation problems, harmonic distortion, malfunctioning of protective devices and overloading and under-loading of distribution feeders. The studying of the possible impacts of PV systems on the electricity network is currently becoming an important issue and is receiving a lot of attention from both researchers and power utilities. The main reason for the importance of this issue is that accurate evaluation of these impacts, as well as providing feasible solutions for the operational problems that might arise due to installing PV systems, is considered a major contribution towards facilitating the widespread use of grid connected PV systems.

The primary objective of the research proposed in this thesis is to facilitate increasing the penetration levels of PV systems in the Zimbabwe utility grid. This can be achieved by properly designing PV systems and quantifying and analysing the impacts of installing large grid-connected photovoltaic systems on the performance of the electric network accurately. The cost effectiveness of these systems is also analysed.

Solar PV technology for a particular site depends mainly on the annual solar intensity distribution for the site, variations in the efficiency of PV module technology with intensity, annual temperature distribution and module temperature coefficient, variations in the solar spectrum distribution and the rate at which the output power of the PV modules degrades with time. Electrical efficiency of the photovoltaic module depends on ambient temperature and the efficiency decreases as the temperature increases.

Table of Contents

Table of Figures

CHAPTER 1

INTRODUCTION TO THE STUDY

1.0 Introduction to the study

This chapter defines the research objectives and the research proposition within the issues related to the design of solar PV plants. It also demonstrates the background to the research, defines the electricity problems for Zimbabwe and how the research seek to solve the problem.

1.1 Background

TD Energy is a Zimbabwean company that has a commendable vision of promoting the development and utilization of green energy technologies, among them solar energy. In the present case TD Energy has reserved about 42 hectares of its land to develop a grid-tied solar plant at Ecosoft, based on photovoltaic conversion. The project is a positive step towards alleviating Zimbabwe's electricity generation deficit using environmentally friendly and indigenous resource that is ubiquitously abundant in the country. The project will generate financial and economic benefits and create employment during its planning, construction and operation stages, at the same time helping to reduce the fossil fraction in the Zimbabwe energy mix.

The site is located along Enterprise road across the turn-off to Shamva on the way from Harare to Murewa, and the boundary between Harare and Mashonaland provinces. The site, as presently set up, comprises of a built-up area of about 10% coverage and the land use is chicken breeding. Most of the buildings are sheds meant for chicken breeding. The rest of the buildings are accommodation quarters for the chicken farm workers.

At the present moment, there is a 99kW roof mounted PV system which was installed some time ago. However, the scope of this project will not cover the roofs of these buildings as they have a random azimuth orientation, which will not be optimal for solar energy collection. The design will be centred on the unbuilt area which comprises mainly of slightly south sloping open land of grade of about 5% with an additional part occupied by a hill.

A Zimbabwe Electricity Transmission and Distribution (ZETDC) substation (which will be used for power evacuation) is located about 6 km from the site. The power evacuation transmission line route will be along Enterprise road. Figure 1.1 shows the site location for the solar plant. The project site is located at latitude -17.74° and longitude 31.206°. Access to the solar farm will be achieved by upgrading an existing dirty road which branches off Enterprise road to an all-weather gravel road. A security fence will be erected around the solar farm with guarded gate.

Figure 1.1: Research Project Site - Ecosoft

The demand for power in Zimbabwe is mostly met through conventional plant which generates bulk amount of power centrally. The generation of power using Photovoltaic (PV) technology is very promising in terms of power generation ranging from kWs to MWs and helps to a great extent in the increase of the installed capacity and can help power utility companies in meeting increasing load demand and at the same time minimising distribution losses. The concept of grid-connected solar PV system is mounted on vacant unutilized area of commercial buildings; small-scale industry rooftops are likely to add to generation capacity and thus meet renewables portfolio standard targets of utility. This research analyses and designs a PV array and defines best inverter types sizes for a grid-connected PV system. The proposed site selected is Ecosoft (Harare) with latitude 17.74°S and longitude 31.206°E. With the aid of a PV system design software, various

inputs like peak power, module voltage, global irradiance and tilt angle are provided, and a detailed report on the losses of PV array as well as the inverter and the energy yield are then obtained. The output from the software is also compared with theoretical models.

Currently there is a major challenge of providing reliable and continuous energy supply in Zimbabwe, which has resulted in many power crises in the country over the past decade. Lessons from over-reliance on hydro-electric power generation have led the country to explore alternative forms of energy generation to meet the aspirations for full electrification. Solar power, one of the many renewable energy options, provides attractive benefits like environmental protection, job creation, and global potential for technology transfer and innovation. Zimbabwe, and for that matter, the African continent in general, has the greatest potential for solar power projects with a greater part of the continent receiving about 300W/m^2 of solar radiation annually.

Grid-connected solar Photovoltaic (PV) systems employ the direct conversion of sunlight into electricity which is fed directly into the electricity grid without storage in batteries. This option, like many other renewable energy options, is generally carbon free or carbon neutral and as such does not emit greenhouse gases during its operation, since global warming and climate change are mostly caused by the release of carbon dioxide and other greenhouse gases into the atmosphere.

A look at the world's map of mean solar radiations reveal that, Africa as a continent receives the highest amounts of solar radiation between 300 and 350 W/m^2 annually (Brew-Hammond, et al., 2007). This makes the African continent, of which Zimbabwe is a part, exceptionally suitable for solar energy projects. In spite of this huge potential, Africa still trails the rest of the world in terms of solar energy applications and energy services in general, thus referred to globally as the Dark Continent. From the design and analysis of the grid-connected solar PV system, the researcher seek to come up with standard set of procedures that will make it easy for the institutions to adopt. In the long run, it will help promote the use of grid connected solar PV systems in Zimbabwe.

Zimbabwe's energy requirements are met through a combination of biomass, domestic coal-fired and hydroelectric power plants and imports. The total installed electricity

capacity (2008): 1,990MW which is attributed to Hydropower plants at 57% and Thermal power plants 43% (IRENA, 2010). At least 35% of electricity required is imported from neighbouring countries.

Inadequate power generation, unreliability of sources and financial constraints to importing has led to frequent power shortages resulting in significant under – utilisation of capacity in manufacturing, mining and agriculture sectors.

- More than half of the total energy supply is still from biomass products.
- The large unsustainable fuel wood consumption (primarily for cooking) has caused severe wood shortages in most rural areas

Zimbabwe Energy Generation status at a glance

Table 1.1: Zimbabwe Generation Status (ZESA, 2017)

Gen Station	Energy
Hwange	546 MW
Kariba	694 MW
Harare	0 MW
	0 MW
Bulawayo	0 MW
Imports	0-350 MW
Total	1620MW

1.2 Problem Statement

Poor solar field design and grid integration practices that lack adequate data and analysis lead to low energy performance and frequent equipment failure for large scale solar Photovoltaic (PV) grid integrated power systems, which affects the technical viability and cost effectiveness of these systems.

1.3 Justification

Globally, the demand for electricity is expected to increase rapidly due to the global population growth and industrialisation. The increase in the energy demand requires electric power utilities to increase their generation capacities. A large share of electricity

at the moment is generated from fossil fuels, especially coal due to its low prices. However, the increasing use of fossil fuels accounts for a significant portion of environmental pollution and greenhouse gas emissions, which are considered the main reason behind the global warming. To overcome the problems associated with generation of electricity from fossil fuels, renewable energy sources can be participated in the electricity energy mix for the utilities. One of the renewable energy sources that can be used for this purpose is the energy received from the sun. The use of photovoltaic (PV) systems for electricity generation is not new, it started in the seventies of the 20th century and is growing rapidly worldwide at the moment. World over, many organizations expect a bright future for these systems. Taking for example, the European Photovoltaic Industry Association (EPIA) expects that the global cumulative PV capacity will reach 200 GW by the year 2020 and 800 GW by the year 2030 (IRENA, 2010). PV systems are usually used in three main fields of satellite applications, where the solar arrays provide power to satellites, off-grid applications, where solar arrays are used to power remote loads that are not connected to the electric grid, and grid connected applications, in which solar arrays are used to supply energy to local loads as well as to the utility grid. Grid connected PV systems currently dominate the PV market, especially in Europe, Japan and USA but it is still to find its way in Zimbabwe. The most common in Zimbabwe are the off grid PV systems.

Another major issue that faces the widespread of PV systems is that the increasing installation of grid-connected PV systems, especially large systems in the order of megawatts, might lead to some operational problems in the utility grid. This issue, which is the main focus of the research presented in this thesis, can be tackled by accurately evaluating the impacts of installing PV systems on the performance of the grid and finding solutions that can reduce the operational problems that might arise due to their installation.

This research seeks to motivate the uptake of grid connected solar PV in Zimbabwe and also addresses the economic viability of the systems.

1.4 Aim and Objectives

The aim of this project to determine the viability, cost effectiveness and best practices for Grid connected Solar PV plants in Zimbabwe.

The research objectives are as follows:

i) To review the literature for the design of large scale Photovoltaic Systems connected to the utility grid

ii) To design a PV system with regards to PV system design and grid integration

iii) To assess the impact of connecting the designed PV system on the utility grid (ZETDC)

iv) To determine the cost effectiveness of PV Solar Farms in Zimbabwe

1.5 Research questions

i) How is the design of large scale Photovoltaic Systems connected to the utility grid in Zimbabwe be compared to the literature of solar PV design?

ii) How do you design a PV system with regards to PV energy generation capacity and grid integration?

iii) What is the impact of connecting the designed PV system on the utility grid (ZETDC)?

iv) What is the cost effectiveness of PV Solar Farms in Zimbabwe?

1.6 Summary Methodology

The following research methodology was used:

i) Collection of the metrological data of the area

ii) Determine the area to be covered PV modules

iii) Calculate the total energy to be produced on the two scenarios

iv) Calculate the inverter size and the number of inverters to be installed

v) Quantity the PV modules, inverters, cables and all other accessories to come up with the cost

vi) Perform economic appraisal for the project and calculate the annualised cost of electricity for the design

1.7 Dissertation Structure

The study comprises of five chapters as follows;

- Chapter 1: Introduction

The chapter introduces the study and discusses the background of the company, the research problem, objectives, questions and the scope of the study.

- Chapter 2: Literature Review

  The chapter is a detailed review of the literature on the design of solar PV plants,

- Chapter 3: Research Methodology

  The chapter covers the description of the research methodology adopted for the study and discusses how the research was carried out, sampling methods, research instruments used as well as the techniques for data processing, analysis and presentation.

- Chapter 4: Data Collection

  This chapter is a presentation of the findings of the research as well as discussion of the findings relative to the research hypothesis and research objectives.

- Chapter 5: Design/analysis

  This chapter outlines the design of the PV system and the several options considered

- Chapter 6: Discussion of results

  This chapter is a presentation of the findings of the research as well as discussion of the findings relative to the research hypothesis and research objectives

- Chapter 7: Economic analysis

  This chapter covers economical study to determine the production cost of electricity per kWh for the designed system.

- Chapter 8: Recommendations

  This chapter outlines the conclusion and recommendations emanating from the research. In addition, the chapter also suggests areas of further study as highlighted by the research findings.

1.8 Assumptions and Limitations

In order to complete the objectives, this project is based on the following assumptions:

i) Permission will be granted from Ecosoft to use their site for study of the PV system

ii) Access to the necessary licences

Limitations

The researcher might not commission the project during the timelines of the project as it is still at design stage. Hence the commissioning and actual grid connection of the designed system is beyond the scope of this project.

1.9 Time Schedule

The proposed programme is as follows:

i) Submit initial proposal by the 17th of February 2017

ii) Approval of the Project Proposal by the 28th of February 2017

iii) Chapter 2 submission 31st of March 2017

iv) Chapter 3&4 submission by the 30th of April 2017

v) Chapter 5&6 by the 31st of May 2017

vi) Chapter 7&8 submission by the 30th of June 2017

vii) Final document submission by the 4th of July 2017

CHAPTER 2

LITERATURE REVIEW

2.0 Literature Review

2.1 Introduction

The chapter presents the literature review. It starts with the background and theoretical concepts that relates to solar photovoltaic design for grid connected systems. The grid connected solar photovoltaic designs which were conducted in various countries and their implementation are then presented.

Definition of terms

Latitude (φ) – the angular location North or South of the Equator, North is positive; −90◦ ≤ φ ≤ 90◦.

Declination (δ) – the angular position of the sun at solar noon (i.e., when the sun is on the local meridian) with respect to the plane of the equator, north positive; −23.45◦ ≤ δ≤ 23.45◦.

Slope (β) – the angle between the plane of the surface in question and the horizontal; 0◦ ≤ β ≤ 180◦. (β > 90◦ means that the surface has a downward-facing component

Surface azimuth angle (*γ)* - deviation of the projection on a horizontal plane of the normal to the surface from the local meridian, with zero due south, east negative, and west positive; −180◦ ≤ *γ* ≤ 180◦.

Hour angle (*ω)* - angular displacement of the sun East or West of the local meridian due to rotation of the earth on its axis at 15˚ per hour; morning negative, afternoon positive.

Angle of incidence (*θ)* - angle between the beam radiation on a surface and the normal to that surface.

Zenith angle θ_z - angle between the vertical and the line to the sun, i.e. the angle of incidence of beam radiation on a horizontal surface.

Solar altitude angle (α_s) – angle between the horizontal and the line to the sun and it is the complement of the zenith angle.

Solar azimuth angle (γ_s) - angular displacement from south of the projection of beam radiation on the horizontal plane. Displacements east of south are negative and west of south are positive.

According to (Cooper, 1969), the declination δ can be found from the approximate equation below:

$$\delta = 23.45 \sin\left(360 * \frac{284+n}{365}\right) \quad \text{.....Equation 1}$$

2.2 PV Module Power Output

According to (Dash & Gupta, 2015), the photovoltaic module performance is rated under standard test conditions (STC) i.e. irradiance of 1000 W/m², solar spectrum of Air Mass 1.5 and module temperature at 25°C. Therefore, photovoltaic modules manufacturers provide ratings at Standard Test Conditions. PV modules however operates over a large range of environmental conditions in the field. This therefore leaves the manufacturer's information not sufficient to determine the actual performance of the photovoltaic module under field conditions. The actual performance of a PV module at a particular site depends on the effective efficiency and effective global irradiance. This can be illustrated by the following equation:

$$P_{pv} = \frac{\eta_{pv}}{\eta_r} \times \frac{G_T}{G_r} \times P_{rated} \quad \text{.....Equation 2}$$

Where η_{pv}= actual module operating efficiency under arbitrary weather conditions

η_r= array efficiency measured at reference cell temperature

G_T=resultant global irradiance due to the weather conditions on the particular site due to tilt

G_r= the STC global irradiance

2.2.1 PV Module Efficiency

According to (Evans, 1981), the efficiency, η_{pv}, of a photovoltaic array (or cell) is a function of the cell temperature (T_c) and array irradiation (G_T) and is characterised by the following equation:

$$\eta_{pv} = \eta_r[1 - \beta(T_c - T_r) + \gamma log_{10} I_{array}] \quad \text{.....Equation 3}$$

where β is defined by (Spiegel, et al., 1981) as a temperature coefficient for cell efficiency and is relatively constant for the range of operating temperatures encountered in flat-plate arrays

T_c is the cell temperature

T_r is the reference cell temperature at which η_r is determined,

γ is a radiation intensity coefficient for module/cell efficiency

I_{array} is the radiation incident on the array per unit area.

Often γ is negligible i.e. approximately equal to zero γ =0, (Hove, 2000) and subtracting T_a, from the two temperature terms in parentheses in Equation (2), T_c and T_r, respectively, results in:

$$\eta_{pv} = \eta_r[1 - \beta(T_c - T_a) - \beta(T_a - T_r)] \quad \text{Equation 4}$$

An energy balance of the array equates the solar energy gain in the array to the electrical output and thermal losses as:

$$\tau\alpha I_{array} = \eta_{pv} I_{array} + U_L(T_c - T_a) \quad \text{Equation 5}$$

where $\tau\alpha$ is the transmittance-absorbance product of the array and U_L is the thermal loss coefficient per unit area between array and ambient. η_{pv} in Equation. (3), is in the order of $0.1\tau\alpha$, (Evans, 1981), so that Equation. (4) can be estimated by:

$$T_c - T_a = 0.9\frac{\tau\alpha}{U_L} I_{array} \quad \text{Equation 6}$$

$\tau\alpha/U_L$ can be determined from measurements of cell temperature ambient temperature and solar radiation at Nominal Operating Cell Temperature (NOCT) conditions I_{array}=800Wm^2 =2.88MJ/m^2/h, T_a=20^{o}C, wind speed =1m/s and $\eta_{pv} = 0$.

From equation (4) above substituting $T_{c,NOCT}$ for T_c, $T_{a,NOCT}$ for T_a and $\eta_{pv} = 0$ thus $\tau\alpha/U_L$ will be obtained as (Hove, 2000):

$$\tau\alpha/U_L = \frac{(T_{c,NOCT} - T_{a,NOCT})}{I_{array,NOCT}} \quad \text{Equation 7}$$

Assuming $\tau\alpha/U_L$ to be constant over the relevant operating temperature range (Hove, 2000), Equation (5) with $\tau\alpha/U_L$ obtained from Equation (6), can be used in Equation (3) to obtain:

$$\eta_{pv} = \eta_r[1 - 0.9\beta \frac{I_{array}}{I_{array,NOCT}}(T_{c,NOCT} - T_{a,NOCT}) - \beta(T_a - T_r)]$$ .....Equation 8

∴ The electrical energy output, Qe, of the modules array is given by:

$$Q_e = \eta_{pv} A I_{array}$$ .....Equation 9

where η_{pv} is obtained from Equation (8) and A is the array area.

2.3 Solar Radiation

The sun is the primary source of energy to the Earth. This energy is radiated in all directions into space through short waves and is known as solar radiation. About two billionths or (two units of energy out of 1,00,00,00,000 units of energy radiated by the sun) of the total solar radiation reaches the earth's surface (Magee, 2010). This is the only major source of energy on the earth for most of the physical and biological phenomena. The incident solar radiation that comes through short waves is termed as insolation (Klaus, et al., 2014). The amount of insolation received on the earth's surface is far less than that is radiated from the sun because of the small size of the earth and its distance from the sun. In addition, water vapour, dust particles, ozone and other gases present in the atmosphere absorb a small amount of insolation (Magee, 2010).

2.3.1 Factors influencing Insolation

The amount of insolation received on the earth's surface is not uniform everywhere. It varies from place to place and from time to time (Sukhatme, 1999). The tropical zone receives the maximum annual insolation. It gradually decreases towards the poles. Insolation is more in summers and less in winters.

The following factors influence the amount of insolation received.

i) The angle of incidence

ii) Duration of the day. (daily sunlight period)

iii) Transparency of the atmosphere

The Angle of Incidence

Since the earth is round, the sun's rays strike the surface at different angles at different places. The angle formed by the sun's ray with the tangent of the earth's circle at a point is called angle of incidence. It influences the insolation in two ways. First, when the sun

is almost overhead, the rays of the sun are vertical. The angle of incidence is large, hence they are concentrated in a smaller area, giving more amount of insolation at that place. If the sun's rays are oblique, angle of incidence is small and sun's rays have to heat up a greater area, resulting in less amount of insolation received there. Secondly, the sun's rays with small angle, traverse more of the atmosphere, than rays striking at a large angle. The longer the path of sun's rays, greater is the amount of reflection and absorption of heat by atmosphere. As a result, the intensity of insolation at a place is less.

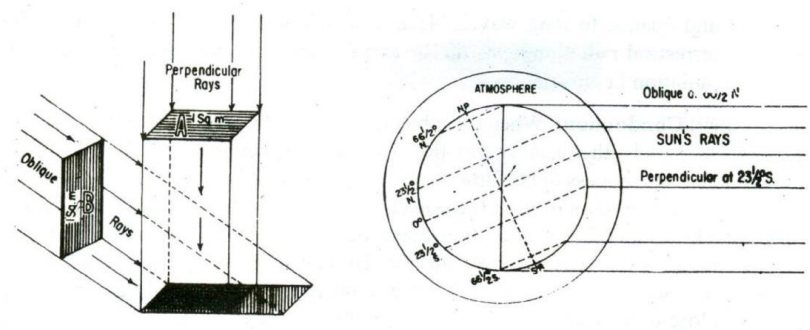

Figure 2.1: Effect of angle of incidence on insolation

Duration of the day

Duration of the day varies from place to place and season to season. It decides the amount of insolation received on earth's surface. The longer the duration of the day, the greater is the amount of insolation received. Conversely shorter the duration of the day leads to receipt of less insolation.

Transparency of the atmosphere

Transparency of the atmosphere also determines the amount of insolation reaching the earth's surface. The transparency depends upon cloud cover, its thickness, dust particles and water vapour, as they reflect, absorb or transmit insolation. Thick clouds hinder the insolation to reach the earth while clear sky helps it to reach the surface. Water vapour absorb insolation, resulting in less amount of insolation reaching the surface.

2.3.1.1 The angle of incidence related to solar radiation received on solar collector

The amount of sun's radiation received on a certain surface or solar collector on the earth is changes throughout the year. The amount of radiation received is determined by the

position of the sun in the sky and the orientation of the surface. In order to receive maximum solar energy, the collector's surface should be perpendicular to the sun's rays (Duffie & Beckman, 2006). This however can be achieved when the solar trackers are used to follow the sun instantaneously. This phenomenon is rather costly to employ hence the angles of collector's surface could be changed manually every day or month or season in order to adjust the collector almost perpendicular to the sun's rays (Foster, et al., 2010). of past studies in this field investigated the monthly slope angle of the solar collectors and the results showed that the slope angle depends on latitude.

The diagram below shows the incidence solar radiation on flat and tilted surface.

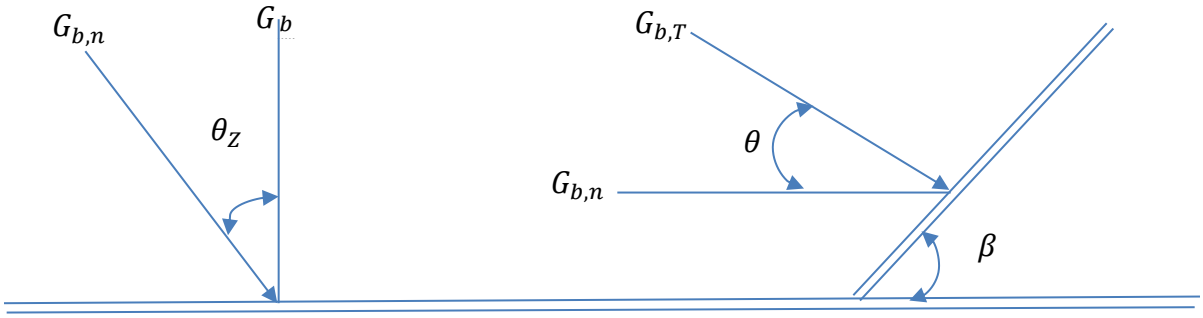

Figure 2.2: The incidence angle on a surface

$$G_b = G_{b,n}Cos\theta_Z \quad \text{.....Equation 10}$$

$$G_{b,T} = G_{b,n}Cos\theta \quad \text{.....Equation 11}$$

Radiation of the sun consists of two components, i.e. beam and diffuse radiation. The angle of incidence of beam radiation on a surface is related to some other angles as shown in Equation below.

$$Cos\theta = Sin\delta Sin\emptyset Cos\beta - Sin\delta Cos\emptyset Sin\beta Cos\gamma + Cos\delta Cos\emptyset Cos\beta Cos\omega + Cos\delta Sin\emptyset Sin\beta Cos\gamma Cos\omega + Cos\delta Sin\beta Sin\gamma Sin\omega \quad \text{.....Equation 12}$$

For a horizontal surface, the angle of incidence is the zenith angle of the sun, θ_Z. Its value must be between 0^o and 90^o when the sun is above the horizon.

$$\therefore Cos\theta_Z = Cos\emptyset Cos\delta Cos\omega + Sin\emptyset Sin\delta \quad \text{.....Equation 13}$$

When the beam radiation arrives perpendicularly to a surface, the surface will receive more radiation. Some solar collectors 'track' the sun by moving in certain ways to minimize the angle of incidence of beam radiation, θ or θ_Z, on the surfaces. Doing so will make $Cos\theta$ as maximum as possible. Thus, it will maximize the incident beam radiation.

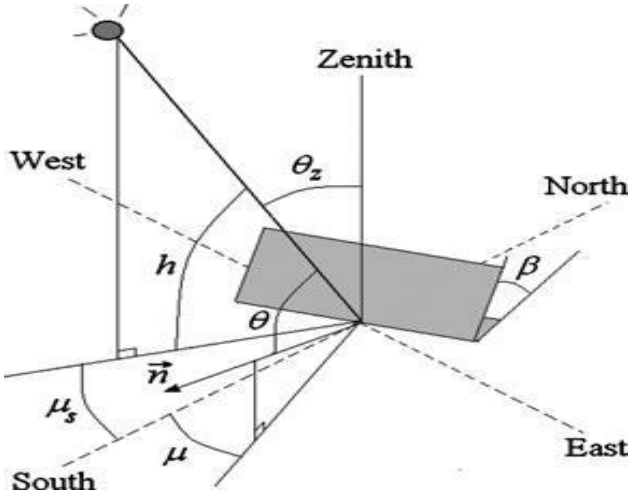

Figure 2.3: Angles Describing the position of the sun

2.3.1.2 Azimuth and Inclination

When the latitude of the designed solar system is other than equator the face of a fixed panel system should be oriented to the optimum direction in order to maximize the energy production. This orientation is commonly defined by terms of azimuth and inclination. Azimuth defines the horizontal direction angle or the point of the compass where panels are facing and inclination defines the angle or tilt from horizontal the panels should have. Azimuth range is from 0° (South) to +180° (West) and to -180° (East). Some applications Use also normal compass definition where 180° is south etc. Inclination range is from horizontal 0° to vertical 90°. Figure 2.4 below illustrates this:

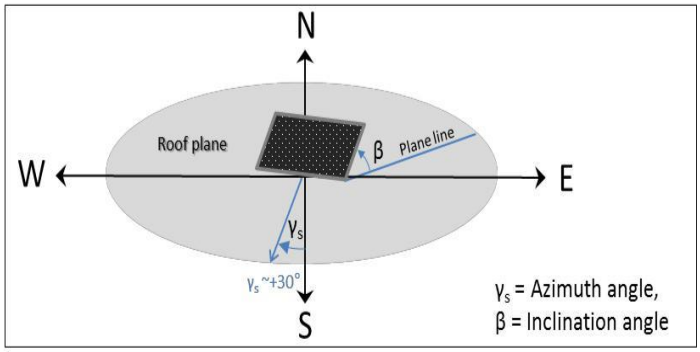

Figure 2.4: Azimuth and inclination angles of a solar panel

The best and most used azimuth angle for fixed solar systems in northern hemisphere is usually 0° i.e. the panel faces are towards south and vice versa for Southern Hemisphere. The best azimuth angle for Southern Hemisphere is 180° and collectors will be facing North. The reason for this is that sun altitude angle is at its highest when it is in south. The bigger the altitude angle the smaller the irradiance attenuation effect and generally less shadowing problems to deal with.

2.3.1.3 Optimum tilt angle

In their research, (Moon, et al., 1981) noted that there was wide study on the optimum solar collector's tilt angle. As alluded by (Moon, et al., 1981), the use of solar tracking systems is the best way to collect maximum daily energy on a solar collector. According to (Markvart, 1994) and (Yakup & Malik, 2001), it is possible to collect 40% or more solar energy by using a two-axis tracking system. The main disadvantage of these systems is their high cost and they consume energy during their operation hence a source of energy loss. Choosing the best direction for solar collectors is however the more practical and economic way. According to (Elminir, et al., 2006), there are mainly two factors that affect the optimum tilt angle of a solar collector which are:

i) The reflection properties of sky and ground and actual climatic conditions of the site, regarding snow fall and dust,
ii) the maximisation of the amount of collectable radiation in the whole year or a certain period of time.

The theoretical and experimental results indicate that the sky radiation is not isotopically distributed at all times (Dave, 1977). Many models proposed over the last few years to optimize solar collectors tilt angles were based on the consideration of sky and ground reflection. In their research (Temps & Coulson, 1977) noted that the main influencing factor of the solar collector is the direct solar radiance.

According to (Shariah, et al., 2002), the amount of solar radiation reaching the collector surface is changed by tilt angle variations. The optimum tilt angle was proposed based only on the latitude (Shariah, et al., 2002). Many researchers have come up with different values. According to (Duffie & Beckman, 2006), the tilt angle should be 10°–15° more

than the latitude during winter and 10°–15° less than the latitude during summer. Other authors, Lunde (Lunde, 1980) and Garg (Garg, 1982) obtained the optimum tilt angle, $\beta_{opt} = \varphi \pm 15°$. Experimental results done by (Asowata, et al., 2012) also proved that the optimum tilt angle for the winter months is approximately equal to $\beta_{opt} = \varphi \pm 10°$.

2.3.1.4 Inter-row Shading and Array Spacing

When designing a solar array having more than one row of solar panels, the mutual shading of adjacent rows i.e. inter-row shading needs to be taken into account. This is especially important for PV systems due to significant power loss shading can cause. In inter-row shading the shading is uniform i.e. while the rows are spaced evenly also the shadow caused by the adjacent row is uniform and similar for all rows except of course for the first row of the array. The amount and configuration of the bypass diodes is important in relation to the panel orientation (portrait or landscape). If orientation is wrong one, in multi row array, the shading of the bottom row of cells i.e. about 15cm of one panel can cut down the power by 90% of the whole row instead of 20% of properly configured and oriented solar panels.

Depending on the position of the Sun a panel row can be partly or totally shaded. The effect of shading is a change in the current-voltage (I-V) characteristics of the system, and consequently a reduction in power output. When a system is being designed, it is of interest to have detailed knowledge of this energy loss in order to determine its impact on the overall economy of the system. For a certain shading in the system the optimum inclination is generally not the same as for an unshaded row.

The generation of photovoltaic systems is significantly influenced by external and internal loss factors (Nemet and Husmann, 2012). Therefore, the design process of photovoltaic systems requires information on performance characteristics under various environmental conditions for estimating real power generation.

2.4 Solar Panels

Figure 2.5: Polycrystalline solar panels in operation

A solar cell as illustrated in Figure 2.9(a) is a device that converts the energy of sunlight directly into electricity by the photovoltaic effect. The solar cells are then wired in series and placed into a frame. This is now called the solar panel see Figure 2.10. The size of the frame can vary with manufacturers as a result of the technology used. A protective coating on the top covers and protects (and sometimes increases the output) of the solar cells. On the market today, the size of a PV-cell is usually 10 x 10 cm with thickness of 0.1 to 0.4mm. Any number of cells can be connected in series and most commercial modules sold today incorporate 72 cells. The PV-cells made from silicon each capable of producing DC-voltage of 0.5V. The type, quality, number and arrangement of the PV-cells used in constructing the panel determine the maximum DC-power output and the measures of the panel frame.

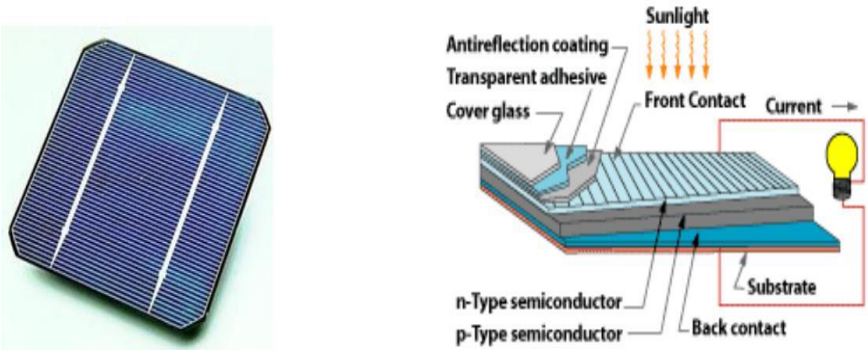

a) b)

Figure 2.6: A silicon cell made from a mono-crystalline silicon wafer (a) and (b) illustration of a typical solar cell

There are three general families of PV panels on the market today which are namely single crystal silicon, polycrystalline silicon, and thin film.

2.4.1 Monocrystalline silicon modules

Monocrystalline modules are composed of cells cut from a piece of continuous crystal. The material forms a cylinder, which is sliced into thin circular wafers. The cells may be the cells may be fully round or they may be trimmed into other shapes, retaining more or less of the original circle to minimize waste. The cells have a dark blue uniform colour because each cell is cut from a single crystal.

Figure 2.7: Monocrystalline Silicon module

Advantages of monocrystalline silicon modules

The monocrystalline modules have the following advantages:

i) They have the highest efficiency rates of between 15-20% since they are made out of the highest-grade silicon.

ii) Monocrystalline silicon solar panels are space-efficient and yield the highest power outputs thus require the least amount space as compared to any other types. They produce up to about four times the amount of electricity as thin-film solar panels.

iii) Monocrystalline solar panels have the longest lifespan, about 25years.

iv) They perform better than similarly rated polycrystalline solar panels at low-light and low-temperature conditions.

Disadvantages

i) Monocrystalline solar panels are the most expensive. For this reason, most homeowners tend to favour polycrystalline silicon solar panels (and in some cases thin-film) as they are cheaper.

ii) Entire circuit breaks down if one solar panel is partially covered with shade, dirt or snow. It is therefore recommended to choose micro-inverters instead of central string inverters if there are space challenges. This is because for micro-inverters only the shaded module will be affected and not the entire array.

iii) The Czochralski process used to produce monocrystalline silicon results in large cylindrical ingots where four sides are cut out of the ingots to make silicon wafers hence significant amount of the original silicon ends up as waste.

iv) Monocrystalline solar panels tend to be more efficient in cold weather and become less efficient when temperature goes up.

2.4.2 Polycrystalline silicon modules

Polycrystalline cells are made from similar silicon material except that instead of being grown into a single crystal, they are melted and poured into a mould. This forms a square block that can be cut into square wafers with less waste of space or material than round single-crystal wafers. As the material cools, it crystallizes in an imperfect manner, forming random crystal boundaries. The efficiency of energy conversion is slightly lower. This merely means that the size of the finished module is slightly greater per watt than most single crystal modules. The cells look different from single crystal cells as shown in Figure 2.8. The surface has a jumbled look with many variations of blue colour

Advantages

Polycrystalline modules offer the following advantages:

i) The production process is simpler and cheaper hence reduces amount of waste silicon.

ii) Polycrystalline solar panels have higher heat tolerance and hence perform better than monocrystalline at high temperatures. Heat can affect the performance of solar panels and shorten their lifespans.

Disadvantages

i) The efficiency of polycrystalline-based solar panels is typically 13-16%.

ii) Lower efficiency because of lower silicon purity

iii) Produce lower yield than monocrystalline silicon thus covers a larger surface area for the same electrical power output.

2.4.3 Thin film panels

In thin film panels, the active material is deposited as a microscopically thin layer on a sheet of metal or glass. Individual PV cells are deposited next to each other, instead of being mechanically assembled. Thin film technology is also called amorphous silicon, meaning "not crystalline". The active material may be silicon, or it may be a more exotic material such as cadmium telluride.

Some of thin film modules perform slightly better than crystalline modules under low light conditions. They are also less susceptible to power loss from partial shading of a module. The disadvantages of thin film technology are lower efficiency and uncertain durability. Current thin film materials tend to be less stable than crystalline, causing degradation over time.

2.4.4 Characteristics of Solar Cell and Bypass Diode Operation

The properties of a solar cell are defined as current versus voltage as shown in Figure 2.8. The point where the graph intercepts the current axis represents zero voltage and is the short-circuit current (Isc). The point where the graph intercepts the voltage axis represents zero current and is the open-circuit voltage (Voc).

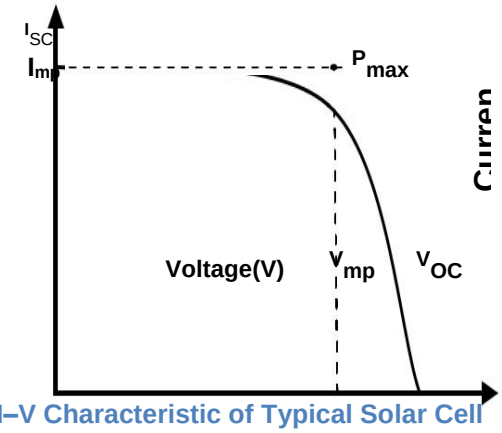

Figure 2.8: I–V Characteristic of Typical Solar Cell

From Figure 2.8 of the typical characteristic, the maximum power point (P_{max}) lies in the region of the knee of the curve. This point is calculated by the multiplication of the operating current (I_{mp}) and operating voltage (V_{mp}):

$$P_{max} = I_{mp}V_{mp} \quad \text{Equation 14}$$

Fill factor (FF) is defined as the ratio of the maximum power from a solar cell to the product of V_{oc} and I_{sc}:

$$FF = \frac{I_{mp} * V_{mp}}{I_{sc} * V_{oc}} \text{.....Equation 15}$$

The efficiency (η) of a solar cell is determined as the fraction of the incident power that is converted to electricity:

$$\eta = \frac{P}{P_{in}} = \frac{I_{mp} * V_{mp}}{P_{in}} = \frac{I_{sc} * V_{oc}}{P_{in}} * FF \text{.....Equation 16}$$

Operation Characteristics of Bypass Diodes

Mismatch caused by partial shading occurs on all types of PV installations; nearby shade obstructions such as buildings, trees, and telephone poles as well as self-shading from adjacent PV modules occur. If shading occurs to the series connection PV module, the output current is limited to the current of the shaded PV module. In this case, a solar cell that has a relatively lower current would initiate reverse voltage, which causes hot-spot heating and power degradation.

A bypass diode is therefore installed to minimize the power loss and prevent hot-spot heating. The bypass diode allows the current from good solar cells to flow in an external circuit. The bypass diode is connected in parallel with substrings in a reverse bias condition and starts working when it obtains the reverse voltage (Kim, et al., 2007). When the current of a solar cell is reduced while the shading is generated, current mismatch with other solar cells that are connected in series occurs and substrings are under reverse bias (Abete, et al., 1991).

The effect of a bypass diode on an I–V curve can be determined by first finding the I–V curve of one solar cell with a bypass diode and then combining this curve with the curves of other solar cells. The combined I–V curve is shown in Fig. 2.9 below.

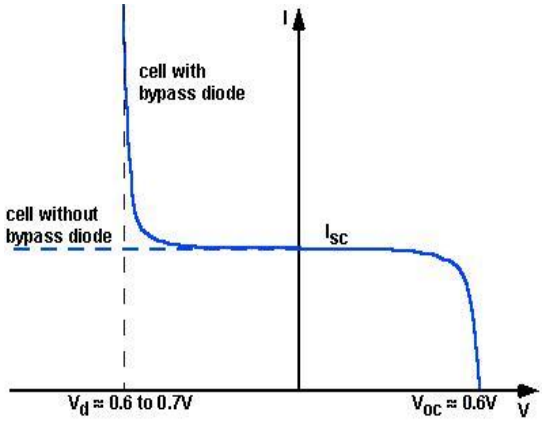

Figure 2.9: I–V Curve of Solar Cell with Bypass Diode

2.4.5 Effect of temperature

Solar modules like all other semiconductor devices, are sensitive to temperature. When the temperature rise, it reduces the band gap of a semiconductor, thereby affecting most of the semiconductor material parameters. The decrease in the band gap of a semiconductor with increasing temperature can be viewed as increasing the energy of the electrons in the material. Lower energy is therefore needed to break the bond. In the bond model of a semiconductor band gap, reduction in the bond energy also reduces the band gap. Therefore, increasing the temperature reduces the band gap.

In a solar cell, the parameter most affected by an increase in temperature is the open-circuit voltage. The impact of increasing temperature is shown in the figure below.

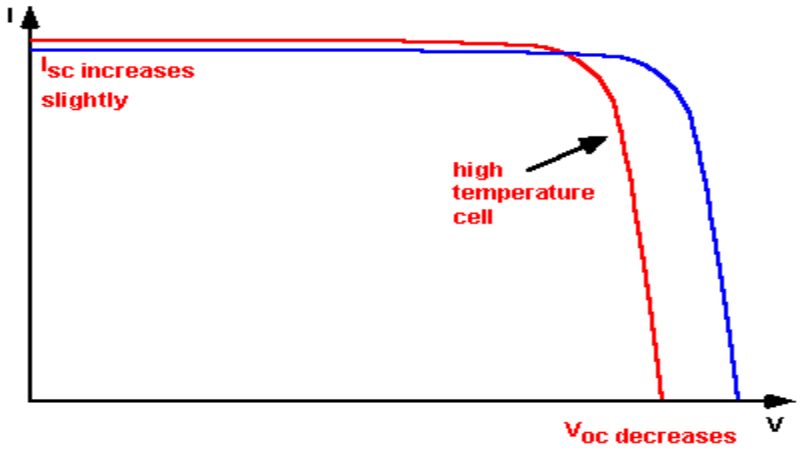

Figure 2.10: The effect of temperature on the IV characteristics of a solar cell.

The open-circuit voltage decreases with temperature because of the temperature dependence of I_0. The equation for I_0 from one side of a *p-n* junction is given by;

$$I_o = qA\frac{Dn_i^2}{LN_D} \quad \text{.....Equation 17}$$

where:

q is the electronic charge

A is the area;

D is the diffusivity of the minority carrier given for silicon as a function of doping

L is the minority carrier diffusion length;

N_D is the doping; and

n_i is the intrinsic carrier concentration

In the above equation, many of the parameters have some temperature dependence, but the most significant effect is due to the intrinsic carrier concentration, n_i. The intrinsic carrier concentration depends on the band gap energy (with lower band gaps giving a higher intrinsic carrier concentration), and on the energy which the carriers have (with higher temperatures giving higher intrinsic carrier concentrations). The equation for the intrinsic carrier concentration is;

$$n_i^2 = 4\left(\frac{2\pi kT}{h^2}\right)^3 * (m_e m_h)^{\frac{3}{2}} * e^{\left(-\frac{E_{GO}}{kT}\right)} = BT^3 e^{\left(-\frac{E_{GO}}{kT}\right)} \quad \text{.....Equation 18}$$

where:

T is the temperature;

h and k are constants

m_e and m_h are the effective masses of electrons and holes respectively;

E_{GO} is the band gap linearly extrapolated to absolute zero; and

B is a constant which is essentially independent of temperature.

Substituting these equations back into the expression for I_0, and assuming that the temperature dependencies of the other parameters can be neglected, gives;

$$I_o = qA\frac{D}{LN_D}BT^3 * e^{\left(-\frac{E_{GO}}{kT}\right)} \approx B'T^{\gamma} e^{\left(-\frac{E_{GO}}{kT}\right)} \quad \text{.....Equation 19}$$

where B' is a temperature independent constant. A constant, γ is used instead of the number 3 to incorporate the possible temperature dependencies of the other material parameters. For silicon solar cells near room temperature, I_0 approximately doubles for every 10 °C increase in temperature.

The impact of I_0 on the open-circuit voltage can be calculated by substituting the equation for I_0 into the equation for V_{oc} as shown below;

$$V_{oc} = \frac{kT}{q}\ln\left(\frac{I_{sc}}{I_o}\right) = \frac{kT}{q} lnI_{sc} - \frac{kT}{q} lnB'T^{\gamma} e^{\left(-\frac{E_{GO}}{kT}\right)} \quad \text{Equation 20}$$

$$\therefore V_{oc} = \frac{kT}{q} lnI_{sc} - lnB' - \gamma lnT + \frac{qV_{GO}}{kT} \quad \text{Equation 21}$$

where $E_{G0} = qV_{G0}$. Assuming that dV_{oc}/dT does not depend on $dI_{sc}/dT, dV_{oc}/dT$ can be found as;

$$\frac{dV_{oc}}{dT} = \frac{V_{oc} - V_{GO}}{T} - \gamma\frac{k}{q} \quad \text{Equation 22}$$

The above equation shows that the temperature sensitivity of a solar cell depends on the open circuit voltage of the solar cell, with higher voltage solar cells being less affected by temperature. For silicon, E_{G0} is 1.2, and using γ as 3 gives a reduction in the open-circuit voltage of about 2.2 mV/°C;

$$\frac{dV_{oc}}{dT} = -\frac{V_{GO} - V_{oc} + \gamma\frac{k}{q}}{T} \approx -2.2mV\ per\ ℃\ for\ Si \quad \text{Equation 23}$$

The short-circuit current, I_{sc}, increases slightly with temperature, since the band gap energy, E_G, decreases and more photons have enough energy to create e-h pairs. However, this is a small effect and the temperature dependence of the short-circuit current from a silicon solar cell is;

$$\frac{1}{I_{sc}} * \frac{dI_{sc}}{dT} \approx 0.0006\ per\ ℃\ for\ Si \quad \text{Equation 24}$$

The temperature dependency FF for silicon is approximated by the following equation;

$$\frac{1}{FF} * \frac{dFF}{dT} \approx \frac{1}{V_{oc}} * \frac{dV_{oc}}{dT} - \frac{1}{T} \approx -0.0015\ per\ ℃\ for\ Si \quad \text{Equation 25}$$

The effect of temperature on the maximum power output, P_m, is;

$$P_{Mvar} = \frac{1}{P_M} * \frac{dP_M}{dT} = \frac{1}{V_{oc}} * \frac{dV_{oc}}{dT} + \frac{1}{FF} * \frac{dFF}{dT} + \frac{1}{I_{sc}} * \frac{dI_{sc}}{dT} \quad \text{Equation 26}$$

Where;

$$\frac{1}{P_M} * \frac{dP_M}{dT} \approx -(0.004\ to\ 0.005) per\ ℃\ for\ Si \quad \text{Equation 27}$$

2.4.6 Effect of Light intensity

The change in the light intensity incident on a solar cell changes the short-circuit current, the open-circuit voltage, the Fill Factor (FF), the efficiency and the impact of series and shunt resistances. The light intensity on a solar cell is called the number of suns, where 1 sun corresponds to standard illumination at AM1.5, or 1 kW/m^2. A PV module designed to operate under 1 sun conditions is called a "flat plate" module while those using concentrated sunlight are called "concentrators".

Under concentration, V_{oc} increases logarithmically with light intensity, as shown in the equation below;

$$V'_{oc} = \frac{nkT}{q}\ln\left(\frac{XI_{sc}}{I_o}\right) = \frac{nkT}{q}\left[\ln\left(\frac{I_{sc}}{I_o}\right) + lnX\right] = V_{oc} + \frac{nkT}{q}lnX \quad \text{.....Equation 28}$$

where X is the concentration of sunlight.

From the equation above, a doubling of the light intensity (i.e. X=2) causes 18 mV rise in V_{OC}.

According to (Cotal, et al., 2009), concentrating PV system is cheaper than a corresponding flat-plate PV system since you only require a small area of solar cells. The efficiency benefits of concentration may be reduced by increased losses in series resistance as the short-circuit current increases and also by the increased temperature operation of the solar cell. As losses due to short-circuit current depend on the square of the current, power loss due to series resistance increases as the square of the concentration.

Low Light Intensity

According to (Kim, et al., 2007), solar cells experience daily variations in light intensity, with the incident power from the sun varying between 0 and 1 kW/m^2. When light intensity decreases, the bias point and current through the solar cell also decreases, and the equivalent resistance of the solar begin to approach the shunt resistance. When these two resistances are similar, the fraction of the total current flowing through the shunt

resistance increases, thereby increasing the fractional power loss due to shunt resistance. Consequently, under cloudy conditions, a solar cell with a high shunt resistance retains a greater fraction of its original power than a solar cell with a low shunt resistance.

Air Mass

As defined by (Duffie & Beckman, 2006), Air Mass (AM) is the path length which light takes through the atmosphere normalized to the shortest possible path length (that is, when the sun is directly overhead). The Air Mass quantifies the reduction in the power of light as it passes through the atmosphere and is absorbed by air and dust. The Air Mass is defined as:

$$AM = 1\cos(\theta) \quad \text{Equation 29}$$

where θ is the angle from the vertical (zenith angle). When the sun is directly overhead, the Air Mass is 1.

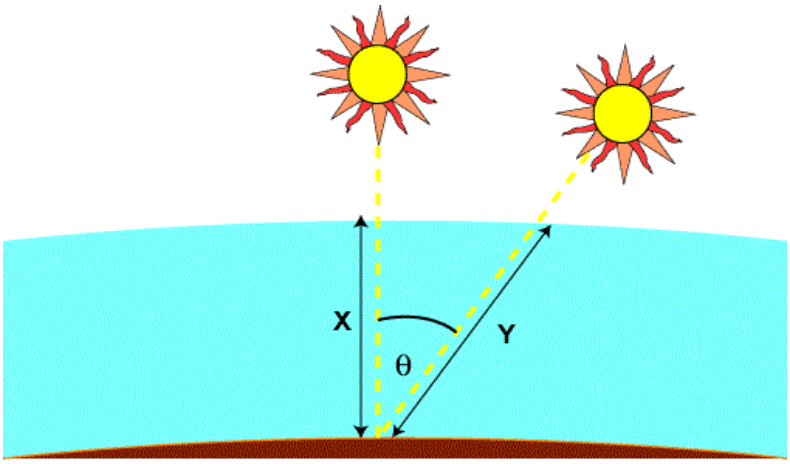

Figure 2.11: Air mass

From the figure above, the air mass represents the proportion of atmosphere that the light must pass through before striking the Earth relative to its overhead path length, and is equal to Y/X.

2.5 PV Inverters

The photovoltaic cells produce Direct Current (DC) power. However, this cannot be fed directly into the utility grid. The utility grid in Zimbabwe uses Alternating Current (AC) for transmission and distribution of electricity. Therefore, the inverter is essential for converting the DC power from the PV modules with the required output voltage and frequency by the inverter, making it ready to be used by electrical appliances or exported to the electrical grid.

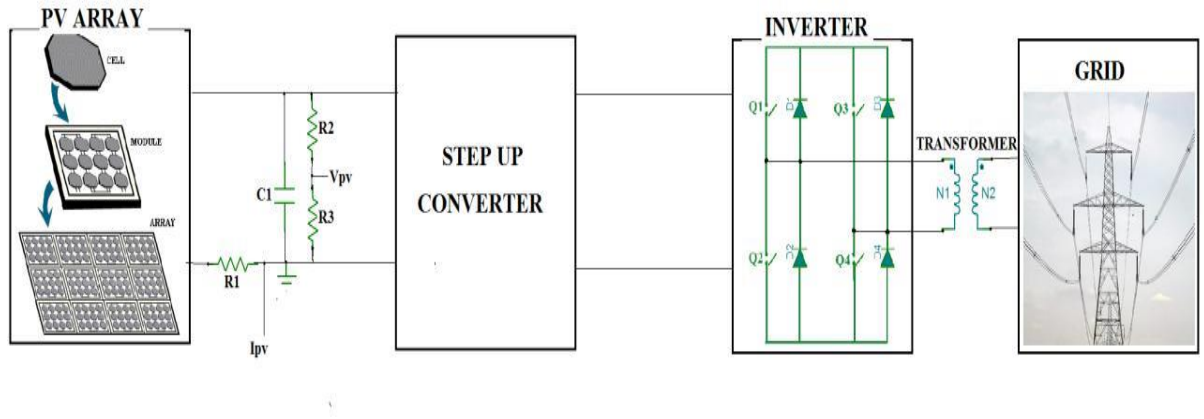

Figure 2.12: Ideal circuit of single phase grid connected inverter

Figure 2.13 shows the equivalent circuit of a single-phase full bridge inverter connected to utility grid. When the PV array provides small amount DC power it is fed to the step-up converter. The step-up converter then boosts the PV array's output power and then feed to the inverter block. The inverter converts DC into AC with the help of the Pulse Width Modulation (PWM) gate switching pulses.

2.5.1 Grid – connected Inverters

There are two main types of inverters on the market which are Grid-connected and Stand-Alone inverters. the grid-connected inverter uses a grid sensing device and a digital signal processor (DSP) to ensure the inverter has a grid to connect to and "copy" its voltage amplitude and frequency as illustrated in. This is to ensure the grid-connected inverter produces exactly the same voltage and frequency as available on the grid, this is also known as "grid-compatible sine wave AC electricity". If the grid sensing device in Figure 2.14 does not find the voltage and frequency to copy, then switches in the inverter will disconnect it from the grid.

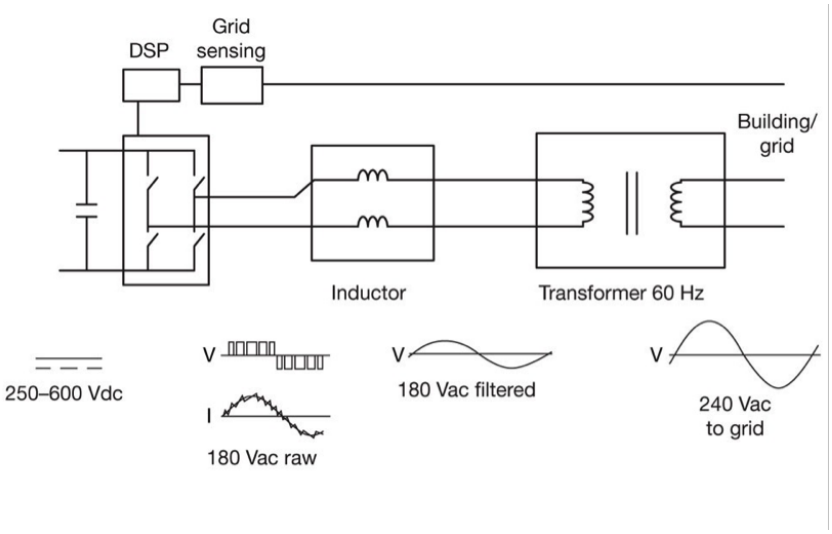

Figure 2.13: The basic topology of a grid connected, single phase, transformer-based inverter

2.5.2 Maximum Power Point Tracking (MPPT)

To keep the output efficiency of the inverter as high as possible, grid-connected inverters normally use Maximum Power Point Tracking (MPPT) so the inverter can operate near the maximum power point. The MPPT is an electrical system, which uses several different module electrical operating points to optimise the module performance. The tracker searches for the array's MPP at some specific times of the day to ensure that the environmental conditions have not moved the MPP [3]. The basic principle of the MPPT algorithms is the use of $P/V = 0$ (from $P = I*V$) to find the array output MPPT. The algorithm measures both P and V to find the array's momentary operating region and is using this when increasing or decreasing $V_{Reference}$. By doing this, the MPPT algorithm ensures that the PV system operates by the MPP of the array at all-time. This method can, however, not track the MPP under rapid and instant changes in irradiance conditions. A more complex method called" the incremental conductance method" is an alternative but will only be mentioned in this thesis.

2.5.3 Power Rating of Inverters

Depending on how large the PV array the customer wants to connect to a single inverter, different types of inverters are then developed for the market according to their power ratings. This varies from small modular inverters (micro inverters in AC PV modules) to large PV-inverters generating 100 kW or more.

2.5.4 Central Inverters

According to (Stapleton, et al., 2010), central inverters are inverters normally used in large grid connected PV systems with a power rating from 30 kW to 1 MW. The main advantage of this system is that all the components are located at one location for maintenance, good inverter efficiency and relatively lower cost per Watt.

2.5.5 String Inverters

A string inverter is the most common inverter used in small grid-connected PV-systems. Some string inverters can serve up to two or three strings of PV modules, with an inverter power rating from 1kW to 12kW. However, with a single MPPT it is recommended to use a multi-string inverter for arrays over 5kW. The downside of having multiple strings in one string inverter is that only one MPPT is installed in each inverter. If one string is shaded then this will affect the output of the entire array, instead of just one string. Individual string inverters for each string could be an alternative but would also be costly. As illustrated in Figure 2.15, PV arrays based on string inverters are more flexible than PV arrays based on central inverters since they are both easier and cheaper to extend.

2.5.6 Multi String Inverters

The multi string inverter is an improvement of the string inverter where multiple MPPT's can be installed in one inverter. Multiple strings can then be controlled independently and the array can be easily extended, providing high efficiency without any troubles for the customer. The multi string inverter is, however, more expensive than a string inverter because of the multiple MPPTs. One of the increased costs is the installation of extra DC protection in each string when multiple strings are using one DC – AC inverter.

2.5.7 Modular Inverters (Micro inverters in AC-Modules)

The modular inverters only need to convert 100-300 W and are therefore very small. The transformer-less inverter is connected to the back of each module in the array, next to the junction box as a separate module or integrated into the junction box. The advantage of using this inverter is the removal of DC cabling in the array connections. DC cables can carry higher voltages than AC cables, which will have lower voltages but higher currents. AC cables with larger cross section area and a wider isolation is therefore needed. Like in Figure 2.15, cables from AC-modules are connected together in parallel and then fed into the utility grid as a single phase. An array with modular inverters can easily be extended in the future by adding more modules. One disadvantage is if the modular inverter breaks down or need to be serviced, the whole module needs to be removed for it to be fixed. However, this could be compensated by better design for serviceability. The micro inverter is also very expensive compared to other inverters in terms of cost per power rating. It also produces more harmonics, which reduces the power quality and because of demanding grid codes could make it harder to be approved for grid connection. It would also be more challenging and costly to integrate an array with micro inverters in smart grids, because a communication cable must be added to each PV module.

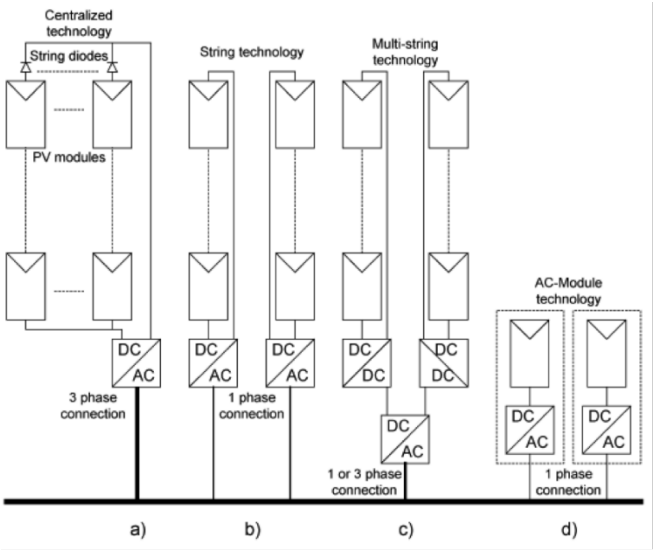

Figure 2.14: An overview of the different inverter options: a) Central inverter, b) String inverter, c) Multi string inverter, d) Modular inverter.

2.6 Grid connection

Zimbabwe Electricity Transmission and Distribution Company, (ZETDC) has the sole responsibility for operating, maintaining and ensuring the power quality in the grid. The grid application in Zimbabwe is regulated by ZERA who regulates any person or private companies that operate an electricity undertaking which generates, transmit, distributes, or retail electricity for commercial purposes in excess of 100Kilowatts (kW). The documentation can be found on http://www.zera.co.zw/index.php/electricity/electrcity-page.

2.6.1 Islanding

Islanding is a critical phenomenon and is at the time not wanted on the utility grid. It occurs when the PV system keeps on feeding electrical power to a utility grid that is isolated from its utility voltage source. The utility grid can be isolated when a grid and a PV-inverter are separated by accident, on purpose or by damage, (Kjaer, et al., 2005). This is usually divided between wanted- and unwanted islanding, where wanted islanding occurs when renewable energy sources are connected to make a micro grid as shown in Figure 2.18. During islanding, this micro grid is isolated from the utility grid and the renewable sources are used to power it. This micro grid is then called an island.

Unwanted islanding can present a high risk for utility workers maintaining the grid as well as causing unwanted incidents on the utility grid. Utility workers arriving to do scheduled maintenance work somewhere on the isolated island might think that it is not energised since the switch (showed as CB1 in Figure 2.18) has to be manually disconnected. Just a few tens of seconds would be lethal if utility workers had commenced maintenance work on the grid immediately after the switch (CB1) was disconnected. Even though the grid is manually disconnected from the micro grid, local production units can produce power a few more seconds until the grid-sensing device cannot find the grid, or until the inverter anti islanding device kicks in. The AC switches (CB1 and CB2) should therefore have an indicator on each side, indicating if AC power is present or not, and to clarify this by an alarm or a light.

Figure 2.18 is an example where the local production unit is the micro grid. PCC is the Point of Common Connection where the micro grid is connected to the main grid, CB1 is the circuit breaker between the main grid and the micro grid and CB2 is the AC circuit breaker between the grid connected inverter and the grid it is connected to. In situations where the PV system is placed on the roof, the PCC is situated in the house switchboard

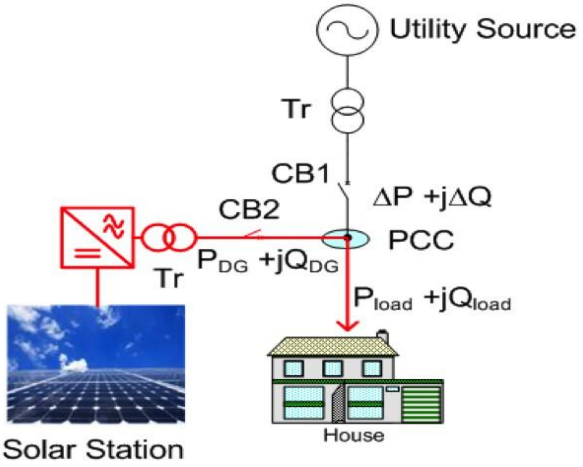

Figure 2.15: Solar station disconnected from the utility grid, and operating as an isolated island

where the power Pload + jQload is supplied to the house and a Pload + jQload is supplied through a smart meter to the main grid. CB1 is still the circuit breaker connecting or disconnecting the main grid to the micro grid. In cases where the grid needs to be disconnected for maintenance, the switch CB2 must be disconnected prior to

disconnecting CB1, and connected after CB1 to avoid islanding. It must, therefore, be possible to remotely control the inverter so this can be done directly by the utility company. Many inverters now have communication terminals e.g. CAN interface (Controller Area Network) that are intended for smart grids or to communicate between a master and several slave inverters. This allows many local PV or Wind production units to supply a micro grid and be remotely operated by the local utility company.

2.6.2 Grid Integration

The transmission grid is changing and becoming more complex to manage and more utilities globally are experiencing grid challenges such as:

i) Increase in global demand for electricity
ii) Thermal plant retirements coupled with an increase in renewable generation, often remote from load centres
iii) Stringent requirements by regulatory authorities on power quality
iv) Interconnected grids and
v) Ageing transmission infrastructure

These challenges can make power flow stability more complex for network operators to manage with stability issues under fault clearing and post-fault conditions. The increase in load demand and renewable integration combined with ageing infrastructure can cause voltage on the grid to fluctuate. The grid also experiences other issues including harmonics, flicker phenomena, unbalanced loads and power oscillations which can impact power quality and power transfer capability. Additionally, the ability to implement a more flexible solution is highly desired as utilities today are facing a highly dynamic grid, which requires solutions that can accommodate more drastic changes than in the past.

The Static Synchronous Compensator (STATCOM)

The solution is a custom designed system to be installed on transmission grids. It provides grid operators with reactive power compensation and improved range of operational voltage with a faster response time and a smaller footprint than traditional Static Var Compensator (SVC) solutions. A shunt connected STATCOM system is able to generate capacitive or inductive output current independent of the AC system voltage. STATCOM solutions can help utilities achieve the following:

i) Increase system stability and power quality by providing:
   - Voltage control and support
   - Reactive power control
   - Power oscillation damping
   - Power transfer capacity increase

ii) Grid code compliant renewable integration by providing:
   - Fault ride through support
   - Voltage control and support

Key features of the STATCOM system include:

i) Usually connected to High Voltage (HV) grid via a step down power transformer
ii) Always a symmetrical power rating in the inductive and capacitive operating regions
iii) Hybrid STATCOM solutions available for increased power rating including: -- Thyristor Switched Components,
iv) Mechanically Switched components -- or Static Var Compensator (SVC)
v) Reduced footprint compared to a classical SVC solution

The diagram below shows a typical arrangement of the SVC System

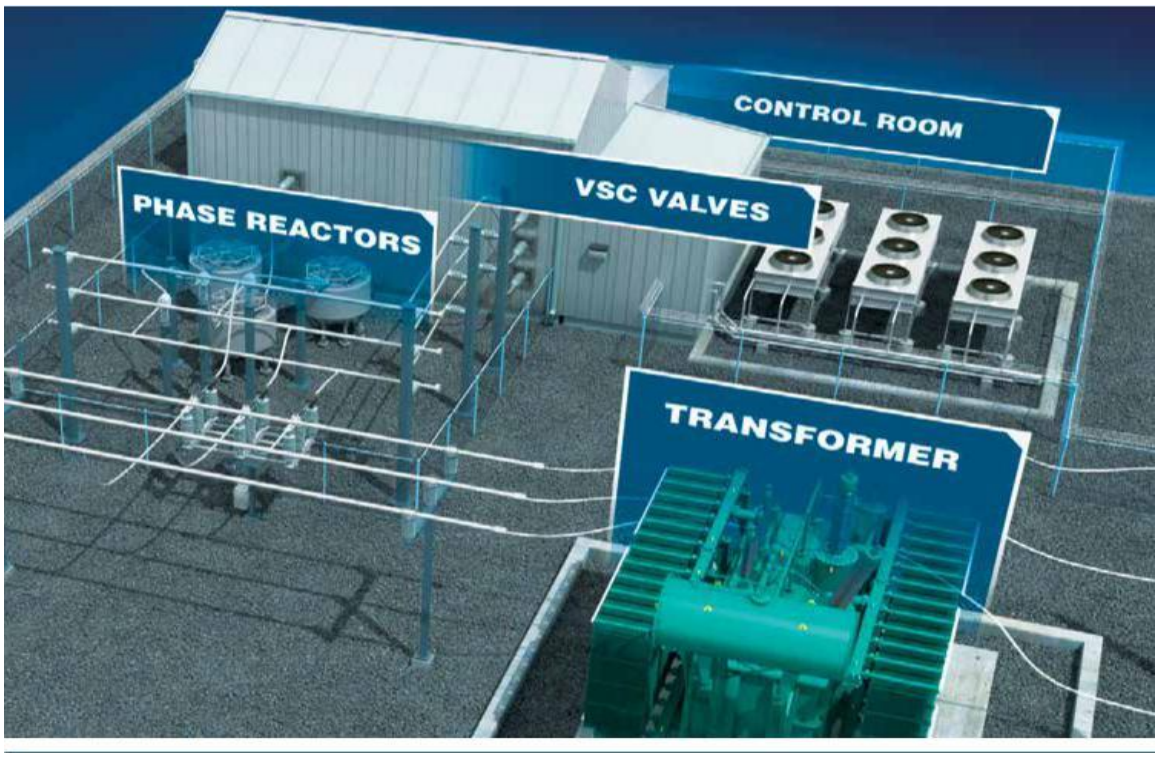

Figure 2.16: Typical arrangement of the SVC System

2.6.3 Compensation Principle of Static Synchronous Compensator (STATCOM)

Static Synchronous Compensators (STATCOM) consist of a voltage source converter (VSC) connected to the grid by phase reactors and a step-up transformer. STATCOMs use Insulated Gate Bipolar Transistors (IGBT) in a modular multi-level converter (MMC) configuration. The STATCOM generates or absorbs reactive power by producing a controlled voltage waveform.

The STATCOM system is shunt connected to the transmission grid. There are Voltage Transformers (VTs) in the STATCOM that measure the voltage of the grid. The Advanced Digital Control (ADC) takes the VT input and controls the individual sub-modules, so that they produce a voltage waveform that is either:

i) The same as the system, when there are no grid issues

ii) Lower in magnitude than the system, making the STATCOM act as an inductive device and absorbing reactive power from the grid

iii) Higher in magnitude than the system, making the STATCOM act as a capacitive device and generating reactive power to the grid

Ultimately the STATCOM continually monitors the grid voltage and constantly adjusts its reactive power output in response to system disturbances and thus improves grid stability

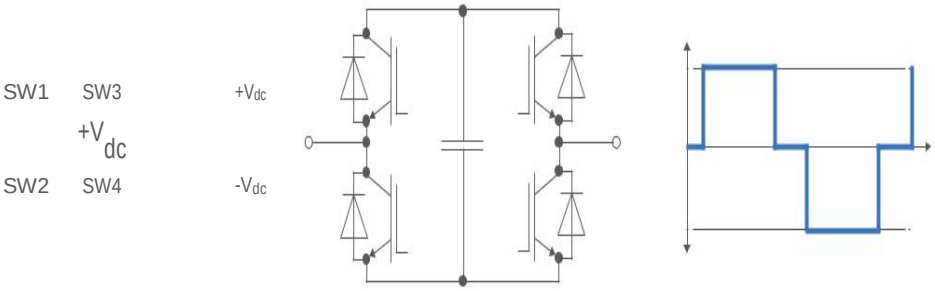

Figure 2.17: Typical full bridge valve sub-module and its output waveform

Figure 2.20 above illustrates how the controlled switching of the IGBT valves in a single sub-module creates the basic three-level waveform that the STATCOM uses to control the reactive power contribution to the grid. When multiple such sub-modules are connected in series, as shown in Fig. 2.21, it can be seen that how the voltage waveform can be built up with better resolution to deliver improved performance, higher rating and enhanced controllability of the STATCOM.

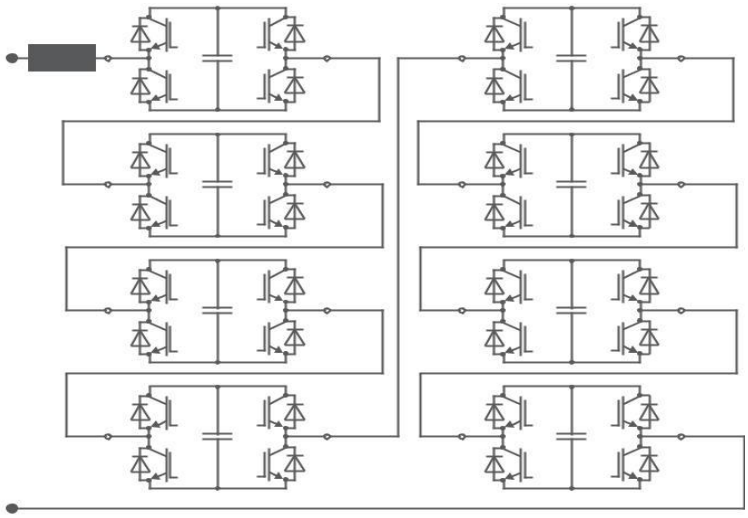

Figure 2.18: Multiple sub-module operation and resulting waveform

2.7 Feed-in Tariff

According to (Couture, et al., 2010) , a feed-in tariff (FIT) is an energy supply policy that promotes the rapid deployment of renewable energy resources. A FIT offers a guarantee of payments to renewable energy developers for the electricity they produce. Payments can be composed of electricity alone or of electricity bundled with renewable energy

certificates. These payments are generally awarded as long-term contracts set over a period of 15-20 years.

FIT policies can be implemented to support all renewable technologies including wind, Photovoltaics (PV), Solar thermal, Geothermal, Biogas, Biomass, Fuel cells, Tidal and wave power. As long as the payment levels are differentiated appropriately, FIT policies can increase development in a number of different technology types over a wide geographic area. At the same time, they can contribute to local job creation and increased clean energy development in a variety of different technology sectors.

Benefits of FIT policies

The benefits and impacts of FIT policies include:

i) The rapid renewable energy development seen in jurisdictions with FIT policies has helped reduce the environmental impacts of electricity generation, while providing valuable air quality and other environmental benefits.

ii) Fixed prices created by FITs for renewable energy sources can also help stabilise electricity rates which can entice new business and attract new investment.

iii) Due to the guaranteed terms and low barriers to entry offered by FIT policies, they have been highly successful at driving economic development and job creation.

iv) Data from countries like Germany and Spain demonstrate that well-designed FIT policies can positively impact job creation and economic growth. A growing body of evidence from Europe and Ontario, Canada demonstrates that FIT policies have on average fostered more rapid RE project development than other policy mechanisms.

Implementation Issues

Despite the many benefits, FIT policies pose a few challenges as well.

i) FIT policies do not address the barrier posed by the high up-front costs of RE systems, in contrast to rebate programs and other up-front "capacity-based" incentives. FIT policies are designed to offer stable revenue streams through long-term purchase contracts, requiring that the high up-front costs be amortized over a long period of time.

ii) Well-designed FIT policies require a significant up-front administrative commitment to design the policy and to establish FIT payments based on the levelised cost of

renewable energy generation. Detailed analyses on technology cost and resource quality are needed to ensure FIT payments are adequate to guarantee cost recovery without leading to windfall profits.

iii) FIT policies designed to include guaranteed grid interconnection, regardless of location on the grid, could lead to less-than-optimal project siting. Accordingly, if projects are sited far from load centers or transmission or distribution lines, interconnection costs increase. This puts upward pressure on policy costs. However, this challenge can be largely overcome if FIT policies encourage siting projects near load centers by creating an incentive—either a bonus or a higher price based on higher spot-market prices—or if the policies require developers to bear a portion, if not the entirety, of the costs of grid connection.

iv) Due to changes in technology costs and market prices over time, FIT policies must be adjusted periodically to account for these changes. Accounting for changes in technology costs accurately remains a challenge. Changing payment levels too often can be undesirable as well, as it creates investor uncertainty and increases overall market risk. One way to resolve this issue is to adjust the policy through a tariff degression, where the FIT payments decline by a pre-determined percentage each year. This can be coupled with periodic policy adjustments that occur every several—three to four—years. To be successful, these adjustments require a detailed methodology to track market changes effectively from year to year. Ultimately, the challenge is to provide a flexible policy framework without jeopardizing investor confidence.

Design Best Practices

Many successful FIT policies base the prices offered to suppliers on the levelized cost of renewable energy generation to ensure a reasonable rate of return. Other design best practices include:

i) Offering long-term, must-take contracts

ii) Differentiating FIT prices by technology type, project size, and resource quality

iii) Including a design feature that incorporates an incremental decrease in the FIT prices over time to encourage innovation and accelerate the pace of deployment

iv) Incorporating the costs of the policy into the electricity rate base

v) Minimizing transaction costs by providing streamlined administrative procedures.

2.8 Net- metering

Net-metering, in essence, allows small scale renewable energy power producers to "bank" or "store" their electricity in times of over-production (e.g. for solar energy during peak production in the day) in the national grid, and to balance out their grid consumption with this banked or stored electricity during other times (e.g. during night, morning and evening hours).

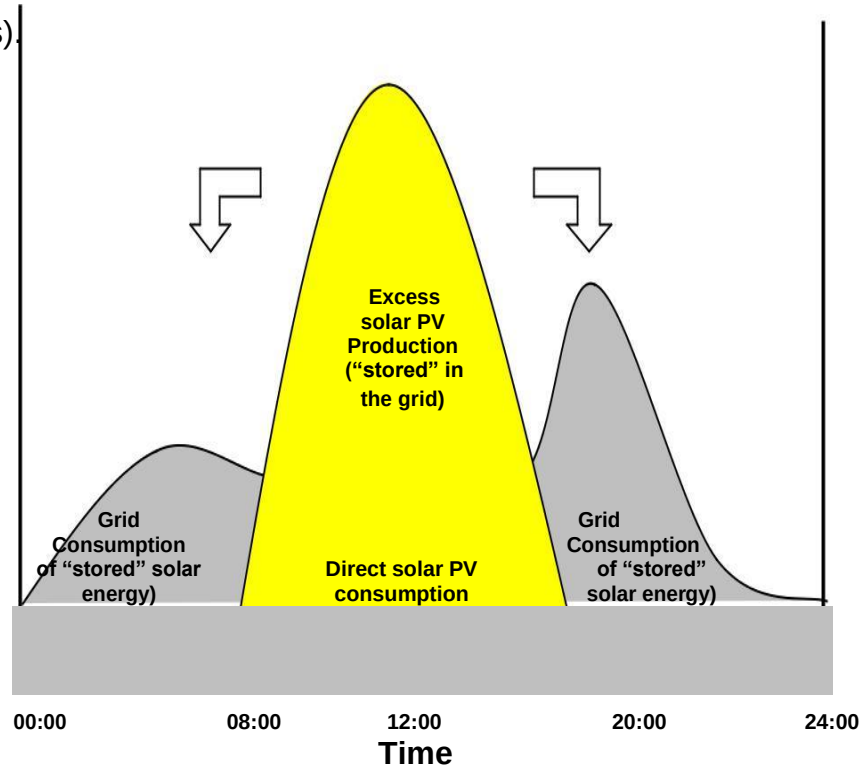

Figure 2.19: Principle of PV electricity production and daily demand

The system in theory offers a wide range of advantages as listed below:

i) There is generation of additional power in the national grid, without the need for investment by the utilities or conventional IPP's

ii) There is promotion of small scale investments, value addition and market development

iii) There is no direct payment by the grid operator (as opposed to a FIT)

iv) There is consumer savings on power bills

However, there are some issues for the grid operators like the technical feasibility of grid connection and impact on grid stability, revenue loss for the grid operator and potential compensation mechanisms and other direct and indirect benefits for the grid operator.

2.9 Net Metering or Feed-in-Tariffs

The success story of grid connected PV is largely based on Feed-in-Tariffs (FiT). More countries have opted towards that option. Net-metering is a different regulatory instrument, which will open up a different market segment with different project types and regulatory requirements. Even before FiTs were widely introduced, net-metering was actively practiced by PV installers in many countries including Germany. Net-metering continues to be a driver of emergent PV industries where Governments do not support consumer FiTs (i.e. in many US states). In the following table both instruments pros and cons are presented.

Table 2.1: Strengths and weaknesses of net-metering versus Feed-in Tariff

	Feed-in tariff FIT	**Net metering**
	Key elements:	**Key elements**
Strengths	Strong security of investment, both for project developers as well as for financiers	Very easy to set-up and implement
	Everyone can invest, including the utilities themselves	Minimal administrative effort for the utility
	Can be tailored and refined in order to channel investment into desired subsectors and project types	Can also tap the market segments for power generation below the project sizes suitable to the FiT, and thereby leverage otherwise wasted natural/domestic resources
		No actual payments by the utility and little risk of deceptive practices.
Weaknesses	Perception of FiT as a subsidy, even if it designed as a surcharge to all consumers	Not fair to all consumer classes - higher incentive and economic

		attractiveness for consumers with higher tariffs
	Extra metering is required, which should be registered by remote sensing monthly (otherwise there must be monthly down-payments and annual control)	Does not provide very strong security of investment due to the (at least theoretical) possibility of fluctuating end-user tariffs
	Relatively complex regulatory instrument, requiring close management in order to effectively leverage investment while avoiding market distortions	

CHAPTER 3

METHODOLOGY

3.0 Methodology

This chapter will detail the methodology followed in designing the grid connected PV system. The design methodology is basing on creating an optimum design of a grid connected PV system basing on the available land area of 42hactares at the project size. It will also take into consideration the economic viability of the designed system. The main software used for the system design is PVsyst software.

The first step in the software is to input the geographical coordinates of the site and then load the meteorological data of the area.

3.1 Module spacing

There is need to determine the optimum spacing for the modules so as to minimise losses due to shading and also enable maintenance teams to access the modules at the same time maximising the amount of area available. The module spacing was calculated using the following methodology as detailed by Hove in (Hove, 2004).

With designed panel inclination (β), minimum altitude angle (α), and panel length (L), the row spacing (S), L_s is the shaded part of the panel, θ_z is the zenith

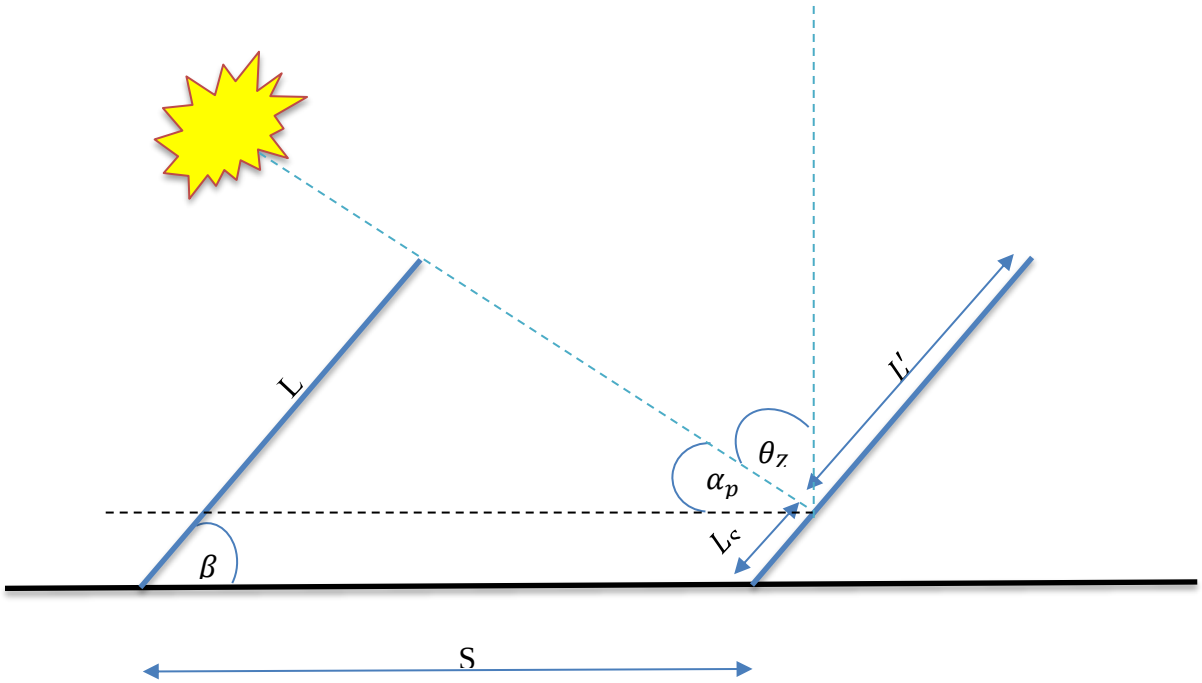

Figure 3.1: Side view of tilted PV-array showing the minimum altitude angle and other dimensions

The following procedure for determining the minimum fraction of L_s/L can be determined by trial and error using the following steps:

i) Input the latitude of the area, the length of panel, L, the time of the day, t, the day number, n,

ii) Calculate the hour angle, (ω)

$$\omega = 15° * (t - 12) \quad \text{.....Equation 30}$$

Where *t* is the time of day

iii) Calculate the declination angle (δ) from approximate equation of (Cooper, 1969)

$$\delta = -23.45Sin(360\frac{284+n}{365}) \quad \text{.....Equation 31}$$

iv) Calculate the zenith angle from θ_s

$$Cos\theta_z = Cos\varphi Cos\delta Cos\omega + Sin\varphi Sin\delta \quad \text{.....Equation 32}$$

v) Calculate solar azimuth angle, γ_s

$$\gamma_s = sign(\omega)\left|\cos^{-1}\left(\frac{\cos\theta_z \sin\varphi - \sin\delta}{\sin\theta_z \cos\varphi}\right)\right| \quad \text{Equation 33}$$

vi) Calculate solar altitude angle, α_s

$$\alpha_s = 90 - \theta_z \quad \text{Equation 34}$$

vii) Calculate solar profile angle, α_p

$$\tan\alpha_p = \frac{\tan\alpha_s}{\cos(\gamma_s - \gamma)} \quad \text{Equation 35}$$

viii) Calculate the fraction L_s/L from (Hove, 2004)

$$\frac{L_s}{L} = 1 - \frac{S}{L}\frac{\tan\alpha_p}{sin\beta + \tan\alpha_p tan\beta} \quad \text{Equation 36}$$

3.2 Array Sizing

When designing a grid-connected PV system the properties of both the chosen PV module type and the chosen inverter type have to be taken into account. In order to produce at optimal power output, the array has to be matched to the inverter. The following methodology was used in the PVsyst design software:

i) Determining the optimum tilt angle

The researcher chose seasonal tilt angle adjustment. To determine the optimum tilt angles for the two seasons, the researcher first selected fixed tilt and determine the tilt angle that will produce maximum energy yield for Winter and then do the same for Summer. These angles were then inputted for the seasonal tilt angle adjustment.

ii) System design

- The design is based on the land size sizing and hence using Equation 43, the ground area covered by the collectors can be determined. This was then used to determine the area covered by the collectors in the design. Also to take note, there are some other equipment like inverters, transformers, junction boxes and the substation which are competing for the same area. Hence the design methodology was then based on collector area of 20 hectares.

- The module sizes were then selected basing on the maximum available on the market to minimise on the land covered and maximise on the energy output.

iii) Inverter selection

- The methodology for inverter size commenced by determining the desired nominal inverter power, Pnom. According to (Kjaer, et al., 2005), the PnomAC= 6% PnomDC.
- Then can now determine the feasible inverter size basing on the desired PnomAC. Due to the size of the system a maximum possible inverter is chosen. Each inverter will be paired with a transformer in the field.

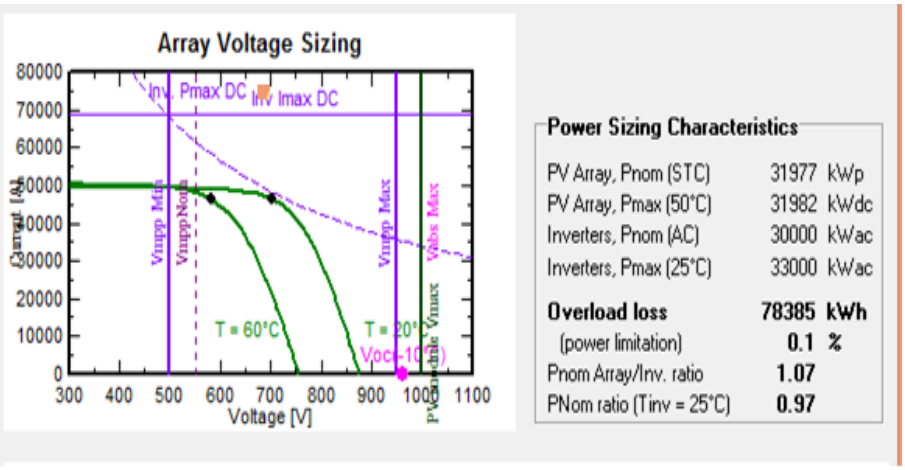

Figure 3.2: Array/Inverter Sizing conditions

The following conditions have to be met for the array and inverter matching:

- Maximum array operating output voltage in worst case scenario (i.e. at min. module operating temperature 20°C) should be lower than the max. V_{MPPT} of the inverter.
- Minimum array operating output voltage in worst case scenario (i.e. at max. module operating temperature 60°C) should be higher than the min. V_{MPPT} of the inverter.
- The absolute maximum array voltage in open circuit (i.e. V_{oc} at 10°C) should stay below the absolute maximum inverter´s input voltage.

iv) Horizon Shading

The horizon shading was measured at site with a compass at different azimuth.

3.3 Cable Sizing

The optimal cable sizing for the PV system methodology in this paper was based on (Maillo, 2013). A photovoltaic system array consists of a number of strings and these strings are connected in parallel to a junction box. In each string there are a number of PV modules connected in series. Therefore, for any given string in a PV array, the overall voltage of this string is the sum of the voltages of each module in the string. This voltage is the applied voltage at the level of junction box. It can be expressed as in the following Equation:

$$V = V_{mpp} * N_{modules} \quad \text{.....Equation 37}$$

Where:
$N_{modules}$ is the number of modules connected in series in a string and
V_{mpp} is the voltage of one module at maximum power point.
The current value of a string is same as the current value of one module, because in a string the modules are connected in series and uniform current flows. Therefore, for a number of strings connected in parallel per junction box, the current at the level of junction box is the sum of the current of each string connected to that junction box. It can be expressed by the following Equation:

$$I = I_{mpp} * N_{strings} \quad \text{.....Equation 38}$$

Where;
I_{mpp} is the current of a string at maximum power point.
$N_{strings}$ is the number of strings per junction box.
The maximum allowed voltage drop must be according to the installation standards. In Zimbabwe, the maximum allowed voltage drop between the PV array and inverter shall be less than 4% as per British Standard on Electrical Wiring Installations BS767. The resultant voltage from Equation (44) is multiplied by the maximum allowed percentage voltage drop ($\Delta V\%$) to get the voltage drop (ΔV) value.

Thus

$$\Delta V = 0.04V \quad \text{.....Equation 39}$$

The voltage drop value will be used in the following Equation (Maillo, 2013):

$$A = L * {}^{I}/_{\gamma} * \Delta V \quad \text{.....Equation 40}$$

Where:

A = Cross section area of the cable *(mm²)*.

L = Length of the cable *(m)*

I = Nominal Current *(Amps)*

γ = Conductivity of copper *(m/Ω. mm²).*

ΔV = Maximum voltage drop *(V).*

The result of Equation (47) represents the cable cross section area *(A)*, which is calculated according to maximum allowed voltage drop in (*mm²*).

It is important to note that, if the cable section, which has been resulted from the maximum allowed current calculations, is bigger than the cable section, which has been resulted from the maximum allowed voltage drop calculations, and vice versa, the bigger cable section must be selected, because the resulting cable section must fulfil both criteria maximum allowed current and maximum voltage drop standards.

3.4 Economic analysis

PVSyst software has the option of inputting the costs into the project. The costs were broken down into four main groups namely the Civil works, PV array field, grid connection and Transport. This was used to calculate the Levelised Cost of Electricity (LCOE). Another model from theory was also used to compare with the results from the software. The payback period and Internal Rate of Return was then calculated.

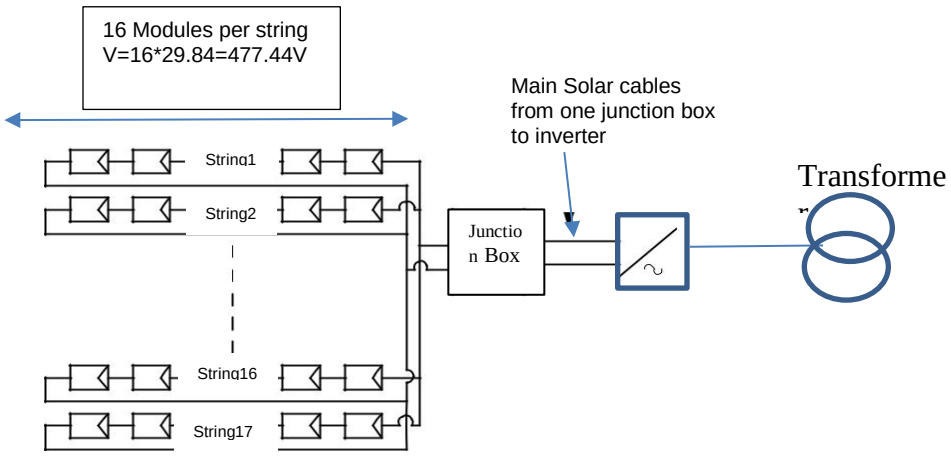

CHAPTER 4

DATA COLLECTION

4.0 Data collection

This chapter presents the data collection methods and the data which was used for the project.

The geographical site coordinates are Latitude -17.74° and Longitude 31.206°. The area reserved for the solar project is 42 hectares.

Horizon:

Table 4.1: Horizon Table

Azimuth	**Angle**
-120°	-10°
-40°	-5°
+40°	+5°
+120°	+10°

PVsyst uses Meteonom 7.1 which indicates the monthly meteorological data for the area as shown on Table 4.2 below:

Table 4.2: Ecosoft Zimbabwe Monthly Metreological Data

	Global Irradiation (kWh/m².day	*Diffuse (kWh/m².day*	*Temperature (°C)*	*Wind Velocity (m/s)*
Jan	*5.21*	*2.81*	*21.4*	*2.9*
Feb	*5.21*	*2.39*	*21.1*	*2.9*
Mar	*4.9*	*2.71*	*20.5*	*2.9*
Apr	*5.19*	*1.79*	*18.7*	*2.8*
May	*4.74*	*1.53*	*16.7*	*2.5*
Jun	*4.17*	*1.65*	*14.8*	*2.91*
Jul	*4.42*	*1.61*	*14.5*	*2.99*
Aug	*5.16*	*1.67*	*16.8*	*3.31*
Sep	*5.76*	*2.16*	*19.6*	*3.81*
Oct	*6.14*	*2.18*	*21.8*	*4*
Nov	*5.92*	*2.94*	*21.6*	*3.6*
Dec	*5.64*	*2.56*	*21.3*	*3.09*
Year	***5.21***	***2.17***	***19.1***	***3.1***

4.1 Climatological Data Relevant to Solar Power Production

Figure 4.1 shows the long-term monthly averages for solar global horizontal irradiance and irradiation incident on the plane of the collector for the project site. While Figure 4.2 and Figure 4.3 show the monthly average ambient temperature and wind speed at the site respectively.

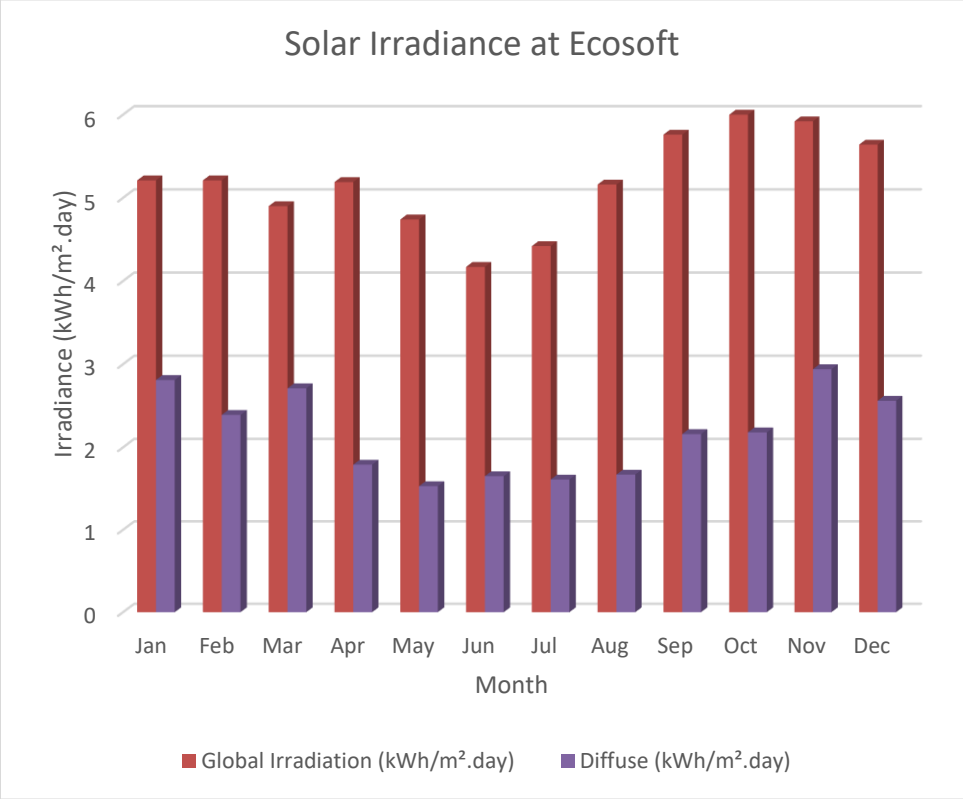

Figure 4.1: Solar irradiation at project site

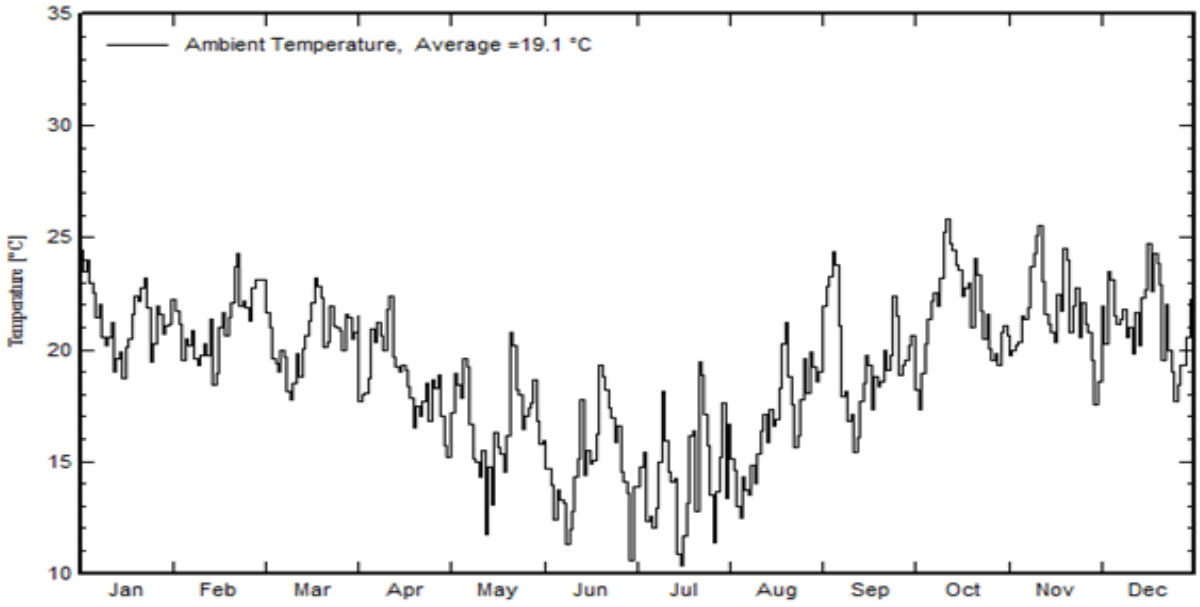

Figure 4.2: Monthly variation of ambient temperature

The monthly variation of wind speed for the area is as shown on Figure 4.3 below:

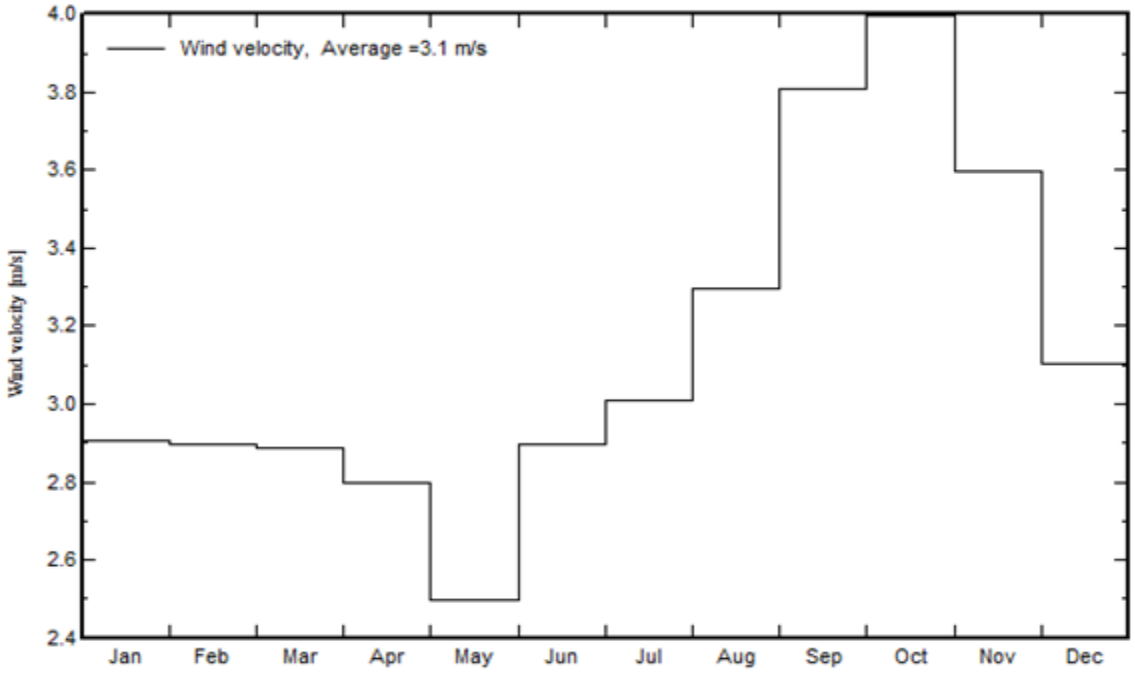

Figure 4.3: Monthly variation of wind speed

CHAPTER 5

DESIGN/ANALYSIS

5.0 Design/ Analysis

Many factors are involved in determining how the PV system should be designed, and then installed, these factors are explained and discussed in this chapter. This chapter detail the design of the Ecosoft PV system and the grid integration. This project uses PVsyst as the main software for the design of the PV system and Sincal Software for the grid impact study.

5.1 PVSyst

In their study conducted in SouthAfrica using the PVsyst software, (Okello, et al., 2015) found a good approximation made by the software to measured energy output for a 3.2kWp system. In light of this the author found it proper to select the particular software for design and optimization of the system for the location. The PVsyst software was developed by André Mermoud and Michel Villoz and is used for the study, sizing and data analysis of complete PV systems. It deals with grid-connected, stand-alone, and pumping PV systems. The software includes extensive met data and PV systems, components databases, as well as general solar energy tool.

Site Selection

The site is being selected based on the primary considerations of availability of land that is fully owned by the project proponent, TD Energy situated at located at latitude -17.74° and longitude 31.206°. The site is also conveniently located near a ZETDC electricity substation, which makes evacuation of power from the Solar PV Power Plant to the grid easy and low cost. According to (Hove & Gotsche, 1999), the average annual solar irradiation is 5.8 kWh/m^2/day or 6.0 kWh/m^2/day (according to the database Meteonom 7.1), is favourable for electricity generation on a year round basis.

5.2 Project Design

The first step is to define your project using the following steps:

Step 1: Definition of the project name and its associated comment.

Step 2: Definition of the **project site**

Step 3: Selection of a meteo file, in PVsyst format *. MET

Step 4: Definition of the project settings.

Step 5: Definition of the PV system in several "Variants" or "Calculation versions"

All calculation variants attached to the project will have the same project's name with extensions **.VC0,** .**VC1**, etc

5.3 Orientation

As highlighted in the literature in chapter 2, the orientation is key to the amount of energy produced by the system. Since the sun position changes throughout the day, the best option is to track the position of the sun to maximise on the system yield. However, this is very expensive and complicated. For the purposes of this project, two orientations adjustments were considered which are fixed tilt and seasonal tilt adjustment. The optimisation of the orientation depends on the planned use for the PV energy produced. In the case for grid-connected systems, the energy is usually sold at a constant price throughout the contract period and hence the relevant optimum is then to maximize the annual energy yield.

Option 1: Fixed tilted plane orientation

In PVsyst there is choice to maximise the Energy Yield with respect to Yearly irradiation yield, Summer or Winter yield. You have to define the tilt of the collector and azimuth for the area. The plane azimuth is defined as the angle between north and collector plane for Southern hemisphere. The angle is taken as negative towards East, i.e. goes in the trigonometric direction. This angle is 0° for the chosen site.

The Global Irradiation received on the collector is maximum at 23° i.e. φ + 5° for the yearly irradiation. The optimisation is with respect to the transposition factor (FT) and the Loss by respect to optimum. The transposition factor is the ratio of the incident radiation (GlobInc) on the plane, to the horizontal irradiation (GlobHor). Therefore, it entails the gain in tilting the collector plane. It is computed by applying the Hay or Perez transposition

model to horizontal hourly values. The table below shows the design considerations for fixed plane tilt option:

Table 5.1: Fixed plane tilt design considerations

Optimisation by respect to:	Plane Tilt	Azimuth	Transposition Factor	Loss by respect to Optimum	Global on collector Plane(kWh/m^2)
Yearly Irradiation Yield	23°	0°	1.07	0%	2030
Summer (Oct-Mar)	10°	0°	0.99	-1.0%	992
Winter (Apr-Sept)	40°	0°	1.26	-0.1%	1132

NB. Although the Summer plane tilt is optimum at 0°, a value of 10° was chosen for the plane tilt to cater for self-cleaning for the collector. This has minimum effect as can be noted from the loss by respect to optimum value of -1%.

Option 2 – Seasonal Tilt Adjustment

For this option, the plane tilt may be adjusted with two values, for winter and summer chosen months. The following parameters were selected:

Table 5.2: Seasonal Tilt Input Parameters

Summer tilt	10°
Winter tilt	40°
Azimuth	0°
Winter months	April-Sept
Summer months	Oct-Mar

From Table 5.2 above, it can be noted that optimising orientation with respect to Winter or Summer alone will result in reduced global irradiation received on the collector and hence the overall yield of the design. Therefore, the researcher chose Option 2 i.e. Winter and summer tilt adjustments.

5.4 Module Spacing

Table 5.3 below shows the results of the spacing between the modules as explained in Chapter 3. From the table it shows that there is minimum shading of the collectors all year round for a ground/collector area ratio of 2.

***Table 5.3: Module* shading profile (Ls/L)**

Time	Jan	Feb	Mar	Apr	May	Jun	Jul	Aug	Sep	Oct	Nov	Dec
6	0.1	0.1	0.1	0.1	1.0	1.0	1.0	1.0	0.1	0.1	0.1	0.1
7	0.0	0.0	0.0	0.0	0.1	1.0	1.0	1.0	0.0	0.0	0.0	0.0
8	0.0	0.0	0.0	0.0	0.0	0.4	0.4	0.0	0.0	0.0	0.0	0.0
9	0.0	0.0	0.0	0.0	0.0	0.0	0.0	0.0	0.0	0.0	0.0	0.0
10	0.0	0.0	0.0	0.0	0.0	0.0	0.0	0.0	0.0	0.0	0.0	0.0
11	0.0	0.0	0.0	0.0	0.0	0.0	0.0	0.0	0.0	0.0	0.0	0.0
12	0.0	0.0	0.0	0.0	0.0	0.0	0.0	0.0	0.0	0.0	0.0	0.0
13	0.0	0.0	0.0	0.0	0.0	0.0	0.0	0.0	0.0	0.0	0.0	0.0
14	0.0	0.0	0.0	0.0	0.0	0.0	0.0	0.0	0.0	0.0	0.0	0.0
15	0.0	0.0	0.0	0.0	0.0	0.0	0.0	0.0	0.0	0.0	0.0	0.0
16	0.0	0.0	0.0	0.0	0.0	0.4	0.4	0.0	0.0	0.0	0.0	0.0
17	0.0	0.0	0.0	0.0	0.1	1.0	1.0	1.0	0.0	0.0	0.0	0.0
18	0.1	0.1	0.1	0.1	1.0	1.0	1.0	0.1	0.1	0.1	0.1	0.1

5.5 System

The "system" as defined in PVsyst is a set of components constituting the PV-array, i.e. the PV modules, strings, inverter, up to the connection to the grid. The sizing was based on the available land area of 42hactres. Taking into consideration a Ground/Collector ratio of 2, a Module area of 20.6972ha resulted in a planned power of 31,977kWp.

The solar plant will consist of 106,590 solar PV modules, each with a rated power of 300Wp to give a total installed PV peak power of 31982kWdc. A GE Solar Module was selected with the following properties:

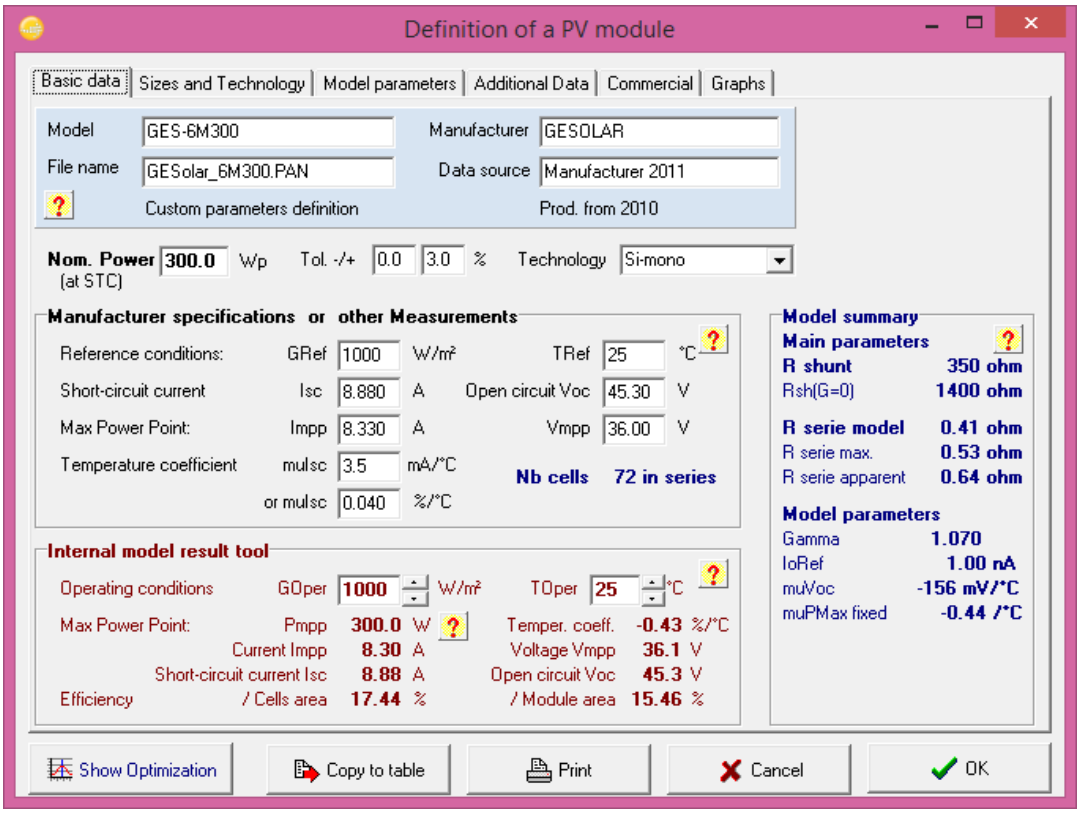

Figure 5.1: PV Module Basic data

The PV modules are connected to DC-AC inverters, which convert the direct current produced by the PV modules to alternating current required by the grid. A 1MW ABB inverter was selected with minimum voltage of 500V. A total of 30 inverters were selected and issues out power at 380V AC. This will however have to be stepped up to 33kV. Each inverter will have its own transformer connected side by side to minimise cable losses. The inverter properties is as shown below:

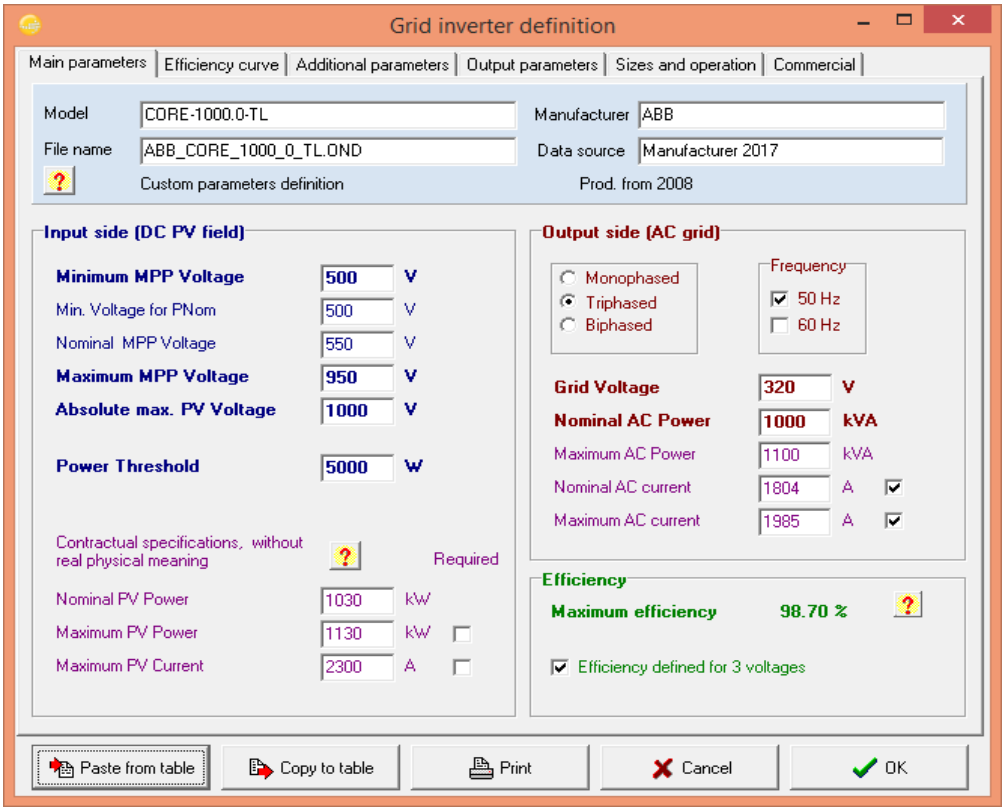

Figure 5.2: Grid inverter properties

5.5.1 Array/ inverter sizing

Number of PV modules in series – 19

Number of strings – 5610

For each inverter there will be 187 strings of PV modules with 19 modules per string connected in series. Each inverter has a ground area of 2.08m^2 and with the transformer a land area of 10m^2 per transformer – inverter combination is reserved. A total of 300m^2 is then required. The transformer will be a 1MVA 0.4/33kV transformer with specifications matching the ZETDC standards specifications as outlined in the Grid Code. The array inverter sizing conditions for the chosen inverter is as shown below:

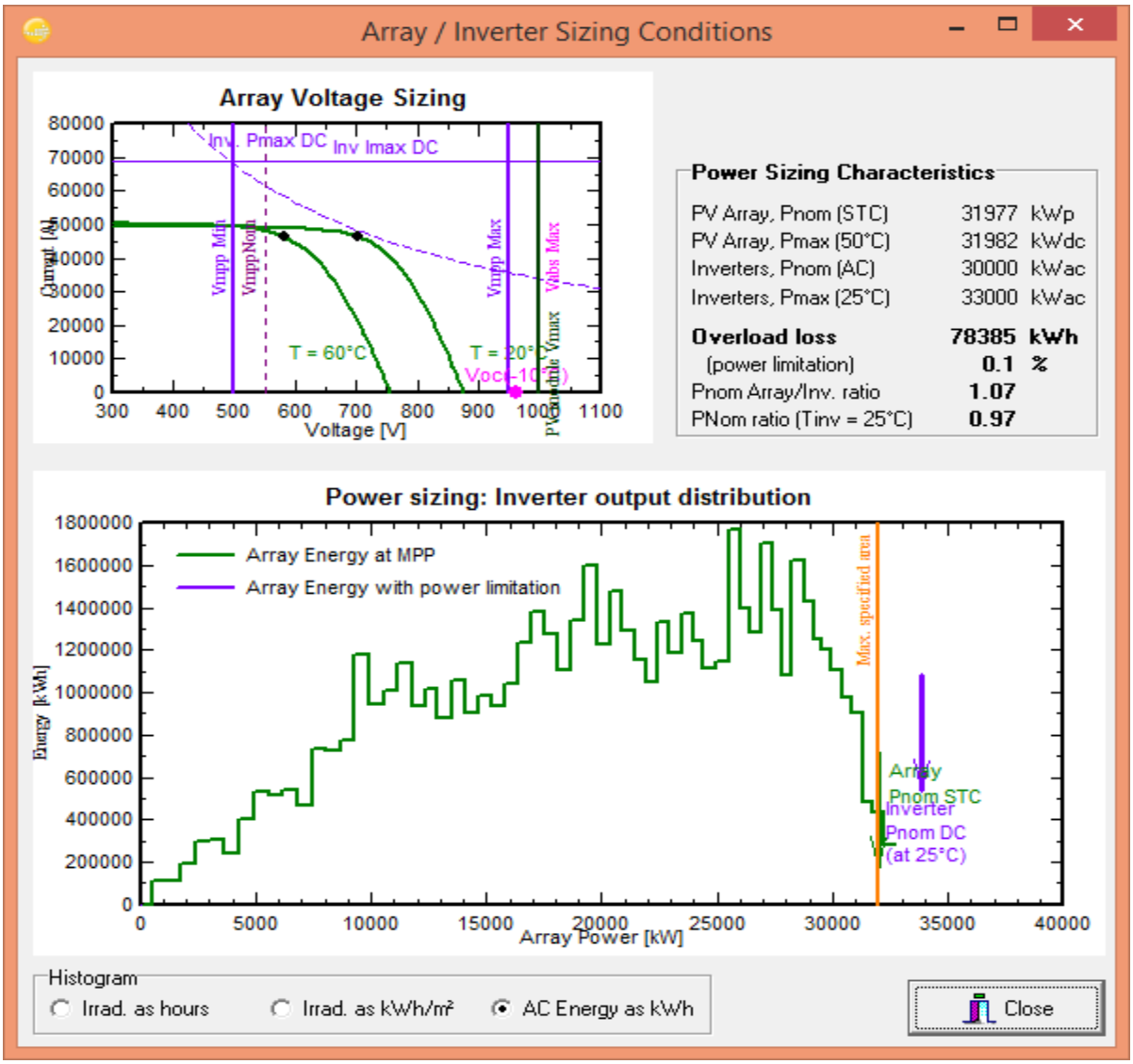

Figure 5.3: Array/Inverter Sizing Conditions

The maximum array operating output voltage in worst case scenario (i.e. at min. module operating temperature 20°C) should be lower than the maximum V_{MPPT} of the inverter. Also the minimum array operating output voltage in worst case scenario (i.e at max. module operating temperature 60°C) should be higher than the minimum V_{MPPT} of the inverter. Finally, the absolute maximum array voltage in open circuit (i.e. V_{oc} at 10°C) should stay below the absolute maximum inverter´s input voltage.

Overload behaviour

With all modern inverters, when the P_{mpp} of the array overcomes its P_{nom} DC limit, the inverter will stay at its safe nominal power by displacing the operating point in the I/V

curve of the PV array (towards higher voltages). It will therefore not undertake any overpower; simply the potential power of the array is not produced. There is no power to dissipate, no overheating and therefore no supplementary ageing.

The summary of the system design is as shown below:

Table 5.4: PV System Design Summary

Orientation parameters	
Field type:	Seasonal tilt adjustment
Tilt: summer = 15°, winter = 35°, Azimut = 0°	
Compatibility between System and Shadings	
Summer orientation	tilt/azim = 15° / 0°
1 sub-array	PNom = 31977 kWp, modules area = 206822 m²
shading 3D fields	31 Tables, : , total rough area , . 246209 m²
Winter orientation	tilt/azim = 35° / 0°
Orientation #2: No Shading field defined	
System parameters	
Sub-array #1	PV Array
PV modules:	5610 strings of 19 modules in series, 106590 to
Pnom = 300 Wp	Pnom array = 31977 kWp, Area = 206822 m²
Inverters (1000 kWac)	30 MPPT inputs, Total 30000
Shading scene parameters	
2 fields defined	Total Area 246209 m²
Field #1: rectangular	(Multi) Rectangular field
Total area = 75989 m²	
Orientation #1	Tilt/Azimut = 15.0° / 0.0°
Field #2: 30 rectangles	(Multi) Rectangular field
Total area = 170220 m²	
Orientation #1	Tilt/Azimut = 15.0° / 0.0°
Fixed plane system	31 tables, Area = 246209 m²
Use in simulation:	No shading calculations

5.6 Detailed Losses

The array losses can be defined as that which penalise the available array output energy with respect to the PV-module nominal power from the manufacturer's STC conditions. PVsyst treats in detail the following loss types in a PV array or system and are explained below:

i) Thermal losses

These are strongly influenced by the thermal behaviour of the field. It is determined by an energy balance between ambient temperature and the cells heating up due to incident irradiance. These factors depend on the mounting mode of the modules (sheds, roofing, facade, etc...).

In this project, the researcher proposed free mounted modules with free air circulation. For the design U_c=29W/m^{2}k and U_v=0 therefore U=29W/m^{2}k determined by equation 50 below:

$$U = U_c + U_v * v \quad \text{.....Equation 41}$$

Where, (U in [W/m²·k], v = wind velocity in [m/s]) $U_{c=}$ constant loss factor and U_v is wind loss factor

Ohmic losses

The proposed PV system will have the strings of PV modules arranged in a group as shown in the schema below:

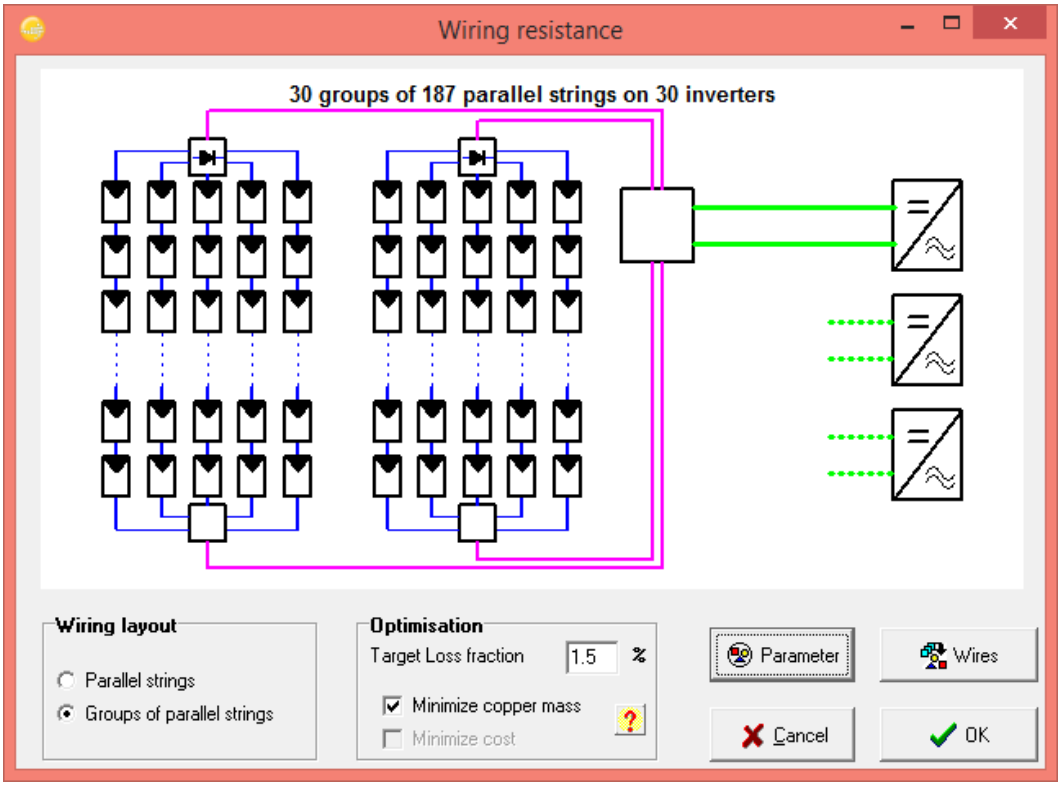

Figure 5.4: Wiring Schema

Table 5.9 below show the summary of values provided for all the losses both array and system losses and ageing of the PV modules:

Table 5.5: Summary Loss Table

	Description	Loss Type	Value
Ohmic Losses	DC Ohmic Losses	Global Wiring resistance	0.1749mΩ
		Voltage Drop across series diode	0.7V
	AC Circuit inverter to injection point	Length inverter to injection	100m
		Loss fraction at STC	1.91%
	External Transformer	Iron loss	0.1= 31.4kW
		Resistive/Inductive	1% at STC
	Voltage Drop at STC		6.8V
Module Quality – Light Induced Degradation (LID)	Module Quality	Module efficiency loss	0.8%
	LID	LID loss factor	2%
	Mismatch	Power Loss at MPP	1%
		Loss when running at Fixed voltage	2.5%
Soiling Loss	Yearly Soiling loss factor	Yearly Soiling loss factor	3%
IAM Losses		IAM=1-b_o(1/Cosi-1)	b_o=0.05
Auxilliaries	Auxilliary energy losses	Continuous auxiliary loss (fans etc)	100W per 1000kW inverter power threshold
	Night Loss		300W
Ageing		Individual PV modules	0.2%
	PV module ageing parameters	Average degradation factor	0.4%/year
		Isc dispersion RMS	0.4%/year
		Voc dispersion RMS	0.4%/year
Unavailability	Unavailability of the system	Unavailability time fraction	2%
		Unavailability duration	7.3days/yr
		Number of periods	3

Horizon

The site is characterised by the following horizon profile:

Table 5.6: Horizon Table

Azimuth [°]	Height [°]
-120	10
-40	5
40	5
120	10

The field has clear ground and has no near shadings. The most probable shadings are only due to the collectors probably shading each other.

According to (Hove, 2004), the ration of shaded collector to collector length (Ls/L)= 1.25. from Equation 43, thus S=3.91m to also allow for maintenance staff to pass through and maintain the modules.

5.7 Cable Sizing

As from Equation (44), the voltage across the modules V=36*19=684V; V_{mpp}=36V from Figure 5.2.

The Current of a string at maximum power point is I=8.33A*187=1 557.71A using Equation 45.

Conductivity $\boldsymbol{\gamma}$ of Cu= 59.5m/Ω.mm^2

The cable sizes will be calculated per each circuit and having the Length of the cable per circuit. Table 5.11 below shows the chart for the different cable sizes one can select to get the desired cable size for the circuit. The length is measured from the array to the inverter for the DC cables and from the inverter to the substation for grid connection.

Table 5.7: Cable Size Chart

Length (m)	Conductivity (γ) m/Ω.mm²	Current (I) - Amps	Voltage Drop	Area (mm²)
50	59.5	1557.71	4%	53
70	59.5	1557.71	4%	74
90	59.5	1557.71	4%	95
110	59.5	1557.71	4%	116
130	59.5	1557.71	4%	137
150	59.5	1557.71	4%	158
170	59.5	1557.71	4%	179
190	59.5	1557.71	4%	199
210	59.5	1557.71	4%	220
230	59.5	1557.71	4%	241
250	59.5	1557.71	4%	262
300	59.5	1557.71	4%	315

The nearest cable size is then selected.

CHAPTER 6

DISCUSSION OF RESULTS

6.0 Discussion of Results

The chapter will present the results of the designed system.

Definitions

Reference system Yield (Y_r) – ideal array Yield according to P_{nom} as defined by manufacturer, without any loss and its units are kWh/m²/day.

Array Yield (Y_a) – array daily output energy, referred to the nominal power and its units are kWh/kW_p/ day.

System Yield (Y_f) – system daily useful energy, referred to the nominal power and its units are kWh/KW_p/day.

Performance Ratio (PR) - Y_f/Y_r, is the global system efficiency with respect to the nominal installed power and the incident energy.

6.1 PV Array Output

Appendix A shows the results for the simulation of the design as detailed in Chapter 5. The total installed nominal power at the site P_{nom} is 31977MW. The resultant energy produced at the site for first year (as per simulation report attached) is 51,564MWh. The subsequent energy output for the life of the solar panels is as shown in Table 6.1 below:

Table 6.1*: Annual electricity yield*

Year	Yield (MWh)	Year	Yield (MWh)
Year 1	51,564,000	Year 14	47,612,000
Year 2	51,144,000	Year 15	47,227,000
Year 3	50,928,000	Year 16	46,891,000
Year 4	50,697,000	Year 17	46,604,000
Year 5	50,461,000	Year 18	46,333,000
Year 6	50,220,000	Year 19	46,061,000
Year 7	49,980,000	Year 20	45,791,000
Year 8	49,715,000	Year 21	44,159,000

Year 9	49,431,000	Year 22	45,191,000
Year 10	49,128,000	Year 23	44,866,000
Year 11	48,782,000	Year 24	44,519,000
Year 12	48,397,000	Year 25	44,164,000
Year 13	48,004,000		

6.2 Losses diagram

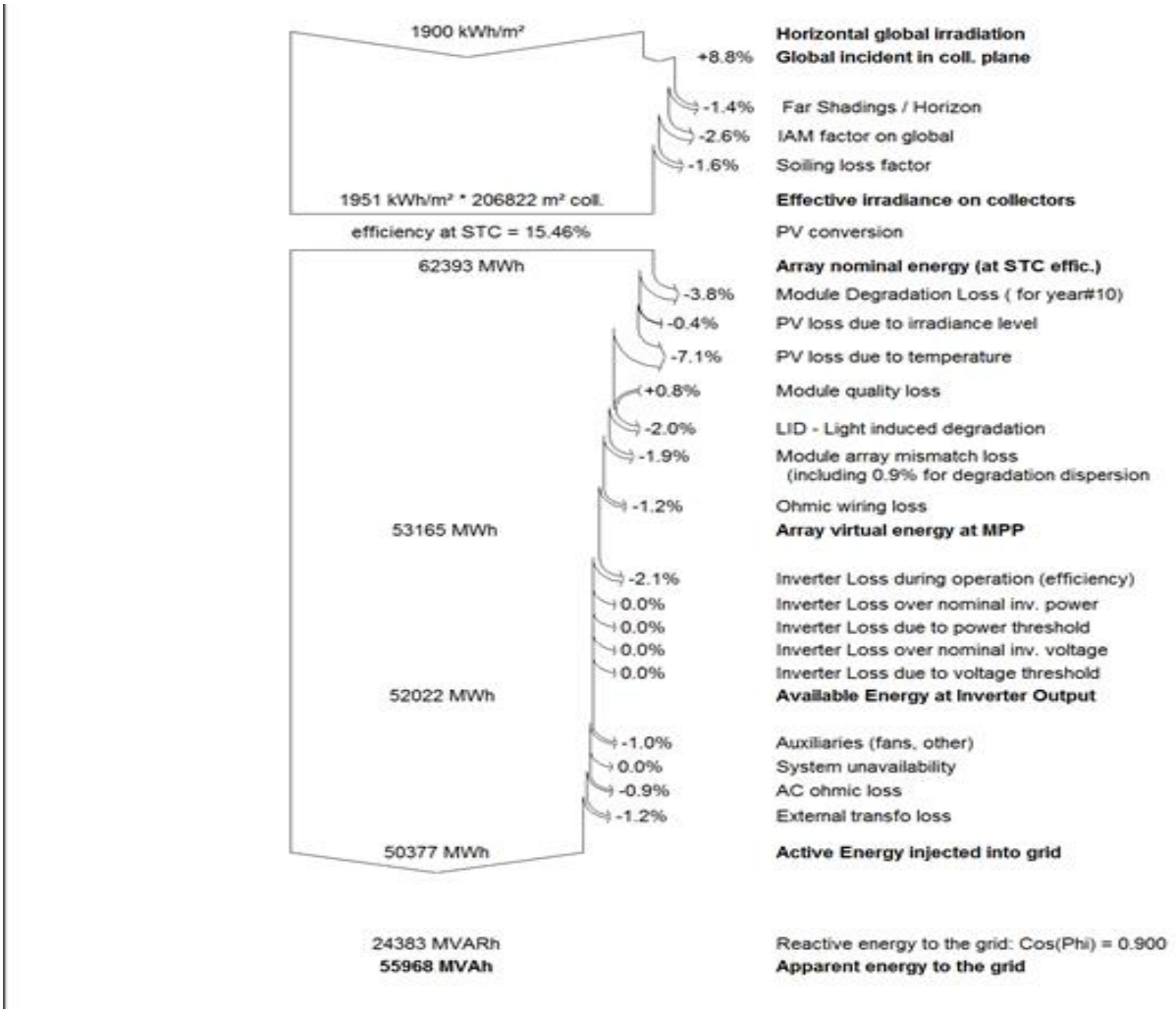

Figure 6.1: Loss Diagram for the Designed PV System

Starting with incident irradiation in the collector plane of 1900kWh/m^2, this is improved by 8.8% due to the correct tilting of the collector. This shows that correctly orienting your collector will play a big role without any additional resources. The shadings due to the

geographical orientation of the site was 1.4%. This is also affected by the shading of the collectors themselves. The incidence angle modifier (IAM) is a function of the tilt and is calculated in the PVSyst software. The IAM loss of 2.6% represents the decrease in the irradiance reaching the PV cells' surface with respect to irradiance under normal incidence due to reflexions increasing with the incidence angle. The soiling factor loss of 1.6% represents the losses due accumulation of dirt and its effect on the system performance is an uncertainty which strongly depends on the environment of the system, raining conditions, etc. it can therefore minimised by regular maintenance. All these losses are referred to as collector losses. The total collector losses for the system was L_c = [(+8.8) +(-1.4) +(-2.6)] %= +4.4%. Therefore, the collected irradiance on the collector is 4.4%*1900kWh/m^2 =1951kWh/ m^2 and is referred to as the Effective irradiance on the collector.

The second level of losses are encountered in the conversion of the irradiance to energy. The module degradation for the 10^{th} year of simulation is 3.8%. PV module degradation gives rise to a progressive loss of efficiency, which is characterised by the "Degradation Loss factor". However, all the modules will not degrade with the same rate. Thus if there is a distribution of loss rates around this average, this will produce an additional loss due to mismatch, increasing with time. PVsyst, software however using the Monte Carlo distribution is able to evaluate the mismatch as function of the age of the system. For the designed system it was found to b 1.9%.

Efficiency of the PV modules decreases for lower irradiances. This for our system, a loss off 0.4% due to irradiance level is a consequence of the intrinsic behaviour of the PV modules as described by the one – diode model. In the one-diode model, the efficiency at low levels depends on the following parameters:

i) The shunt resistance (R_{shunt}) exponential behaviour – when the irradiance diminishes, the R_{shunt} exponentially increases and therefore the corresponding loss diminishes. The lower the R_{shunt} at STC, the more losses to be retrieved by this process, and therefore the higher "low irradiance" efficiency.

ii) The series resistance, (R_{series}) is proportional to the square of the current, thus increases with power. If the R_{series} is high (bad), the losses are higher at STC (or reciprocally the efficiency will be enhanced at low irradiance levels).

Therefore "bad" modules (low R_{shunt}, high R_{series}) have the best performances under low irradiance conditions (with respect to STC specification).

The most significant conversion loss is the loss due to temperature. For a perfectly designed system, there is need to allow free air circulation on the mounting such that the mounting itself will not add to the increase in temperature. For the designed system, it was found to be 7.1%. As the ambient temperature increases, the open circuit voltage decreases and thereby this is the key source of grid voltage fluctuations. This needs to be taken care of when injecting into the grid.

Module quality losses indicates the confidence of the real module's performance, with respect to the manufacturer's specifications. This largely depends on the warranty from the manufacturer. For the designed system, a module quality gain of 0.8% is gained by choosing the best module for the system.

Light induced degradation of 2% is a loss of performances arising in the very first hours of exposition to the sun, with Crystalline modules. Lastly for conversion losses, the wiring ohmic resistance induces losses (I^2 R) between the power available from the modules and that at the terminals of the array. This can be minimised by correctly sizing the cables and also having a design which minimise cable distances. DC cables have high resistance and thus high ohmic losses hence a good designed system should ensure that the DC cables are shorter. For the system the ohmic losses is 1.2%. PVsyst also has a separate special tool for calculation the cable sizes if you have the cable distances.

The resultant array virtual energy at MPP is then 53,165MWh. This translates to a combined loss of 14.8% from the energy collected by the PV modules of 62,393MWh.

The inverter itself when converting from DC to AC also contributes some losses. The designed system had an inverter efficiency loss of 2.1%. There are also other losses which are encountered by the PV system which are due to the auxiliaries, fans, relay and circuit breaker operations to name a few. This loss was 0.1% for the designed system. This gave the output energy of 50,377MWh injected to the grid for the year. This translate to 55,968MVAh Apparent Energy injected to the grid.

6.3 Horizon Shading

The horizon line for the site superimposed on the solar position chart is as shown in figure below:

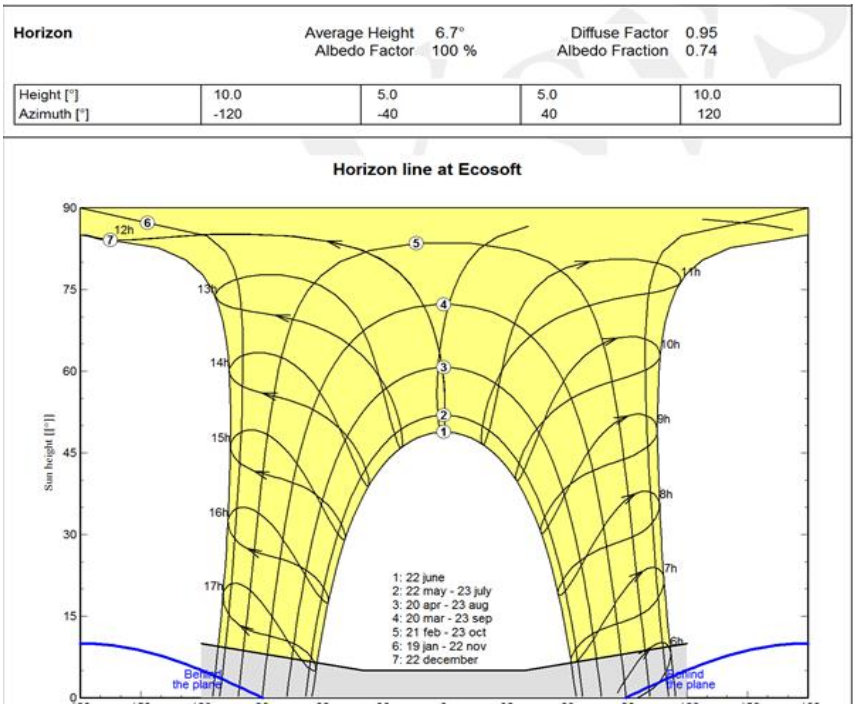

Figure 6.2: Loss Diagram for the Designed PV System

The grey shaded area indicate the times when the collectors will not receive irradiation (shaded). For 22 May,22 June and 23July, the collector will receive irradiation from 7am to 5pm even though sunrise is 6:30am and sunset is 1730hrs. Also for 22 December, 19 January and 22 November, the collector will receive irradiation from 6am to 5:30pm even though sunrise is at 5:30am and sunset is 6pm.

The horizon shading is affected by the general geographic features of the chosen site like mountains, trees or buildings that may provide shading to the collectors. It is however, recommended to site the PV plant away as possible from such obstructions as they greatly affect the yield of the PV system.

6.4 Normalised Energy Yield and Performance Ratio

The simulated results are as shown in the figure below:

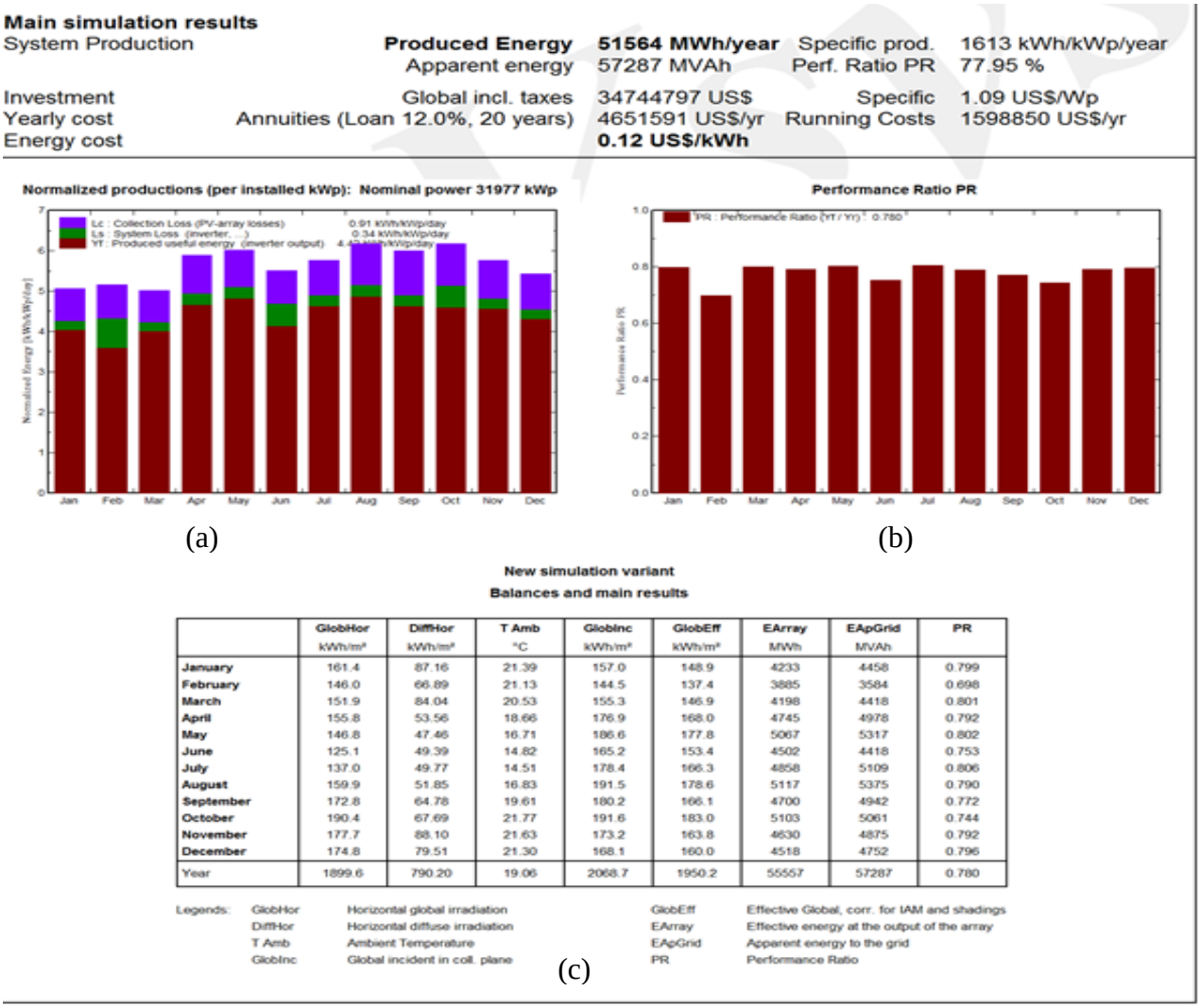

Figure 6.3: Loss Diagram for the Designed PV System

Basing on the installed Watt-peak (W_p), the collection losses (L_c) are 0.91kWh/W_p/day and system losses, L_s are 0.34 kWh/W_p/day. The produced useful energy was 4.42 kWh/W_p/day. The yield is almost constant throughout. This is due to the seasonal tilt adjustment thus maximising energy yield for all the months throughout the year. This can also be seen from almost a flat graph of performance ratio. As defined in the literature, the performance ratio is the global system efficiency with respect to the nominal installed power and the incident energy. An average value of 0.78 in the design was achieved by simply maximising the energy yield through seasonal tilt adjustment. The performance ratio =Yf/Yr plays a critical role in the efficiency of the system for the designed PV system. More often, for a poorly designed system, it will have wide variations for the winter and summer months. The PR for the system can also be improved by continuously tracking

the sun but however as discussed in the literature, this option is rather expensive. However, for an average PR of 0.78, the system is performing well.

From Figure 6.4(c), it can be seen than the winter months produce high Effective energy at the end of the array (EArray). This is so because the ambient temperature is low, and hence the PV modules perform better at low ambient temperatures. The Global Horizontal irradiation and Horizontal diffuse irradiation is low for the winter months but the resultant Global Incidence on the collector plane tend to favour the winter months than the summer counterparts. This is so due to the effect of ambient temperature on the collector efficiency. Therefore, it is very critical to optimise the orientation of the collectors with respect to the seasons.

6.5 Grid Impact Analysis

The technical appraisal of for the system performance with or without Ecosoft plant revealed that there was need to upgrade some portions of the ZETDC electric grid to cater for the additional load. However, the simulations in the Sincal software indicated that all the options were technically feasible. The detailed report from ZETDC is attached in Appendix B. The nominal voltage profile for the proposed injection substations improved as can be seen from Table 6.5 below:

Table 6.2*: Voltage Profiles for the Proposed Injection Substations*

Substation	Before Injection	After Injection	
		Option 1	**Option 2**
ECOSOFT Solar Park 33kV	-	99.48%	108.34%
Highlands Park 33kV	94.56%	98.22%	
Greystones 33kV	93.27%		96.17%

From Table 6.5 above, it can be seen that there is improvement in voltage profile for Highlands Park 33kV busbar and improvement in voltage profile for Greystones 33kV busbar after injecting the Ecosoft solar Park 33k feeder.

These voltages apply to steady state condition with no prior outage. Of note is the improvement in voltage regulation for Highlands park 33kV busbar for option 1 and improvement in voltage profile for Greystones 33kV busbar for option 2.

SHORT CIRCUIT ANALYSIS

Table 6.3: Short circuit analysis

Bus bar	Before Injection, kA	After Injection - Option 1, kA	After Injection Option 2, kA
Highlands park 33kV	4.02	5.08	
Greystones 33kV	4.90		5.97
Coleford	7.35	7.61	7.93
Ecosoft Solar 33kV	-	3.26	3.37

Table 6.6 above indicate that there is marginal increase in fault levels after the injection of the Ecosoft Solar 33kV feeder. However, the utility equipment is already designed to cater for higher fault levels than these hence thus will not affect existing switchgear.

Conclusion and recommendations

The injection of the 30MW to the ZETDC grid does not cause any negative impact on the Grid for both options and is therefore recommended. The least cost option with a total cost of US$2,735,358.89 was chosen for use in the economic appraisal. The following recommendations were made by ZETDC:

i) The inverters that the client is going to use on the plant to have a capability to regulate reactive power so to avoid voltage fluctuations on the nearby network
ii) The client should also ensure that harmonics arising from the inverters are kept to a minimum level and in accordance with requirements set out in the distribution code.
iii) The client should install a fast-response voltage regulating device on the new plant e.g. STATCOM

Based on the report, as per requirement Static Var compensators were recommended for the site to address issues of voltage fluctuations.

CHAPTER 7

ECONOMIC ANALYSIS

7.0 Economic Analysis

The most critical factors in determining the value of electricity generated by PV systems are firstly the initial cost of the hardware and installation, and secondly the amount of electricity produced annually. When the system produces electrical energy for the grid, the price for which the electrical energy can be sold is also critical. For faster investment payback of grid connected systems, most of the energy should be used on site. That energy is worth the retail rate while selling to the utility is generally valued less because most power companies do not voluntarily want to purchase energy at the retail level from their customers. Net energy billing i.e. net metering allows for larger size systems because the system can be sized for producing all the energy needed on site. In net metering customer pays only for the net power consumed i.e. the customer produced electricity is reduced from the consumed electricity before billing. Net metering typically needs to be mandated by the government to be adopted by power companies. (Foster, et al., 2010)

In Zimbabwe, net metering is not a reality yet even the study of its possibilities has been listed in the program of the sitting government. However, the Feed in Tariff is available and is negotiated through ZERA with the electricity power utility – ZESA.

There are many economic factors that should be considered when purchasing a renewable energy system and these are:

i) Load and energy, calculated by month or day for small systems;
ii) Cost of energy from competing energy sources to meet the need;
iii) Initial installed cost;
iv) Production of energy (size of the system, warranty, solar resource, reliability);
v) Selling price of energy produced and anticipated energy cost changes;
vi) Operation and maintenance costs;
vii) Time value of money (interest rate, fixed or variable)
viii) Inflation;

ix) Legal fees (negotiation of contracts, titles, easements, permits);

x) Depreciation if system is a business expense

7.1 Project Costs and Financial Parameters

The costs of the project include capital costs, operation & maintenance costs and decommissioning costs. These costs together with the life-cycle generation of electricity, the borrowing interest rate, as well as the judicial return on costs due to the investor determine the retail cost of energy from the solar power plant.

Capital Costs

The capital costs of the project can be divided into two:

i) Costs incurred for the services of an Engineering Procurement Company, who will be responsible for the procurement and installation of equipment for the plant and

ii) Development Costs, which are incurred for site preparation, provision of site facilities and obtaining of licenses and permissions.

Table 7.1 below shows the capital costs of the Ecosoft solar plant. The total capital cost of the project is **US$34,184,338.24** which represents a specific investment of $1.07 per Watt.

Table 7.1: Project Capital Costs

ENGINEERING PROCUREMENT (EPC) COSTS					
ITEM	**QUANTITY**	**UNIT**	**UNIT COST (USD)**	**AMOUNT (USD)**	**Remarks**
Solar PV module	31,977,000	Watts	0.40	12,790,800.00	approximate pallet price of Renesola module (http://sunelec.com/solar-panels/renesola-255w-solar-panel.html)
Inverter	30,000,000	Watts	0.15	4,500,000.00	http://www.nrel.gov/docs/fy15osti/64746.pdf
Transformer	30,000	kVA	15.00	450,000.00	
Module Racks	31,977,000	Watts	0.05	1,598,850.00	http://www.nrel.gov/docs/fy15osti/64746.pdf , ex-factory gate prices
Switchgear, combiners, conduits and ancillary equipment	31,977,000	Watts	0.03	959,310.00	http://www.nrel.gov/docs/fy15osti/64746.pdf , ex-factory gate prices
Wiring, conduits	31,977,000	Watts	0.03	959,310.00	
Mounting structure foundations	31,977,000	Watts	0.06	1,918,620.00	http://www.greentechmedia.com/articles/read/pv-bos-cost-analysis-ground-mounted-systems
Connection costs to ZESA grid	31,977,000	Watts	0.090	2,877,930.00	ZETDC estimate during grid impact study (attached)
EPC Labor & Transport	31,977,000	Watts	0.06	1,918,620.00	http://www.nrel.gov/docs/fy15osti/64746.pdf (factored by 0.70)
EPC Mark-up	5%	Above total	35,185,040.00	1,759,252.00	http://www.nrel.gov/docs/fy15osti/64746.pdf
Civil works	31,977,000	Watts	0.06	1,918,620.00	

Sub-total EPC costs				**31,651,312.00**	
DEVELOPMENT COSTS					
Land Cost	42	hectares	20,000.00	840,000.00	$2 per square meter assumed
Land preparation	42	hectares	20,000.00	840,000.00	Includes stump clearing, effluent pond levelling, slope grading and drainage works
Developer's overheads	13%	development costs	1,760,000.00	220,000.00	http://www.nrel.gov/docs/fy15osti/64746.pdf
Entitlement and environmental permits	2%	above cost	31,651,312.00	633,026.24	Includes EIA charges, generation licence, prefeasibility studies, geo-technical studies, fencing, water & electricity installation, etc
Sub-total Development				2,533,026.24	http://www.greentechmedia.com/articles/read/pv-bos-cost-analysis-ground-mounted-systems
TOTAL INVESTMENT COSTS				**34,184,338.24**	**$1.07 per watt**

Operation and Maintenance costs

The operation and maintenance costs for a solar plant include regular solar array cleaning, electrical system checking and repairs and inverter preventative maintenance, among other things. The cost of operation and maintenance for the present solar plant is estimated using figures provided by ScottMadden Managing Consultants (Jacobi & Starkweather, 2010).

The operation and maintenance costs for the project are shown in Table 7.3.

Table 7.2 below shows the cost per kW per year of the main operation and maintenance activities as given by ScottMadden.

Table 7.2: Specific O & M Costs for a solar PV plant

O & M Cost Item	Cost [$/kW/year]
Scheduled Maintenance/ Cleaning	20
Unscheduled Maintenance	2
Inverter Replacement Reserve	10
Insurance, Property Taxes, Owner' Costs	15
Total	**47**

Based on specific O & M costs on Table 7.2 and applying the to our solar plant with installed PV module capacity of 31 977kW, the O & M costs for the Ecosoft solar plant are calculated on Table 7.3 below. The O & M costs are assumed to increase annually at the rate of inflation, 2% per annum. The total Operations and Maintenance costs were

shown for 25years which is the lifespan of the PV module though for FiT the contracts are normally 20years.

Table 7.3: Operation and Maintenance Costs for the Ecosoft Solar Plant

YEAR	Scheduled Mantainace/ Cleaning	Unscheduled Maintenance	Inveter Replacement Reserve	Insurance, Property Taxes, Owner' Costs	TOTAL O & M
1	639,540	63,954	319,770	479,655	1,502,919
2	652,331	65,233	326,165	489,248	1,532,977
3	665,377	66,538	332,689	499,033	1,563,637
4	678,685	67,868	339,342	509,014	1,594,910
5	692,259	69,226	346,129	519,194	1,626,808
6	706,104	70,610	353,052	529,578	1,659,344
7	720,226	72,023	360,113	540,169	1,692,531
8	734,630	73,463	367,315	550,973	1,726,382
9	749,323	74,932	374,662	561,992	1,760,909
10	764,310	76,431	382,155	573,232	1,796,127
11	779,596	77,960	389,798	584,697	1,832,050
12	795,188	79,519	397,594	596,391	1,868,691
13	811,091	81,109	405,546	608,319	1,906,065
14	827,313	82,731	413,657	620,485	1,944,186
15	843,859	84,386	421,930	632,895	1,983,070
16	860,737	86,074	430,368	645,552	2,022,731
17	877,951	87,795	438,976	658,464	2,063,186
18	895,510	89,551	447,755	671,633	2,104,449
19	913,421	91,342	456,710	685,065	2,146,538
20	931,689	93,169	465,845	698,767	2,189,469
21	950,323	95,032	475,161	712,742	2,233,259
22	969,329	96,933	484,665	726,997	2,277,924
23	988,716	98,872	494,358	741,537	2,323,482
24	1,008,490	100,849	504,245	756,368	2,369,952
25	1,028,660	102,866	514,330	771,495	2,417,351

7.2 Levelized Cost of Energy (LCOE)

The method of Levelized Cost of Electricity (LCOE) makes it possible to compare power plants of different generation and cost structures with each other. The basic thought is that one forms the sum of all accumulated costs for building and operating a plant and comparing this figure to the sum of the annual power generation. This then yields the so-called LCOE in $ per kWh. It is important to note that this method is an abstraction from reality with the goal of making different sorts of generation plants comparable. The

method is not suitable for determining the cost efficiency of a specific power plant. For that, a financing calculation must be completed taking into account all revenues and expenditures on the basis of a cash-flow model, by calculating the Net Present Value.

The value of LCOE of solar energy technologies depends significantly on the following parameters:

i) Specific investments – for the construction and installation of power plant
ii) Local conditions – with typical irradiation conditions for different locations and full load hours in the energy system.
iii) Operating costs – during the power plant's operational life time.
iv) Operational life of the power plant
v) Financing conditions – interest rates, demanded return on investment, respective shares of external and equity-based financing, loan maturity periods, etc

For calculating the LCOE for new plants, the following formular is applied:

$$LCOE = \frac{I_o + \sum_1^n \frac{A_t}{(1+i)^t}}{\sum_1^n \frac{M_{t,el}}{(1+i)^t}} \quad \text{Equation 42}$$

Where,

LCOE is the Levelized Cost of Electricity in $/kWh

I_o is the Investment expenditures in $

A_t Annual total costs in $ in year *t*

$M_{t,el}$ is the generated quantity of electricity in the respective year in kWh

i is the real interest rate in %

n is the project economic operational lifetime in years

t is the year of lifetime (1, 2, ...n)

The annual total costs are comprised of fixed and variable costs for the operation of the plant, maintenance, service, repairs and insurance payments. The share of external financing and equity financing can be included in the analysis explicitly through the weighted average cost of capital (WACC) over the discounting factor (interest rate). It depends on the amount of equity capital, return on equity capital over lifetime, cost of

debt and the share of debt used. The intial investment can the be represented by an equivalent series of equal annual costs by applying the cost recovery factor.

7.3 Investment Parameters

Table 7.4 below shows the investment parameters for the solar plant, which enter the calculation for the levelized cost of electricity.

Table 7.4: Project Investment Assumptions

Interest On Loan	12.0%	
Expected Return On Investment	20.0%	
Debt Ratio	85.0%	
Equity Ratio	15.0%	
Corporate Tax	25.0%	
Weighted Average Cost Of Capital (WACC)	15.5%	
Annual Energy Year 1	51,564,000	kWh
Tax on energy sales	0%	
Escalation O & M costs	2%	
Loan Term	15	years
Asset Base (USD)	34,184,338.24	

Table 7.5: LCOE for Ecosoft Solar Plant

YEAR	Generation Costs	Depreciation	Total Annual Costs (USD)	Gearing	WACC	Asset Base	Allowed Return on Investment	Total Costs	Annual Generated Energy (kWh)	Levelized Cost of Energy ($/kWh)
0		-	-			34,184,338	-			
1	1,502,919	1,367,374	2,870,293	0.85	0.155	32,816,965	5,298,572	8,168,865	51,349,000	0.159
2	1,573,391	1,367,374	2,940,765	0.85	0.155	31,449,591	5,086,630	8,027,394	51,144,000	0.157
3	1,604,859	1,367,374	2,972,233	0.85	0.155	30,082,218	4,874,687	7,846,919	50,928,000	0.154
4	1,636,956	1,367,374	3,004,330	0.85	0.155	28,714,844	4,662,744	7,667,073	50,697,000	0.151
5	1,669,695	1,367,374	3,037,069	0.85	0.155	27,347,471	4,450,801	7,487,869	50,461,000	0.148
6	1,703,089	1,367,374	3,070,463	0.85	0.155	25,980,097	4,238,858	7,309,320	50,220,000	0.146
7	1,737,151	1,367,374	3,104,525	0.85	0.155	24,612,724	4,026,915	7,131,440	49,980,000	0.143
8	1,771,894	1,367,374	3,139,268	0.85	0.155	23,245,350	3,814,972	6,954,240	49,715,000	0.140
9	1,807,331	1,367,374	3,174,705	0.85	0.155	21,877,976	3,603,029	6,777,734	49,431,000	0.137
10	1,843,478	1,367,374	3,210,852	0.85	0.155	20,510,603	3,391,086	6,601,938	49,128,000	0.134

11	1,880,348	1,367,374	3,247,722	0.85	0.155	19,143,229	3,179,143	6,426,865	48,782,000	0.132
12	1,917,955	1,367,374	3,285,329	0.85	0.155	17,775,856	2,967,201	6,252,529	48,397,000	0.129
13	1,956,314	1,367,374	3,323,688	0.85	0.155	16,408,482	2,755,258	6,078,945	48,004,000	0.127
14	1,995,440	1,367,374	3,362,814	0.85	0.155	15,041,109	2,543,315	5,906,128	47,612,000	0.124
15	2,035,349	1,367,374	3,402,723	0.85	0.155	13,673,735	2,331,372	5,734,094	47,227,000	0.121
16	2,076,056	1,367,374	3,443,430	-	0.2	12,306,362	2,734,747	6,178,177	46,891,000	0.132
17	2,117,577	1,367,374	3,484,951	-	0.2	10,938,988	2,461,272	5,946,223	46,604,000	0.128
18	2,159,928	1,367,374	3,527,302	-	0.2	9,571,615	2,187,798	5,715,099	46,333,000	0.123
19	2,203,127	1,367,374	3,570,501	-	0.2	8,204,241	1,914,323	5,484,823	46,061,000	0.119
20	2,247,190	1,367,374	3,614,564	-	0.2	6,836,868	1,640,848	5,255,412	45,791,000	0.115
21	2,292,133	1,367,374	3,659,507	-	0.2	5,469,494	1,367,374	5,026,880	44,159,000	0.114
22	2,337,976	1,367,374	3,705,350	-	0.2	4,102,121	1,093,899	4,799,248	45,191,000	0.106
23	2,384,735	1,367,374	3,752,109	-	0.2	2,734,747	820,424	4,572,533	44,866,000	0.102
24	2,432,430	1,367,374	3,799,804	-	0.2	1,367,374	546,949	4,346,753	44,519,000	0.098
25	2,481,079	1,367,374	3,848,453	-	0.2	0	273,475	4,121,927	44,164,000	0.093
AVERAGE TARIFF										0.129

The energy tariff for Ecosoft solar plant is 12.9 cents/kWh as shown on Table 7.5 above. This is almost equivalent to the one calculated by the PVsyst software of 12cents/kWh. Hence the software can also be used but however it disregards decimal places which pose a great challenge in understating the LCOE for the PV system.

7.4 Net Present Value, Payback Period and Internal Rate of Return

The Net Present Value (NPV) for the solar project is calculated on Table 7.6 below. It is the cumulative value of the discounted (at WACC rate) cash flow of the project. The NPV for 25 years of operation can be seen as US#14,044,020 and for 20years of operation is US$11,738,839.

Table 7.6: Cashflows for the Project

Year	Capital Costs	Operation & Maintenance Costs	Total Costs (USD)	KWH	Gross Revenue	Net Revenue	Net un-discounted Cash Flow	Present Value of Net Cash Flow (12% DR)	Cumulative Undiscounted Cash Flow	Cumulative Discounted Cash Flow
0	34,184,338	0	34,184,338		0	0	-34,184,338	-34,184,338	-34,184,338	-34,184,338

1		1,502,919	1,542,540	51,349,000	8,215,840	8,215,840	6,673,300	5,958,304	-27,511,038	-28,226,035
2		1,532,977	1,573,391	51,144,000	8,183,040	8,183,040	6,609,649	5,269,172	-20,901,389	-22,956,863
3		1,563,637	1,604,859	50,928,000	8,148,480	8,148,480	6,543,621	4,657,620	-14,357,768	-18,299,243
4		1,594,910	1,636,956	50,697,000	8,111,520	8,111,520	6,474,564	4,114,702	-7,883,204	-14,184,540
5		1,626,808	1,669,695	50,461,000	8,073,760	8,073,760	6,404,065	3,633,838	-1,479,139	-10,550,702
6		1,659,344	1,703,089	50,220,000	8,035,200	8,035,200	6,332,111	3,208,044	4,852,972	-7,342,657
7		1,692,531	1,737,151	49,980,000	7,996,800	7,996,800	6,259,649	2,831,547	11,112,621	-4,511,110
8		1,726,382	1,771,894	49,715,000	7,954,400	7,954,400	6,182,506	2,497,010	17,295,127	-2,014,100
9		1,760,909	1,807,331	49,431,000	7,908,960	7,908,960	6,101,629	2,200,309	23,396,756	186,209
10		1,796,127	1,843,478	49,128,000	7,860,480	7,860,480	6,017,002	1,937,314	29,413,758	2,123,523
11		1,832,050	1,880,348	48,782,000	7,805,120	7,805,120	5,924,772	1,703,230	35,338,530	3,826,753
12		1,868,691	1,917,955	48,397,000	7,743,520	7,743,520	5,825,565	1,495,277	41,164,095	5,322,030
13		1,906,065	1,956,314	48,004,000	7,680,640	7,680,640	5,724,326	1,311,868	46,888,421	6,633,898
14		1,944,186	1,995,440	47,612,000	7,617,920	7,617,920	5,622,480	1,150,471	52,510,901	7,784,369
15		1,983,070	2,035,349	47,227,000	7,556,320	7,556,320	5,520,971	1,008,661	58,031,872	8,793,030
16		2,022,731	2,076,056	46,891,000	7,502,560	7,502,560	5,426,504	885,180	63,458,376	9,678,210
17		2,063,186	2,117,577	46,604,000	7,456,640	7,456,640	5,339,063	777,604	68,797,439	10,455,814
18		2,104,449	2,159,928	46,333,000	7,413,280	7,413,280	5,253,352	683,144	74,050,791	11,138,958
19		2,146,538	2,203,127	46,061,000	7,369,760	7,369,760	5,166,633	599,881	79,217,424	11,738,839
20		2,189,469	2,247,190	45,791,000	7,326,560	7,326,560	5,079,370	526,562	84,296,794	12,265,401
21		2,233,259	2,292,133	44,159,000	7,065,440	7,065,440	4,773,307	441,815	89,070,101	12,707,217
22		2,277,924	2,337,976	45,191,000	7,230,560	7,230,560	4,892,584	404,335	93,962,685	13,111,552
23		2,323,482	2,384,735	44,866,000	7,178,560	7,178,560	4,793,825	353,727	98,756,510	13,465,279
24		2,369,952	2,432,430	44,519,000	7,123,040	7,123,040	4,690,610	309,027	103,447,120	13,774,306
25		2,417,351	2,481,079	44,164,000	7,066,240	7,066,240	4,585,161	269,714	108,032,281	14,044,020

The NPV for the project is positive and hence the project is viable. The internal rate of return of 18% is above the cost of capital and hence the project is viable.

7.4.1 Payback Period

The simple payback period is about 8 years, while the dynamic payback period is about 13 years, as shown on Figure 7.1 and Figure 7.2, respectively.

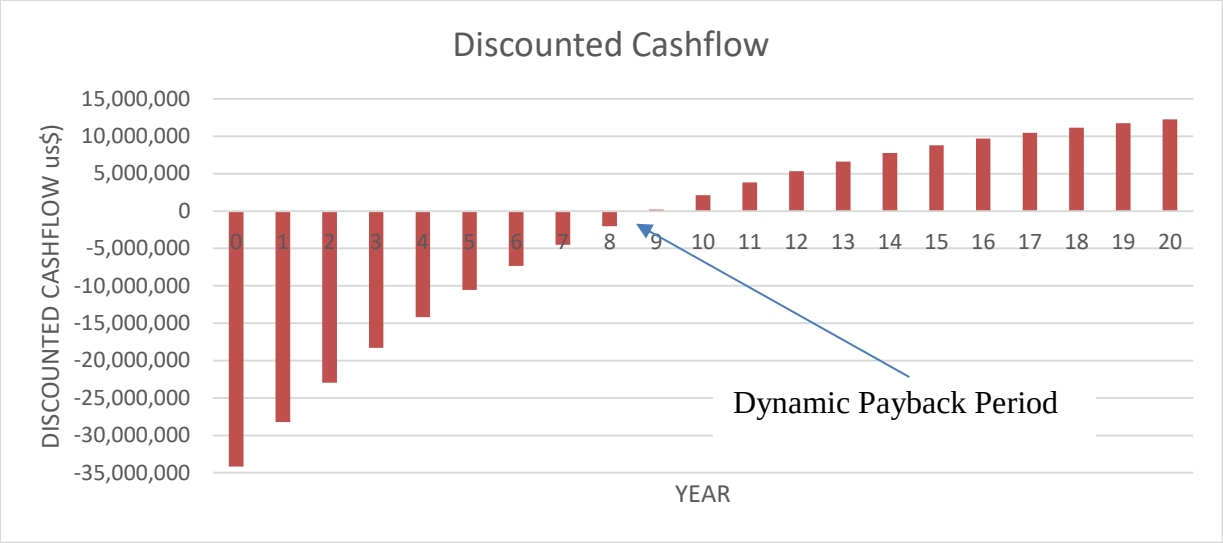

Figure 7.1: Dynamic Payback Period

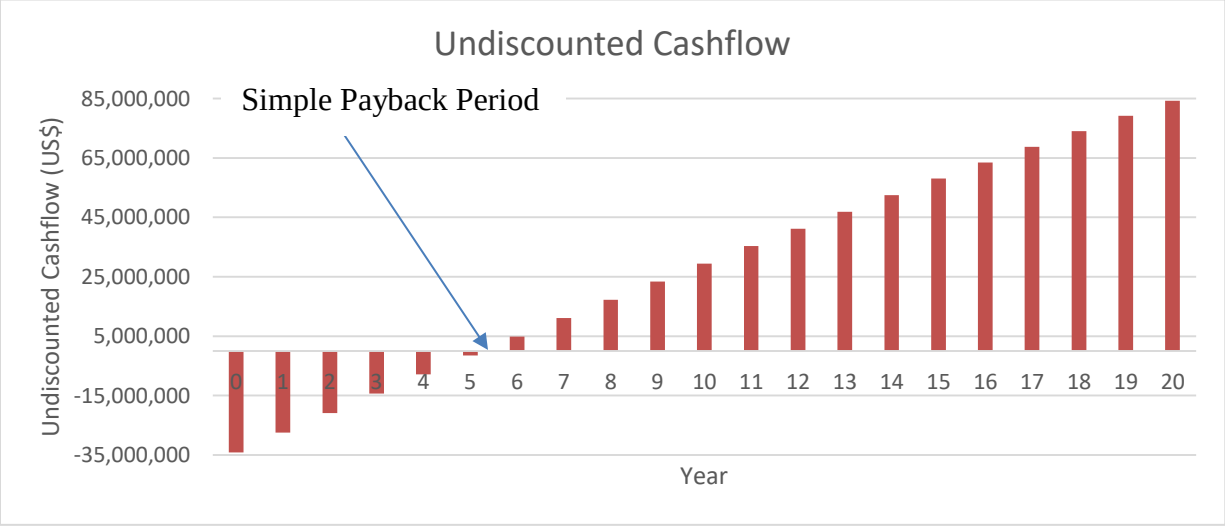

Figure 7.2: Simple Payback Period

The simple payback and dynamic payback periods are short, they translate to about 25% for simple payback and 40% for dynamic payback of the contract period 20years. This makes the investment of the project viable as the initial capital costs are recouped faster and that makes the project worth investing in.

CHAPTER 8

RECOMMENDATIONS AND CONCLUSION

8.0 Conclusion

It is viable to install the PV System on the location as the technical and economic analysis are viable. Ecosoft to apply for 30MW Grid integrated system for the reserved land of 42 hectares at the Ecosoft Plant in Harare. Correct array orientation and selection of the inverters is key for the reliability of the solar system. The LCOE for the research case study of 12.9cents/kWh shows that it is now becoming economically feasible to install grid integrated PV plants in Zimbabwe. This is due to the continued drop in prices of the solar modules and the government policies on the importation of the PV modules. Most of the major components for the grid integrated PV system like transformers, inverters and solar modules are now duty free. Hence the drop in the capital costs.

The energy mix for ZETDC as of June 2017 is as shown in Table 8.1 below:

Table 8.1: ZETDC energy sources (ZETDC, 2017)

	Source	Average Price (c/kWh)	Average Energy Per Month (GWh)
1	Kariba	2.2	300
2	Hwange	7.71	300
3	Small Thermals (Bulawayo, Harare & Munyati)	16 – 17	14.4
4	HCB	6	38
5	Eskom	10c	180
6	IPPs (Hydro)	15	9.6
7	IPPs (PV)	*No PV IPP but price indications from discussions done with prospective PV IPP is 14-16c/kWh*	Nil
	Total		**842**

It shows that Solar PV is now competing in terms of the price with the other sources. And for this reason, the regulator is now recommending a FiT of up to 16c/kWh as can be noted from the ZETDC report above.

To demystify the myth of grid integrated solar energy causing harm to the electricity grid, the grid impact report indicates that the was actually an improvement of the voltages on the nearest substations. Therefore, connecting solar PV plants on the grid does not cause any harm. However, this has to be assessed on case by case basis, and corrective action if needed to be done on the grid before injection to avoid grid disturbances.

It is very crucial for grid integrated PV system PV design engineers to understand the solar engineering aspect of PV design to produce a better yield and also the electrical engineering aspects of grid integration in order to produce maximum energy yield and providing a reliable and stable supply to the grid.

8.1 Recommendations

i) Zimbabwe should embrace solar technology as the solar resource is abundant and will reduce power shortages at the same time embracing clean energy.

ii) Power utility to consider more of distributed generation as this according to the research done by the US department of Energy, the embracing of distributed generation is beneficial to the electric utilities. With Distribution Generation (DG), the electric utilities benefit from increased system reliability, improved power quality, reduction of transmission and distribution losses and also offsets to investments in generation, transmission and/or distribution thereby increasing their revenue

iii) To apply for carbon credits. Carbon credits is the currency for trading carbon emissions. The unit for one carbon credit is equivalent to one tonne of CO_2 emissions. It increases the revenue of the investor and at the same time promotes clean energy.

9.0 References

Abete, A. et al., 1991. *Performance testing procedures for photovoltaic modules in mismatching conditions.* s.l., IEEE.

AFDB, 2011. *Zimbabwe Monthly Economic Review,* Harare: AFDB.

Asowata, O., Swart, J. & Pienaar, C., 2012. Optimum Tilt Angles for Photovoltaic Panels during Winter Months in the Vaal Triangle, South Africa. *Smart Grid and Renewable Energy,* Volume 3, pp. 119-125.

Badescu, V., 2008. *Modeling solar radiation at the earth's surface : recent advances.* Berlin: Springer.

Benford, F. & Bock, J. E., 1939. A time analysis of sunshine. *Transaction of the American Illumination Engineering Society 34, 200-204. ,* Volume 34, pp. 200-204.

Boxwell, M., 2015. *Solar Electricity Handbook: A Simple Practical Guide to Solar Energy - Designing and Installing Photovoltaic Solar Electric Systems.* 9th ed. Coventry: Greenstream Publishing.

Boxwel, M., 2012. *Solar Electricity Handbook: A Simple, Practical Guide to Solar Energy (2012), p. 41–42.* 6th ed. Warwickshire: Greenstream Publishing.

Branker, K., Pathak, M. J. M. & Pearce, J. M., 2011. A review of solar photovoltaic levelized cost of electricity. *Renewable and Sustainable Energy Reviews,* 15(9), pp. 4470-4482.

Brew-Hammond, A. et al., 2007. *Energy Crisis in Ghana: Drought, Technology or Policy?.* Accra: Kwame Nkrumah University.

Chakraborty, S., Simões, M. G. & Kramer, W. E., 2013. *Power Electronics for Renewable and Distributed Energy Systems.* s.l.:Springer-Verlag.

Chauhan, R. K., Rajpurohit, B. S. & Singh, S. N., 2014. DC Grid Interconnection for Conversion Losses and Cost Optimization. In: J. Hossain & A. Mahmud, eds. *Renewable Energy Integration.* s.l.:Springer, pp. 327-345.

Chen, C. J., 2011. *Physics of solar energy.* Hoboken, N.J: John Wiley & Sons.

Chen, Y. & Smedley, K., 2004. A cost-effective single-stage inverter with maximum power point tracking. *IEEE Transactions on Power Electronics*, September, 19(5), pp. 1289-1294.

Cooper, P., 1969. Solar Energy. *The Absorption of Solar Radiation in Solar Stills,* 12(3).

Cotal, H. et al., 2009. III–V multijunction solar cells for concentrating photovoltaics. *Energy Environ-ment Science,* Volume 2, pp. 174-192.

Couture, T., Cory, K., Kreycik, C. & Williams, E., 2010. *A Policymaker's Guide to to Feed-in Tariff Policy Design,* s.l.: NREL.

Darghouth, N., Barbose, G. & Wiser, R., 2011. The impact of rate design and net metering on the bill savings from distributed PV for residential customers in California. *Energy Policy,* Volume 39, pp. 5243-5253.

Dash, P. & Gupta, N., 2015. Effect of Temperature on Power Output from Different Commercially available Photovoltaic Modules. *Int. Journal of Engineering & Research,* 5(1), pp. 148-151.

Dave, J., 1977. Validity of the Isotropic-Distribution Approximation in Solar Energy Estimations. *Solar Energy,* Volume 19, pp. 331-333.

Duffie, J. A. & Beckman, W. A., 2006. *Solar Engineering of Thermal Processes.* New Jersey: John Wiley & Sons. Inc.

Elminir, H. et al., 2006. Optimum Solar Flat-Plate Collector Slope: Case Study for Helwan, Egypt. *Energy Conversion and Management,* Volume 47, pp. 624-637.

Evans, D., 1981. Simplifed method for predicting photovoltaic array output. *Solar energy,* Volume 27, p. 555.

Ferrey, S., 2004. Net zero: distributed generation and FERC's midAmerican decision. *Electical Journal,* Volume 10, pp. 33-42.

Foster, R., Ghassemi, M. & Cota, A., 2010. Solar Energy. *Renewable Energy and the Environment. Boca Raton.*

Fu, W. Q., 2006. *Radiative Transfer.* Wallace: J M & Hobbs.

Garg, H., 1982. *Treatise on Solar Energy;.* New York: JohnWiley & Sons Inc.

Hatano, N., Kishida, Y. & Iwata, A., 2009. STATCOM using the new concept of an inverter system with controlled gradational voltage. *Electrical Engineering in Japan,* 168(4), p. 58–65.

Hove, T., 2000. A method for predicting long-term average performance of photovoltaic systems. *Renewable Energy,* Volume 21, pp. 207-229.

Hove, T., 2004. Methods for calculating the effect on radiation income of inter-row shading in solar energy collector arrays. *Journal of Energy in Southern Africa,* 15(2).

Hove, T. & Gotsche, J., 1999. Mapping Global, Diffuse and Beam Solar Radiation Over Zimbabwe. *Renewable Energy ,* Volume 18, pp. 535-556.

Ibrahim, D., 1995. Optimum tilt angle for solar collectors used in Cyprus. *Renew Energy,* Volume vi, p. 813–819.

IRENA, 2010. *Renewable Energy Country Profiles ,* s.l.: IRENA.

IRENA, 2012. RENEWABLE ENERGY TECHNOLOGIES: COST ANALYSIS SERIES. *Power Sector*, June.

Jacobi, J. & Starkweather, R., 2010. *Scottmadden,* s.l.: Scottmadden.

Kalogrou, S. A., 2014. *Solar Energy Engineering Processes and Systems.* 2nd ed. Kidlington: Academic Press.

Kesraoui, M., Chaib, A. & Lazizi, A., 2016. Grid Connected Solar PV System: Modeling, Simulation and Experimental Tests. *Energy Procedia,* Volume 95, pp. 181-188.

Kim, S. T. et al., 2007. Operation Characteristics of Bypass Diode for PV Module. *Journal of KIEEME,* Volume 21, p. 12.

Kjaer, S., Pedersen, J. & Blaabjerg, F., 2005. A review of single-phase grid-connecte inverters for photovoltaic modules. *IEEE Transactions on Industry Applications,* 41(5), pp. 1292-1306.

Kjaer, S., Pedersen, J. & Blaabjerg, F., 2005. A review of single-phase grid-connected inverters for photovoltaic modules. *IEEE Transactions on Industry Applications*, September, 41(5), p. 1292–1306.

Klaus, J. et al., 2014. *Solar Energy: Fundamentals, Technology, and Systems.* s.l.:s.n.

Lewis, G., 1983. Diffuse irradiation over Zimbabwe. *Solar Energy,* 31(1), pp. 125-138.

Lewis, G., 1983. Estimates of irradiance over Zimbabwe. *Solar Energy,* 31(6), pp. 609-612.

Lunde, P., 1980. *Solar Thermal Engineering: Space Heating and Hot Water Systems.* New York: JohnWiley & Sons Inc.

Magee, S., 2010. *Solar Irradiance and Insolation for Power Systems.* s.l.:Createspace.

Mahalakshmi, R. & Thampatty, K. S., 2015. Grid Connected Multilevel Inverter for Renewable Energy. *Procedia Technology,* Volume 21, p. 636 – 642 .

Maillo, L., 2013. Application note: optimal cable sizing in PV systems: case study, European copper institute. *Leonardo Energy,* Volume 2.

Mani, M. & Pillai, R., 2010. Impact of dust on solar photovoltaic (PV) performance: Research status, challenges and recommendations. *Renewable and Sustainable Energy Reviews,* pp. 3124-3131.

Markvart, T., 1994. *Solar Electricity.* Chichester: John Wiley & Sons.

Markvart, T., 2000. *Solar electricity: Energy Engineering learning package.* Chichester, New York: John Wiley & Sons.

Masters, G. M., 2013. *Renewable and efficient electric power systems.* 2nd ed. New Jersey: Wiley-IEEE Press.

McEvoy, A. J., Markvart, T. & Castaner, L., 2012. *Practical handbook of photovoltaics : fundamentals and applications.* 2nd ed. Waltham, MA: Academic Press.

Moon, E.-J., Lim, J.-H., Seong, Y.-B. & Kim, K.-W., n.d. Characteristics of Power Losses in Photovoltaic Module depending on Shading Patterns and Solar Irradiance.

Moon, S., Felton, K. & Johnson, A., 1981. Optimum Tilt Angles of a Solar Collector. *Energy,* Volume 6, pp. 895-899.

Okello, D., Dyk, E. & Vorster, ,. F., 2015. Analysis of measured and simulated performance data of a 3.2 kWp grid-connected PV system in Port Elizabeth, South Africa. *Energy Conversion and Management,* Volume 100, pp. 10-15.

Parmesano, H., 2003. Standby service to distributed generation projects: the wrong tool for subsidies. *Electrical Journal,* pp. 85-92.

Paulescu, M., Paulescu, E., Gravila, P. & Badescu, V., 2013. Solar Radiation Measurements. In: *Weather Modelling and Forecasting of PV Systems Operation.* s.l.:Springer, p. 358.

Poullikkas, A., Kourtis, G. & Hadjipaschalis, I., 2012. An overview of the EU member states support schemes for the promotion of renewable energy sources. *International Journal Energy Environ,* Volume 4, pp. 553-566.

SAPP, 2011. *Energising the Region for Economic development: Monthly Report,* Harare: SAPP.

Schmid, J. & Schmidt, H., 2003. Power conditioning and photovoltaic powersystems. *Handbook of Photovoltaic Science and Engineering,* pp. 863-903.

Shariah, A., Al-Akhras, M. & Al-Omari, I., 2002. Optimizing the Tilt Angle of Solar Collectors. *Renewable Energy,* Volume 26, pp. 587-598.

Spiegel, M., Klein, S. & Beckman, W., 1981. A simplifed method for estimating the monthly average performance of photovoltaic systems. *Solar Energy,* Volume 26, p. 413.

Stapleton, G., Garrett, S., Neill, S. & McLean, B., 2010. Grid-Connected PV Systems Design and Installation. Global Sustainable Energy Solutions (GSES).

Sukhatme, S., 1999. *Solar Energy.* London: Tata McGraw-Hill Education.

Swartman, R. & Ogunlade, O., 1967. Solar radiation estimates from common parameters. *Solar Energy,* July - December, 11(3-4), pp. 170-172.

Temps, R. & Coulson, K., 1977. Solar Radiation Incident upon Slopes of Different Orientations. *Solar Energy,* Volume 19, pp. 179-184.

Thiel, D. V., 2014. *Research Methods for Engineers,* Cambridge: Cambridge University Press.

Vineet, M., Kamal, B., Piyush, K. & Chandna, V., 2016. *Proceeding of International Conference on Intelligent Communication, Control and Devices.* Singapore: Springer Singapore.

Worden, J. & Martinson, M., n.d. *How Inverters Work..* [Online].

Yakup, M. & Malik, A., 2001. Optimum Tilt Angle and Orientation for Solar Collector in Brunei Da-russalam. *Renewable Energy,* Volume 24, pp. 223-234.

ZESA, 2017. *Power generation stats: ZETDC.* [Online]
Available at: http://www.zesa.co.zw
[Accessed 5 June 2017].

ZETDC, 2017. *ZETDC June Report,* Harare: ZETDC.

10.0 APPENDICES

10.1 APPENDIX A – SIMULATION REPORT

PVSYST V6.62		03/07/17	Page 1/8

Grid-Connected System: Simulation parameters

Project : **Ecosoft Zimbabwe**

Geographical Site	**Ecosoft**		Country	**Zimbabwe**
Situation	Latitude	-17.74° S	Longitude	31.21° E
Time defined as	Legal Time	Time zone UT+2	Altitude	1440 m
	Albedo	0.20		
Meteo data:	**Ecosoft**	Meteonorm 7.1 (1996-2005), Sat=4% - Synthetic		

Simulation variant : **New simulation variant**

Simulation date	03/07/17 13h01
Simulation for the	**first year of operation**

Simulation parameters

Coll. plane: Seasonal tilt adjustment	Azimuth	0°	Winter season	J-A-S-A-M-J
	Summer Tilt	10°	Winter Tilt	35°
Models used	Transposition	Perez	Diffuse	Perez, Meteonorm
Horizon	Average Height	6.7°		
Near Shadings	No Shadings			

PV Array Characteristics

PV module	Si-mono	Model	**GES-6M300**	
Original PVsyst database		Manufacturer	GESOLAR	
Number of PV modules		In series	19 modules	In parallel 5610 strings
Total number of PV modules		Nb. modules	106590	Unit Nom. Power 300 Wp
Array global power		Nominal (STC)	**31977 kWp**	At operating cond. 28446 kWp (50°C)
Array operating characteristics (50°C)		U mpp	612 V	I mpp 46498 A
Total area		Module area	**206822 m²**	Cell area 183382 m²

Inverter		Model	**CORE-1000.0-TL**	
Custom parameters definition		Manufacturer	ABB	
Characteristics		Operating Voltage	500-950 V	Unit Nom. Power 1000 kWac
Inverter pack		Nb. of inverters	30 units	Total Power 30000 kWac

PV Array loss factors

Array Soiling Losses

Jan.	Feb.	Mar.	Apr.	May	June	July	Aug.	Sep.	Oct.	Nov.	Dec.
0.5%	0.5%	1.0%	1.0%	1.0%	3.0%	3.0%	3.0%	3.0%	1.0%	1.0%	0.5%

Thermal Loss factor	Uc (const)	29.0 W/m²K	Uv (wind)	0.0 W/m²K / m/s
Wiring Ohmic Loss	Global array res.	0.22 mOhm	Loss Fraction	1.5 % at STC
Serie Diode Loss	Voltage Drop	0.7 V	Loss Fraction	0.1 % at STC
LID - Light Induced Degradation			Loss Fraction	2.0 %
Module Quality Loss			Loss Fraction	-0.8 %
Module Mismatch Losses			Loss Fraction	1.0 % at MPP
Module average degradation	Year no	1	Loss factor	0.4 %/year
Mismatch due to degradation	Imp dispersion RMS	0.4 %/year	Voc dispersion RMS	0.4 %/year
Incidence effect, ASHRAE parametrization	IAM =	1 - bo (1/cos i - 1)	bo Param.	0.05

System loss factors

AC wire loss inverter to transfo	Inverter voltage	380 Vac tri		
	Wires: 3x30000.0 mm²	100 m	Loss Fraction	1.4 % at STC
External transformer	Iron loss (24H connexion)	31145 W	Loss Fraction	0.1 % at STC
	Resistive/Inductive losses	0.0 mOhm	Loss Fraction	1.0 % at STC

Grid-Connected System: Simulation parameters (continued)

Unavailability of the system	7.3 days, 3 periods		Time fraction	2.0 %
User's needs :	Unlimited load (grid)			
Auxiliaries loss	Constant (fans)	10 W	... from Power thresh.	0.1 kW
	Proportionnal to Power	10.0 W/kW	... from Power thresh.	0.1 kW
	Night consumption	10 W		
Power factor	Cos(phi)	0.900 leading	Phi	25.8°

Grid-Connected System: Horizon definition

Project : **Ecosoft Zimbabwe**

Simulation variant : **New simulation variant**
Simulation for the first year of operation

Main system parameters	System type	**Grid-Connected**		
Horizon	Average Height	6.7°		
PV Field Orientation	Seasonal tilt: summer/winter	10°/35°	azimuth	0°
PV modules	Model	GES-6M300	Pnom	300 Wp
PV Array	Nb. of modules	106590	Pnom total	**31977 kWp**
Inverter	Model	CORE-1000.0-TL	Pnom	1000 kW ac
Inverter pack	Nb. of units	30.0	Pnom total	**30000 kW ac**
User's needs	Unlimited load (grid)		Cos(Phi)	0.900 leading

Horizon Average Height 6.7° Diffuse Factor 0.95
Albedo Factor 100 % Albedo Fraction 0.74

Height [°]	10.0	5.0	5.0	10.0
Azimuth [°]	-120	-40	40	120

Horizon line at Ecosoft

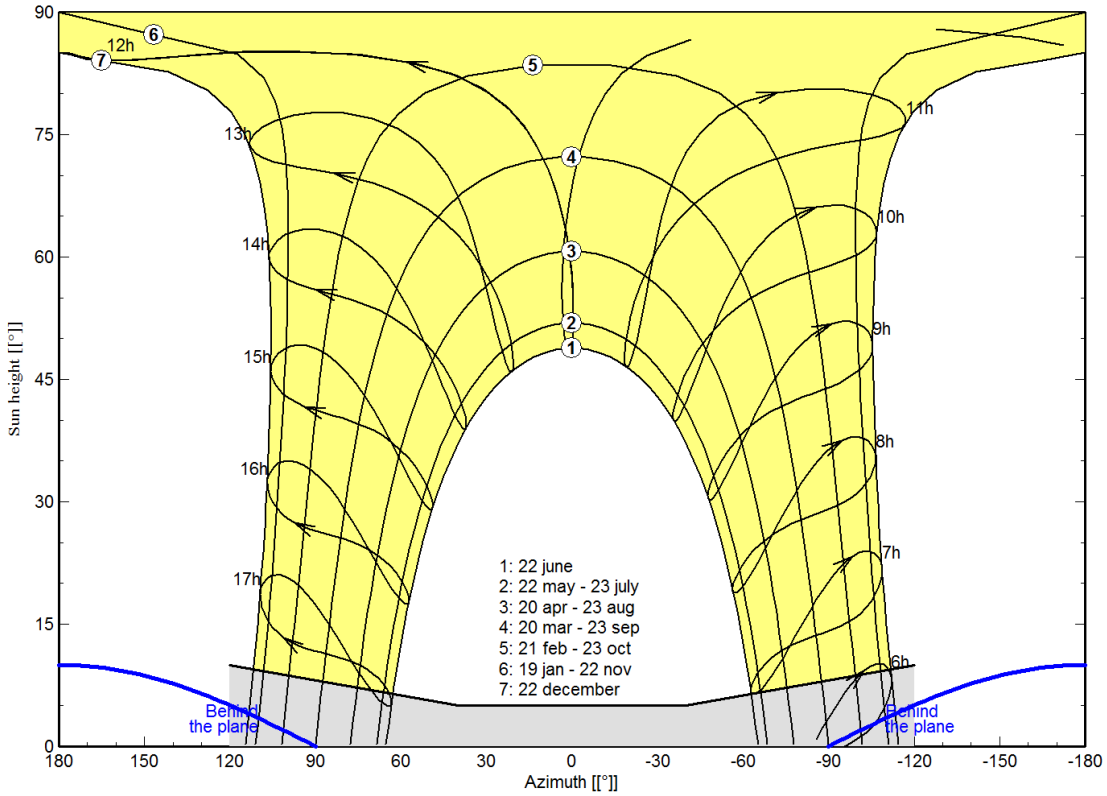

Grid-Connected System: Main results

Project : **Ecosoft Zimbabwe**

Simulation variant : **New simulation variant**
Simulation for the first year of operation

Main system parameters	System type	**Grid-Connected**		
Horizon	Average Height	6.7°		
PV Field Orientation	Seasonal tilt: summer/winter	10°/35°	azimuth	0°
PV modules	Model	GES-6M300	Pnom	300 Wp
PV Array	Nb. of modules	106590	Pnom total	**31977 kWp**
Inverter	Model	CORE-1000.0-TL	Pnom	1000 kW ac
Inverter pack	Nb. of units	30.0	Pnom total	**30000 kW ac**
User's needs	Unlimited load (grid)		Cos(Phi)	0.900 leading

Main simulation results

System Production	**Produced Energy**	**51564 MWh/year**	Specific prod.	1613 kWh/kWp/year
	Apparent energy	57287 MVAh	Perf. Ratio PR	77.95 %
Investment	Global incl. taxes	34744797 US$	Specific	1.09 US$/Wp
Yearly cost	Annuities (Loan 12.0%, 20 years)	4651591 US$/yr	Running Costs	1598850 US$/yr
Energy cost		**0.12 US$/kWh**		

Normalized productions (per installed kWp): Nominal power 31977 kWp

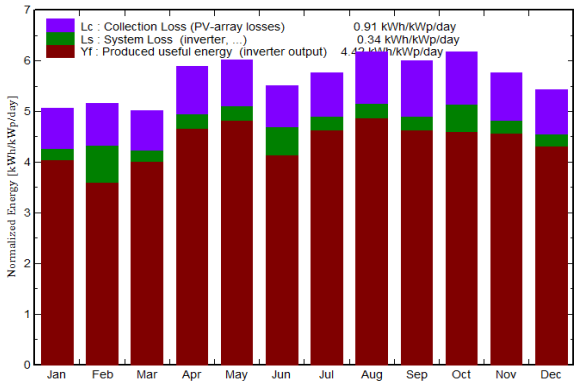

Performance Ratio PR

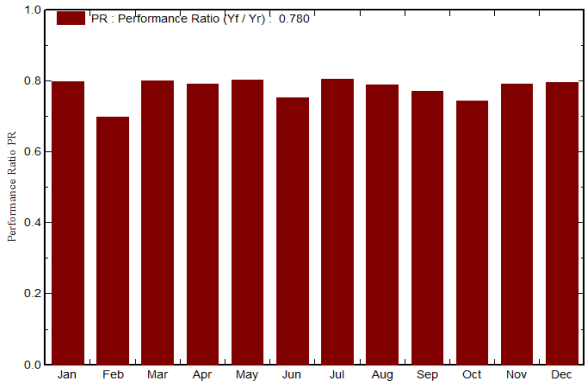

New simulation variant

Balances and main results

	GlobHor kWh/m²	DiffHor kWh/m²	T Amb °C	GlobInc kWh/m²	GlobEff kWh/m²	EArray MWh	EApGrid MVAh	PR
January	161.4	87.16	21.39	157.0	148.9	4233	4458	0.799
February	146.0	66.89	21.13	144.5	137.4	3885	3584	0.698
March	151.9	84.04	20.53	155.3	146.9	4198	4418	0.801
April	155.8	53.56	18.66	176.9	168.0	4745	4978	0.792
May	146.8	47.46	16.71	186.6	177.8	5067	5317	0.802
June	125.1	49.39	14.82	165.2	153.4	4502	4418	0.753
July	137.0	49.77	14.51	178.4	166.3	4858	5109	0.806
August	159.9	51.85	16.83	191.5	178.6	5117	5375	0.790
September	172.8	64.78	19.61	180.2	166.1	4700	4942	0.772
October	190.4	67.69	21.77	191.6	183.0	5103	5061	0.744
November	177.7	88.10	21.63	173.2	163.8	4630	4875	0.792
December	174.8	79.51	21.30	168.1	160.0	4518	4752	0.796
Year	1899.6	790.20	19.06	2068.7	1950.2	55557	57287	0.780

Legends:
- GlobHor — Horizontal global irradiation
- DiffHor — Horizontal diffuse irradiation
- T Amb — Ambient Temperature
- GlobInc — Global incident in coll. plane
- GlobEff — Effective Global, corr. for IAM and shadings
- EArray — Effective energy at the output of the array
- EApGrid — Apparent energy to the grid
- PR — Performance Ratio

Grid-Connected System: Loss diagram

Project : **Ecosoft Zimbabwe**

Simulation variant : **New simulation variant**
Simulation for the first year of operation

Main system parameters	System type	**Grid-Connected**		
Horizon	Average Height	6.7°		
PV Field Orientation	Seasonal tilt: summer/winter	10°/35°	azimuth	0°
PV modules	Model	GES-6M300	Pnom	300 Wp
PV Array	Nb. of modules	106590	Pnom total	**31977 kWp**
Inverter	Model	CORE-1000.0-TL	Pnom	1000 kW ac
Inverter pack	Nb. of units	30.0	Pnom total	**30000 kW ac**
User's needs	Unlimited load (grid)		Cos(Phi)	0.900 leading

Loss diagram over the whole year

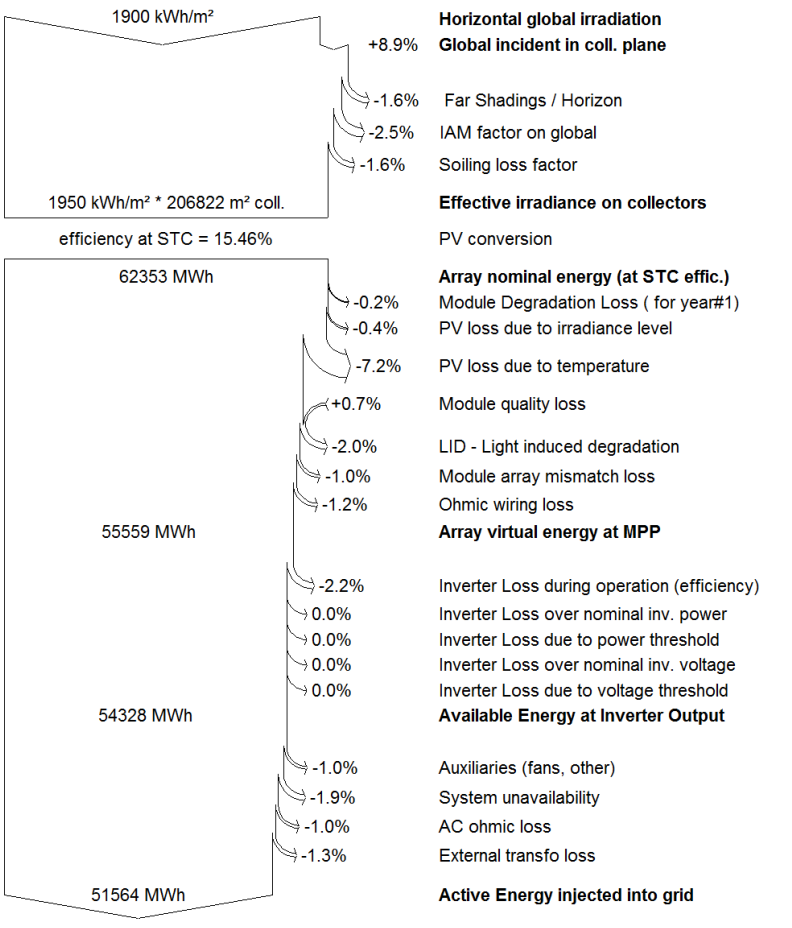

Grid-Connected System: Economic evaluation

Project : **Ecosoft Zimbabwe**

Simulation variant : **New simulation variant**
Simulation for the first year of operation

Main system parameters	System type	**Grid-Connected**		
Horizon	Average Height	6.7°		
PV Field Orientation	Seasonal tilt: summer/winter	10°/35°	azimuth	0°
PV modules	Model	GES-6M300	Pnom	300 Wp
PV Array	Nb. of modules	106590	Pnom total	**31977 kWp**
Inverter	Model	CORE-1000.0-TL	Pnom	1000 kW ac
Inverter pack	Nb. of units	30.0	Pnom total	**30000 kW ac**
User's needs	Unlimited load (grid)		Cos(Phi)	0.900 leading

Investment

PV modules (Pnom = 300 Wp)	106590 units	120 US$ / unit	12790800	US$
Supports / Integration		24 US$ / module	2557094	US$
Inverters (Pnom = 1000 kW ac)	30 units	153900 US$ / unit	4617000	US$
Settings, wiring, ...			959310	US$
Connection to Grid			2378573	US$
Development Costs			2153072	US$
Civil works			1630827	US$
EPC Labour & Transport			1630827	US$
EPC MarkUp			1495364	US$
Substitution underworth			0	US$
Gross investment (without taxes)			**30212867**	**US$**

Financing

Gross investment (without taxes)		30212867	US$
Taxes on investment (VAT)	Rate 15.0 %	4531930	US$
Gross investment (including VAT)		34744797	US$
Subsidies		0	US$
Net investment (all taxes included)		**34744797**	**US$**
Annuities	(Loan 12.0 % over 20 years)	4651591	US$/year
Annual running costs: maintenance, insurances ...		1598850	US$/year
Total yearly cost		**6250441**	**US$/year**

Energy cost

Produced Energy	51564	MWh / year
Cost of produced energy	0.12	US$ / kWh

Grid-Connected System: Long Term Financial Balance

Project : **Ecosoft Zimbabwe**

Simulation variant : **New simulation variant**
Simulation for the first year of operation

Main system parameters	System type	**Grid-Connected**		
Horizon	Average Height	6.7°		
PV Field Orientation	Seasonal tilt: summer/winter	10°/35°	azimuth	0°
PV modules	Model	GES-6M300	Pnom	300 Wp
PV Array	Nb. of modules	106590	Pnom total	**31977 kWp**
Inverter	Model	CORE-1000.0-TL	Pnom	1000 kW ac
Inverter pack	Nb. of units	30.0	Pnom total	**30000 kW ac**
User's needs	Unlimited load (grid)		Cos(Phi)	0.900 leading

Electricity sale

Feed-in Tariff	**0.16**	**US$/kWh**	Warranty over	**20 years**
Annual connexion tax	0	US$		

Long term balance and Running conditions

Annual sale tariff depreciation	0.0	% / year
Annual production reduction	0.0	% / year
Feed-in tariff Warranty over	20	years
Tariff reduction after contractual warranty	**-50**	**%**
Loan duration (payment of annuities)	20	years

Yearly financial balance (kUS$)

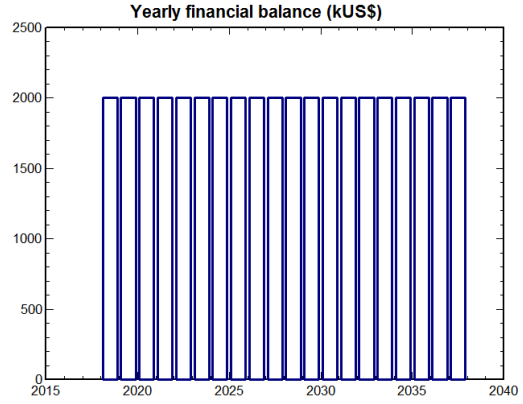

Cumulated financial balance (kUS$)

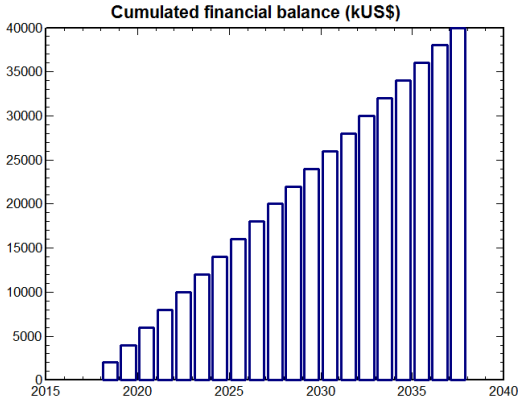

Long term economic balance

Year	Loan 12.0 %	Running costs	Sold energy	Yearly Balance	Cumul. Balance
2018	4652	1599	8250	2000	2000
2019	4652	1599	8250	2000	4000
2020	4652	1599	8250	2000	5999
2021	4652	1599	8250	2000	7999
2022	4652	1599	8250	2000	9999
2023	4652	1599	8250	2000	11999
2024	4652	1599	8250	2000	13999
2025	4652	1599	8250	2000	15999
2026	4652	1599	8250	2000	17998
2027	4652	1599	8250	2000	19998
2028	4652	1599	8250	2000	21998
2029	4652	1599	8250	2000	23998
2030	4652	1599	8250	2000	25998
2031	4652	1599	8250	2000	27998
2032	4652	1599	8250	2000	29997
2033	4652	1599	8250	2000	31997
2034	4652	1599	8250	2000	33997
2035	4652	1599	8250	2000	35997
2036	4652	1599	8250	2000	37997
2037	4652	1599	8250	2000	39997

Grid-Connected System: CO2 Balance

Project : **Ecosoft Zimbabwe**

Simulation variant : **New simulation variant**
Simulation for the first year of operation

Main system parameters	System type	**Grid-Connected**		
Horizon	Average Height	6.7°		
PV Field Orientation	Seasonal tilt: summer/winter	10°/35°	azimuth	0°
PV modules	Model	GES-6M300	Pnom	300 Wp
PV Array	Nb. of modules	106590	Pnom total	**31977 kWp**
Inverter	Model	CORE-1000.0-TL	Pnom	1000 kW ac
Inverter pack	Nb. of units	30.0	Pnom total	**30000 kW ac**
User's needs	Unlimited load (grid)		Cos(Phi)	0.900 leading

Produced Emissions **Total:** **59459.95 tCO2**
Source: Detailed calculation from table below

Replaced Emissions **Total:** **1020976.2 tCO2**
System production: 51564.46 MWh/yr Lifetime: 30 years
Annual Degradation: 1.0 %
Grid Lifecycle Emissions: 660 gCO2/kWh
Source: IEA List Country: Zimbabwe

CO2 Emission Balance **Total:** **826405.8 tCO2**

System Lifecycle Emissions Details:

Item	Modules	Supports
LCE	1713 kgCO2/kWp	4.40 kgCO2/kg
Quantity	31977 kWp	1065900 kg
Subtotal [kgCO2]	54767647	4692305

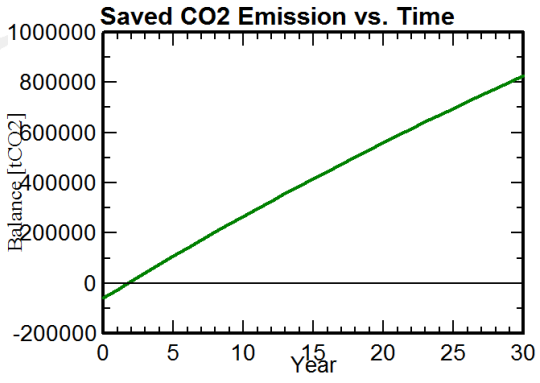

10.2 Appendix B – Global Horizontal Irradiation of Zimbabwe

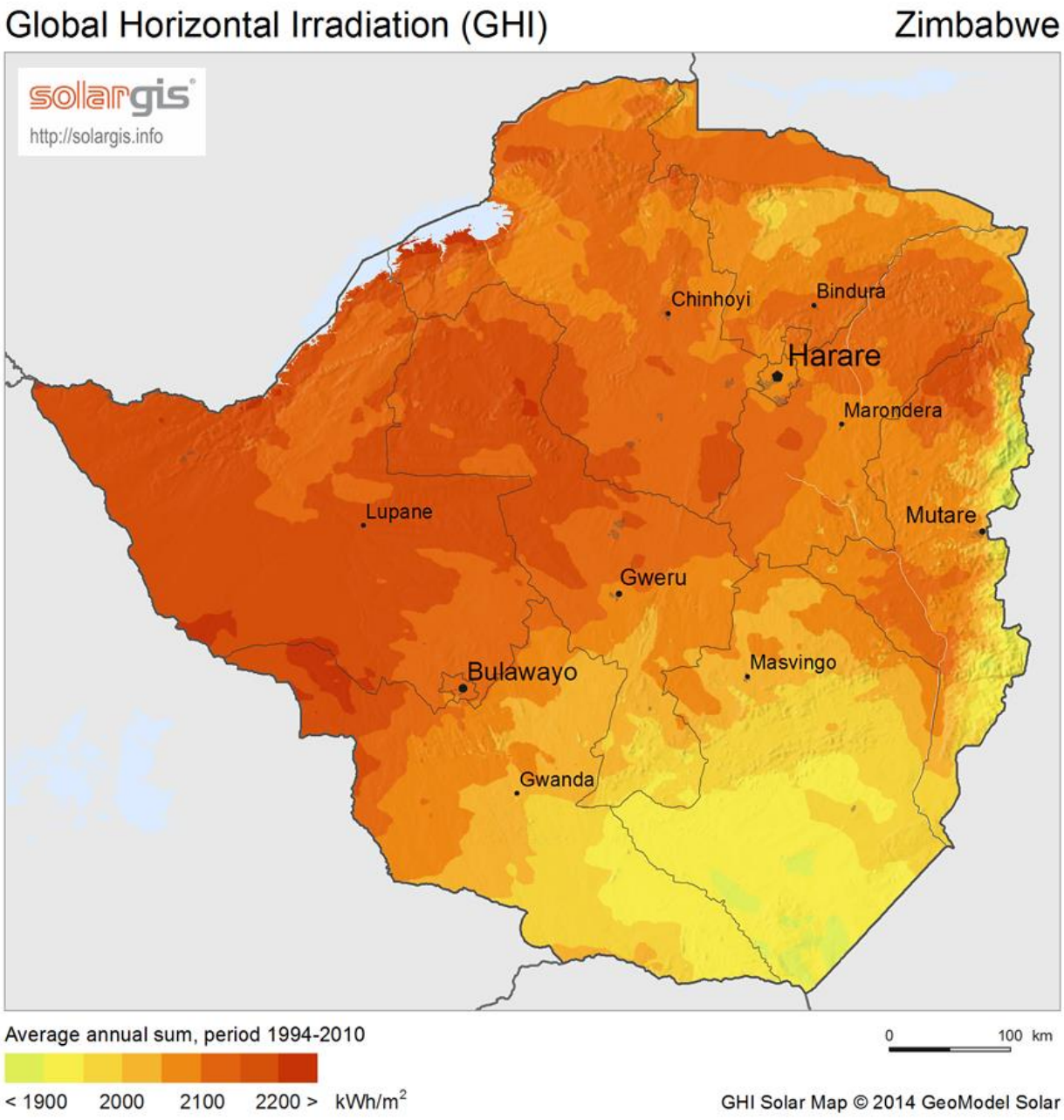

10.3 Appendix C – Grid Impact Assessment

ZIMBABWE ELECTRICITY TRANSMISSION AND DISTRIBUTION COMPANY (ZETDC)

ECOSOFT SOLAR PARK

GRID IMPACT ASSESSMENT

HARARE REGION

JUNE – 2017

Contents

1. PROJECT NAME

ECOSOFT SOLAR FARM

2. PROJECT DESCRIPTION

TDenergy (Pvt) Ltd has applied to connect 30MW power plant located about 7.2 km from Highlands Park 33/11kV substation and about 13.45 km from Greystones 33/11kV substation in Harare. The power station is planned for commissioning in October 2018.

3. Project location

Harare East District, Harare Province

4. PROJECT BACKGROUND

ZETDC has received an application from TDenergy (Pvt) Ltd with a proposal of constructing a 30MW solar power plant using solar photovoltaic technology at Ecosoft solar plant in Harare East, Harare Province.

The proposed site is closer to Highlands Park and Greystones 33/11kV substations in Harare province. According to the client, the proposed gross capacity is 30MW and Net capacity is 30MW generating at Plant Load Factor (PLF) of 22.4%.

The purpose of this feasibility study report is to analyse the impact of connecting the 30MW generation plant to the ZETDC Network.

The geographical location of the proposed power plant is as shown on attached map.

5. PLANNING CRITERIA

The planning criterion used in this analysis is according to the Distribution Planning Manual and is as summarized below

5.1 VOLTAGE DEFINITIONS

Maximum operation voltage (kV)	Nominal system voltage (kV)
145 36 12.1	132 33 11

*standard IEC voltages (IEC 60038 and IEC 60071) and also contained in ZETDC general specification Vol 1. Section 3.4

5.3 **Normal Operation**

With all distribution lines in service, the system must be capable of a satisfactory supply of all distribution loads on the 33kV feeder both during peak and light load conditions

5**.4 Voltage Limits**

In steady state operation, main grid voltages shall be kept within the following limits:

	Maximum (kV/p.u.)	Minimum (kV/p.u.)
33 kV:	36.3./1.1	29.7/0.9

Voltage excursions below 0.85 p.u. any time after a fault has been cleared successfully is considered to be unacceptable.

5.5 Stability Criteria

The system shall withstand a sudden outage of any generating unit or block of units connected to the same transformer without loss of supply.

5.6 Loading Limits

Thermal design ratings shall not be exceeded in steady state operation.

For a single outage, the following load limits shall be applied once the new steady state has been reached, but prior to any operator's intervention:

- Short-time (10 minutes) overloads of up to 15% on distribution lines shall be accepted before operator action can be taken.
- Short-time (10 minutes) overloads of up to 15% on transformers shall be accepted.

5.7 Losses

Losses shall be limited to a maximum of 3% peak on a feeder.

Line Design

All new 11kV and 33 kV lines should be designed for a minimum conductor temperature of 65^{o}C.

5.8 Steady State Stability Limits

When evaluating the system's transfer limits, care should be taken to design the system with adequate margin to avoid voltage collapse phenomena. Note especially that a voltage collapse might occur at voltage levels above the minimum operating levels indicated above. Transfer limits must secure that a single outage does not bring the system into a steady state instability situation. The system should be regarded as unacceptable if the system runs out of voltage control range following a single contingency, even if the deterministic criteria are satisfied.

Assumptions Considered:

The following assumptions were considered;

1. Only steady state conditions were looked at.

6. OPTIONS CONSIDERED

OPTION 1

Case1

This option involves injection into the grid at 33kV and the scope covers construction of 4.3km of twin wolf (2x150mm^2 SCA), 33kV overhead line and laying of 2.9km single core XLPE 300mm2 underground cable from the power plant to 33/11kV substation.

SCOPE OF WORK

The indicative scope of work for the connection of the generation plant to the Grid will involve,

- Construction of a combination of 4.3km, 33kV, 2x 150mm^2, SCA, overhead line rated at 51.68MVA@ 75°C and laying of 3000m of 33kV, 300mm^2 , XLPE underground cable to link Ecosoft Solar Park and Highlands park substation 33kV busbar complete with associated line bays.
- Supply of substation and associated works and accessories
    - ❖ protection equipment,
    - ❖ communication equipment,
    - ❖ metering equipment,
    - ❖ associated switchgear,
    - ❖ 2 x synchronize relays

Case 2

This option involves injection into the grid at 33kV and the scope covers laying of 7.2km of 33kV single core XLPE 300mm2 underground cable from the power plant to 33/11kV substation. This will be implemented in the event of denial of grant of wayleave.

SCOPE OF WORK

The indicative scope of work for the connection of the generation plant to the Grid will involve,

- laying of 7200m of 33kV, 300mm^2 , XLPE underground cable to link Ecosoft Solar Park and Highlands park substation 33kV busbar complete with associated line bays.
- Supply of substation and associated works and accessories
    - ❖ protection equipment,
    - ❖ communication equipment,
    - ❖ metering equipment,
    - ❖ associated switchgear,
    - ❖ 2 x synchronize relays

PROJECT COSTS

OPTION 1: CASE 1

Item	Description	Unit	Quantity	Unit Cost, USD	Total Cost USD
1	Construction of 33kV, twin Wolf (2x150m2 SCA) overhead line 51.68MVA@75°C from the solar plant to Highlands park 33kV busbar.	m	25 800	5.47	141,126.00

2	Lay 2900m of 33kV, 300mm2 XLPE from overhead line to link different portions of the Overhead line and Highlands park Substation 33kV Busbar	m	17 400	85.00	1,479,000.00
3	33kV line bay	ea	2	125,000.00	250,000.00
4	Supply of station interface accessories (protection equipment, communication equipment, metering equipment, associated switchgear, synchronizing relays, etc.) as required.	lot		200,000.00	200,000.00
5	Network reinforcement Up-rate loop cable for the circuit connecting Highlands Park 33/11kV substation and Coleford 132/33kV substation.	m	1500	95.00	142,500.00
6	Labour				110,631.30
7	Administration Costs				55,315.65
	Sub Total				**2,378,572.95**
	VAT 15%				356,785.94
	TOTAL				**2,735,358.89**

OPTION 1: CASE 2

Item	Description	Unit	Quantity	Unit Cost, USD	Total Cost USD

1	Lay 2900m of 33kV, 300mm2 XLPE from overhead line to link different portions of the Overhead line and Highlands park Substation 33kV Busbar	m	43 200	85	3,672,000.00
2	33kV line bay	ea	2	125,000	250,000.00
	Supply of station interface accessories (protection equipment, communication equipment, metering equipment, associated switchgear, synchronizing relays, etc.) as required	lot		200,000	200,000.00
	Labour				213,225.00
	Administration Costs				106,612.50
	Sub Total				**4,584,337.50**
	VAT 15%				687,650.63
	TOTAL				**5,271,988.13**

OPTION 2

This option involves injection into the grid at 33kV and the scope covers construction of 13.45km of a combination of twin Wolf (2x150mm^2 SCA), 33kV overhead line and 300mm^2 XLPE underground cable from the Ecosoft power plant to Greystones 33/11kV substation.

SCOPE OF WORK

The indicative scope of work for the connection of the generation plant to the Grid will involve,

- Construction of 4.3km, 33kV, 2x 150mm^2, SCA, overhead line rated at 51.68MVA@ 75°C from the solar plant and laying of 9.15km of 33kV, 300mm^2, XLPE from the overhead line to Greystones substation 33kV busbar complete with associated line bays.
- Supply of substation and associated works and accessories
    - ❖ protection equipment,
    - ❖ communication equipment,
    - ❖ metering equipment,
    - ❖ associated switchgear,
    - ❖ 2 x synchronize relays

PROJECT COSTS

Item	Description	Unit	Quantity	Unit Cost, USD	Total Cost USD
1	Construction of 33kV, twin dog (2x150mm2 SCA) overhead line rated 51.68MVA@ 75°C from the solar plant to Greystones 33kV busbar.	m	25 800	5.47	141,126.00
2	Laying of 9150m of 33kV 300mm2 XLPE from overhead line to Greystones 33kV busbar.	m	54 900	85	4,666,500.00
3	33kV line bay	ea	2	125,000	250,000.00
4	Supply of station interface accessories (protection equipment, communication equipment, metering equipment, associated switchgear, synchronizing relays, etc.) as required	lot		200,000	200,000.00
	Labour				262,881.30
	Administration Costs				131,440.65
	Sub Total				**5,651,947.95**
	VAT 15%				847,792.19
	TOTAL				**6,499,740.14**

7. TECHNICAL ASSESSMENT OF THE PROPOSED PROJECT

KEY PROJECT ASSUMPTIONS

The following assumptions were considered;

1. A system demand of 648MW
2. All inputs at Dema, Warren and Power Station in service
3. Highlands Park 33/11kV substation on normal feed from Coleford 132/33kV substation.
4. Greystones 33/11kV substation on normal feed from Pomona 132/33kV substation.

TECHNICAL ANALYSES FOR OPTIONS 1 &2

SYSTEM PERFORMANCE WITH AND WITHOUT ECOSOFT SOLAR PARK 30MW PLANT

Load analysis indicated after connecting the solar plant to Highlands Part 33/11Kv substation there is need to upgrade the loop cables between Coleford 132/33Kv substation and Highlands Park substation. However, all the provided options are technically feasible.

THERMAL CONSTRAINT

On connection of Ecosoft Solar 30MW power plant,

- The load analysis indicated a thermal constraint on the two loop cables between Coleford and Highlands park substations under steady state conditions.

VOLTAGE PROFILES:

The nominal voltage profile at Prince Edward Dam and Prospect substations changed with the introduction of the solar plant as follows:

Substation	Before Injection	After Injection	
		Option 1	**Option 2**
ECOSOFT Solar Park 33kV	-	99.48%	108.34%
Highlands Park 33kV	94.56%	98.22%	
Greystones 33kV	93.27%		96.17%

These voltages apply to steady state condition with no prior outage. Of note is the improvement in voltage regulation for Highlands park 33kV busbar for option 1 and improvement in voltage profile for Greystones 33kV busbar for option 2.

SHORT CIRCUIT ANALYSIS

Bus bar	Before Injection, kA	After Injection - Option 1, kA	After Injection Option 2, kA
Highlands park 33kV	4.02	5.08	
Greystones 33kV	4.90		5.97
Coleford	7.35	7.61	7.93
Ecosoft Solar 33kV	-	3.26	3.37

There is a marginal increase in fault levels which does not however affect existing switchgear.

SYSTEM LOSSES:

The impact of Ecosoft Solar 30MW plant to system losses was appraised with and without the plant.

	Option 1		Option 2
	Case 1	Case 2	
Percentage increase in System losses %			

Connection of the solar plant will result in a marginal increase in system losses by 1.1% and 0.9% for Option 1 and Option 2 respectively

LEAST COST ANALYSIS

A least cost analysis was carried out on the two options as both are technically feasible. Table below shows the results:

Option	Life Cycle Costs(20yrs), USD
1.1	
1.2	
2	

8. RECOMMENDATIONS

1. From the grid impact assessment carried out there is no significant negative impact on the ZETDC grid resulting from connection of **ECOSOFT solar** power plant for both options
2. However, it is encouraged that the inverters that the client is going to use on the plant have a capability to regulate reactive power so to avoid voltage drops on the nearby network

3. The client should also ensure that harmonics arising from the inverters are kept to a minimum level and in accordance with requirements set out in the distribution code.
4. The client should install a fast-response voltage regulating device on the new plant e.g. STATCON

Furthermore the plant will need to comply with the requirements for connection of generators to the ZETDC grid and ZETDC's specifications and standards

9. CONCLUSION

All the two options appraised were found to be technically feasible. The project doesn't cause any negative impact on the Grid for both options and is therefore recommended. **Option 1**: **Case 1** is recommended as it is the least cost option.

10. Attachments

10.1 Option 1.1Load flow/before upgrade

10.2 Option 1.1 load flow/After upgrade

10.3 Option 1.2 Loadflow

10.4 Option 2 Loadflow

10.3 Site map

Grid Status before connection of Ecosoft solar plant

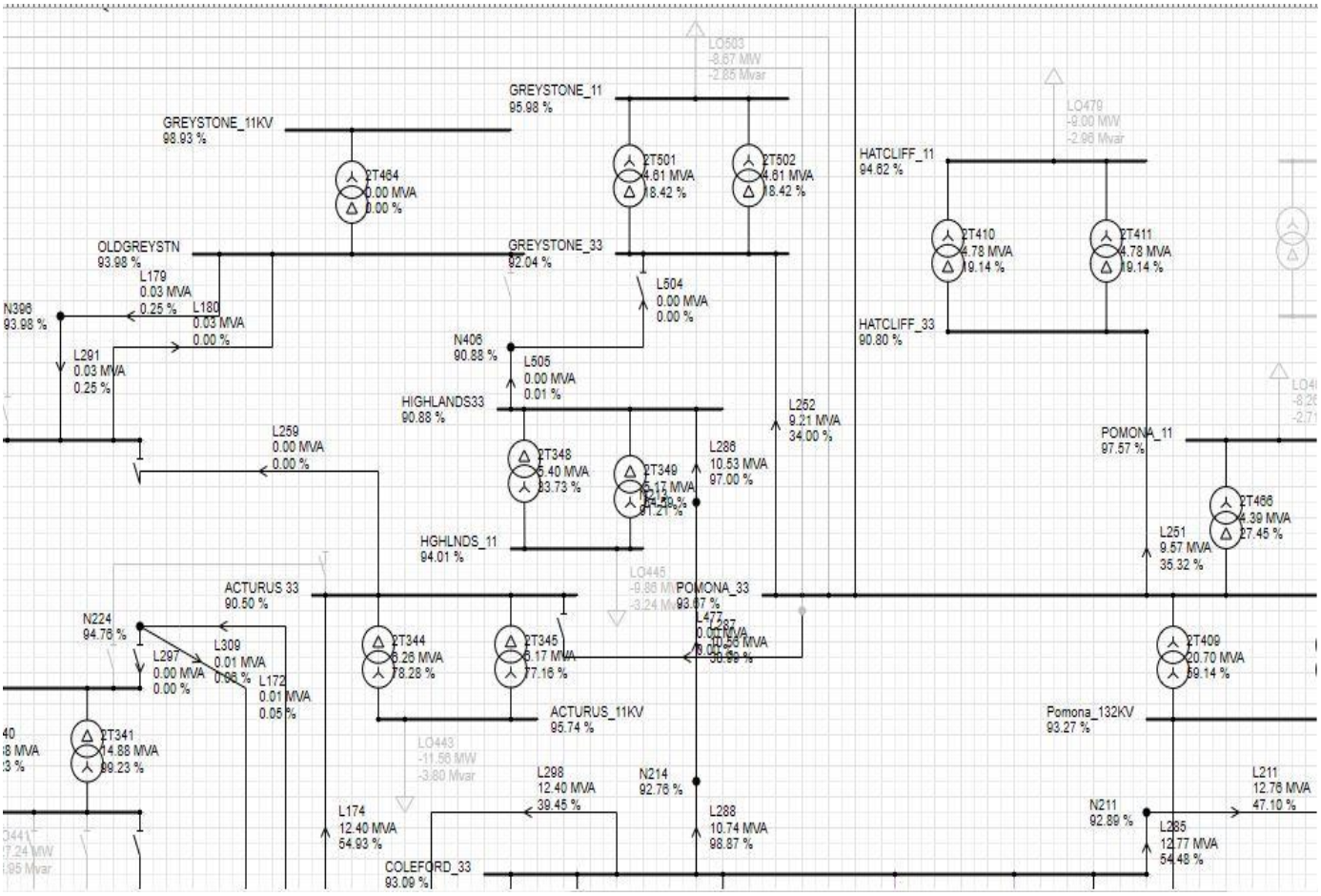

10.1 OPTION 1 .1 before upgrading loop cables connecting Coleford and Highlands Park

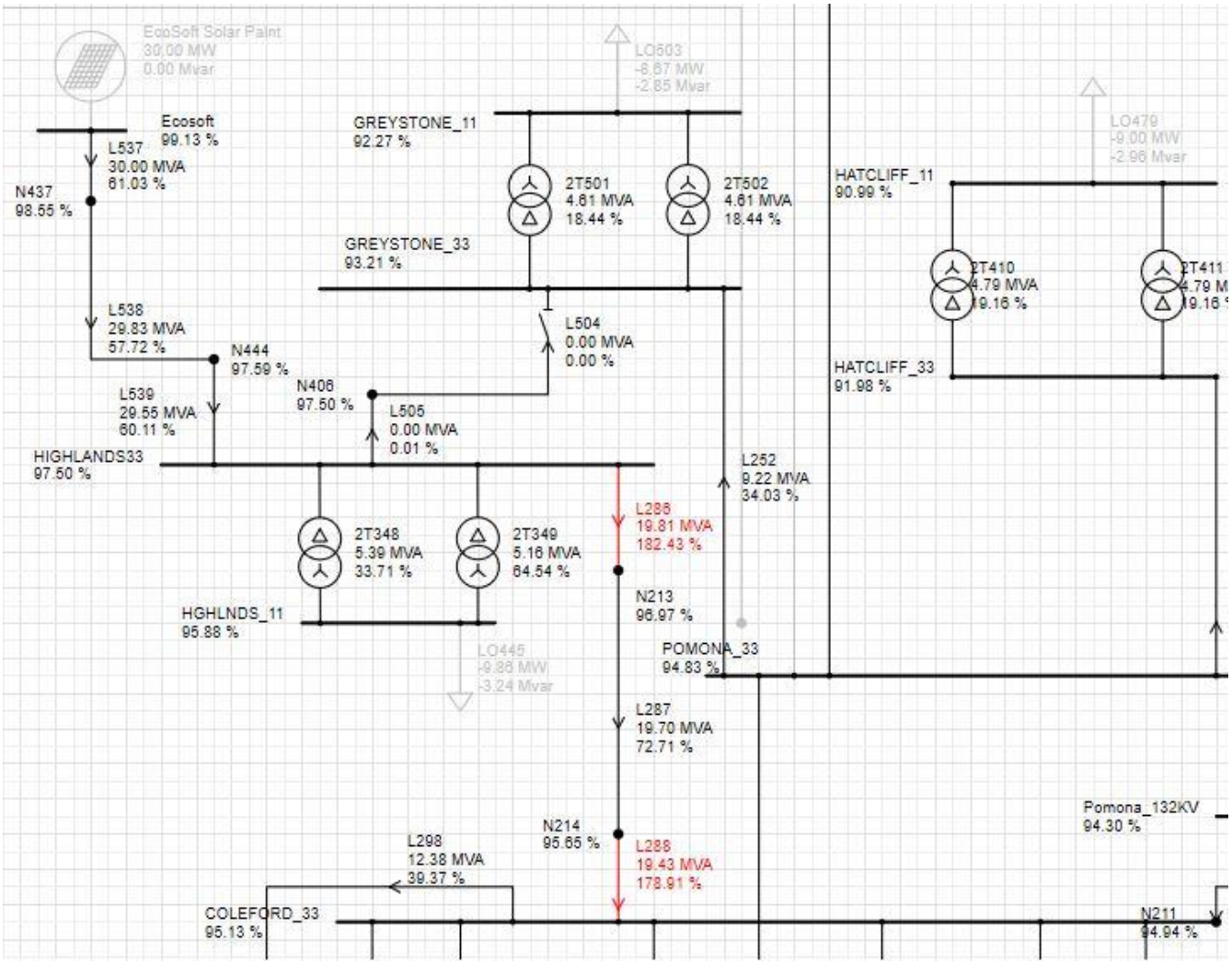

10.2 OPTION 1.1 After upgrading loop cables connecting Coleford and Highlands park

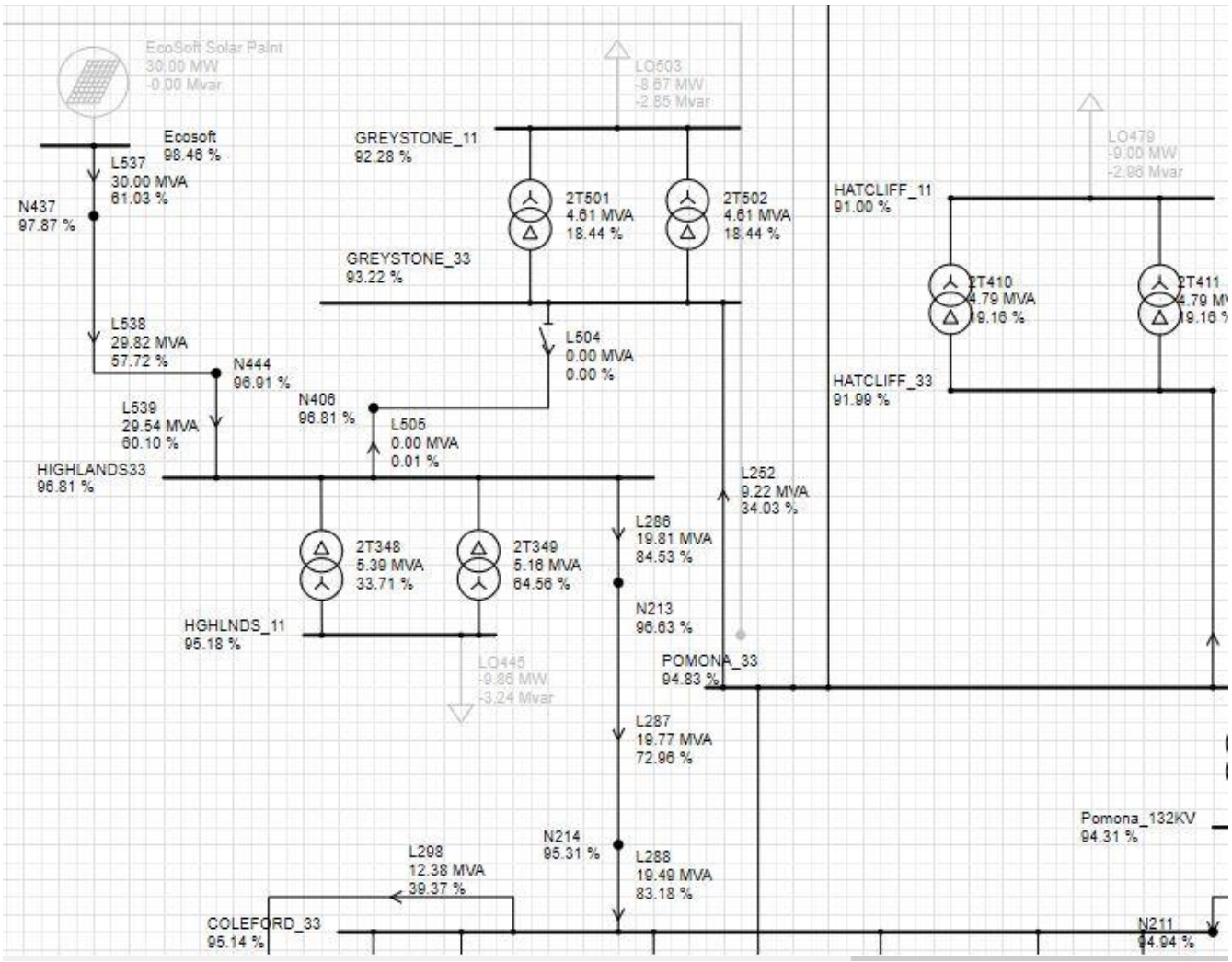

10.3 OPTION 1.2 –Highlands park –Ecosoft /CABLE

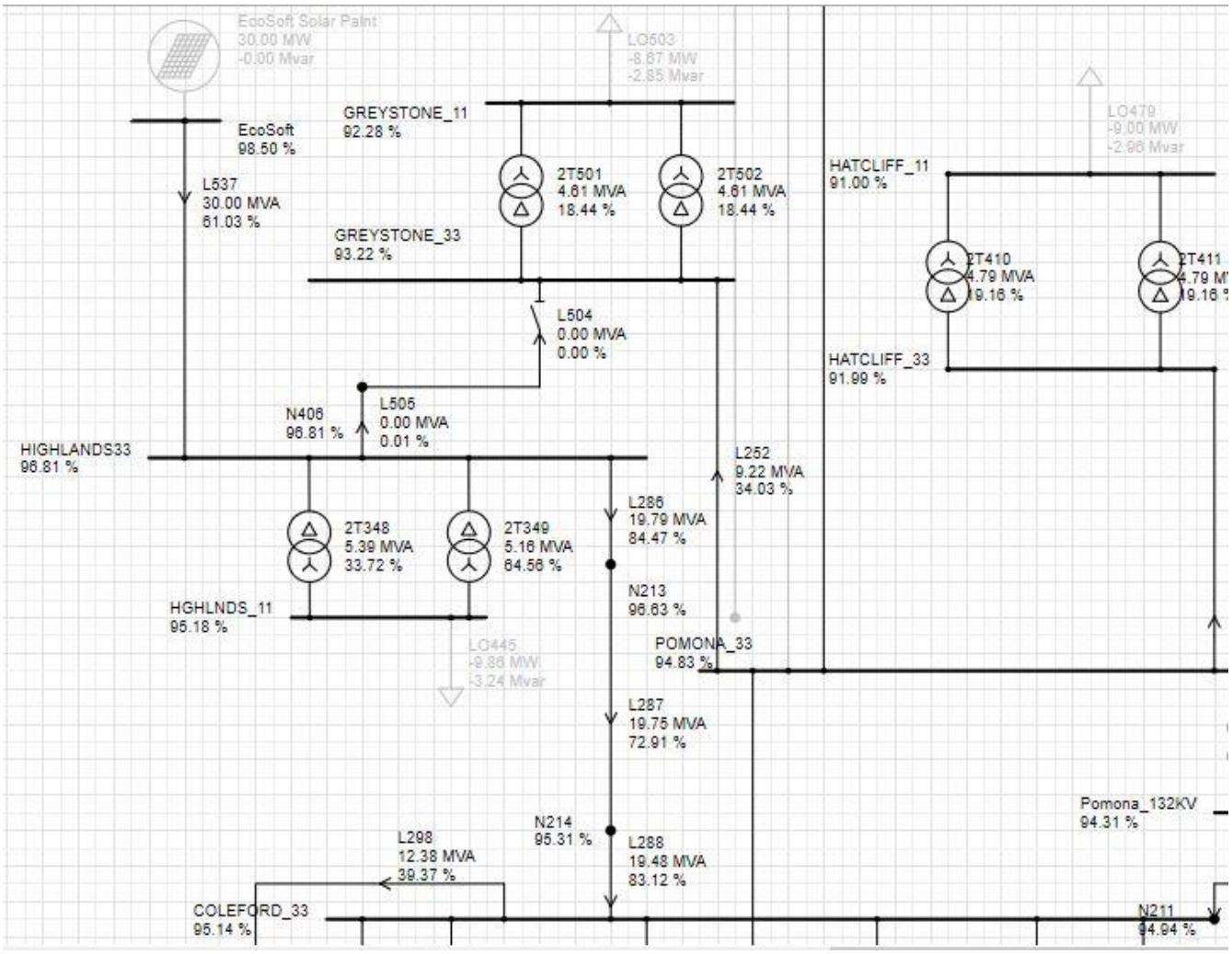

10.4 OPTION 2-Ecosoft-Greystones

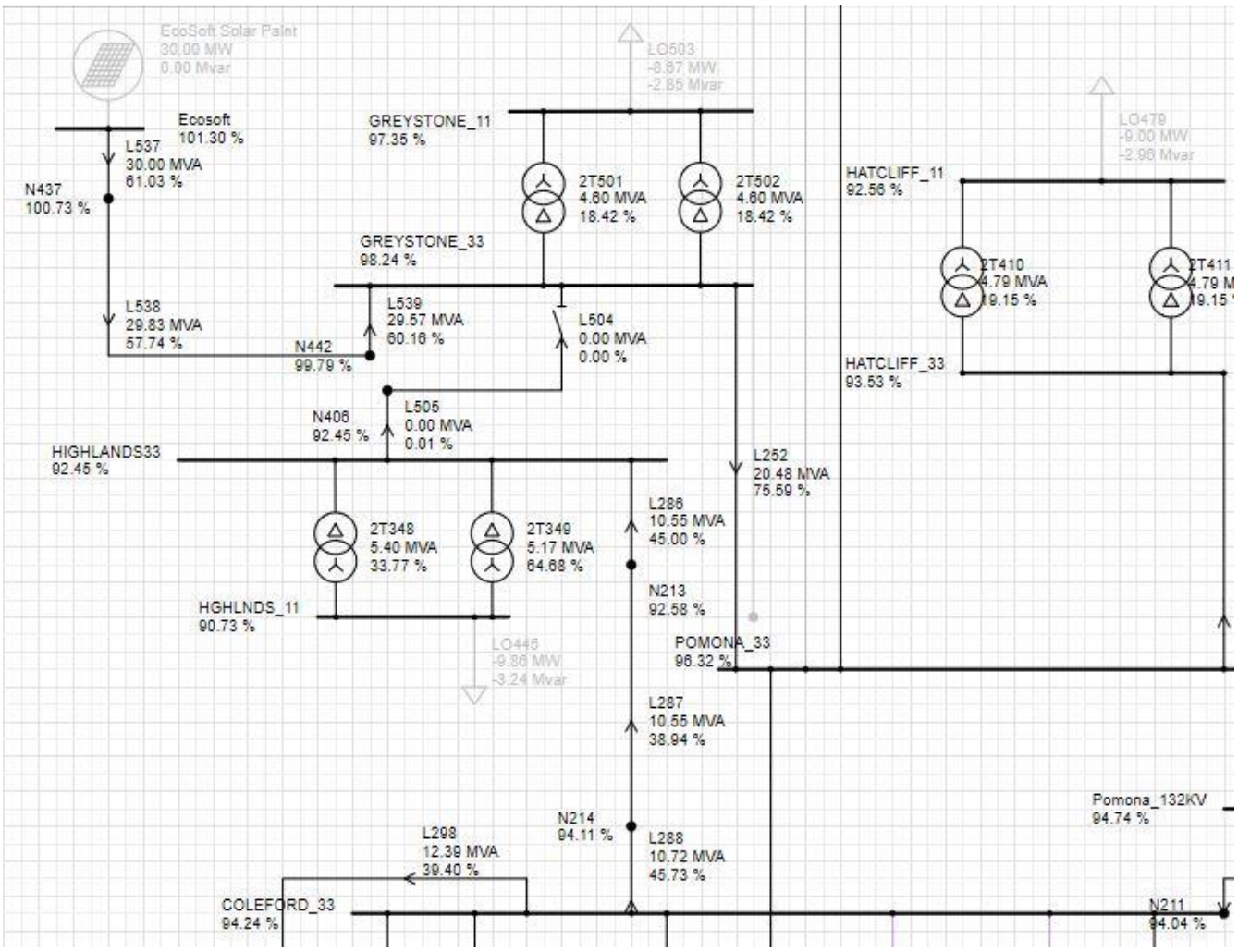
EcoSoft Solar Paint
30.00 MW
0.00 Mvar
LO503
-8.87 MW
-2.85 Mvar
Ecosoft
101.30 %
L537
30.00 MVA
61.03 %
N437
100.73 %
GREYSTONE_11
97.35 %
2T501
4.60 MVA
18.42 %
2T502
4.60 MVA
18.42 %
GREYSTONE_33
98.24 %
L538
29.83 MVA
57.74 %
N442
99.79 %
L539
29.57 MVA
60.16 %
L504
0.00 MVA
0.00 %
N406
92.45 %
L505
0.00 MVA
0.01 %
HIGHLANDS33
92.45 %
2T348
5.40 MVA
33.77 %
2T349
5.17 MVA
64.68 %
HGHLNDS_11
90.73 %
LO445
-9.86 MW
-3.24 Mvar
L252
20.48 MVA
75.59 %
L286
10.55 MVA
45.00 %
N213
92.58 %
POMONA_33
96.32 %
L287
10.55 MVA
38.94 %
N214
94.11 %
L288
10.72 MVA
45.73 %
L298
12.39 MVA
39.40 %
COLEFORD_33
94.24 %
LO479
-9.00 MW
-2.96 Mvar
HATCLIFF_11
92.56 %
2T410
4.79 MVA
19.15 %
HATCLIFF_33
93.53 %
Pomona_132KV
94.74 %
N211
94.04 %